

ANALYSIS OF AN ELECTRONIC PHASE SHIFT CIRCUIT
FOR STARTING A SINGLE PHASE INDUCTION MOTOR

MAHBUBUR RAHMAN



A thesis

submitted to the Department of Electrical and
Electronic Engineering in partial fulfilment
of the requirements for the
degree of
Master of Science in Engineering (EEE)

DEPARTMENT OF ELECTRICAL AND ELECTRONIC ENGINEERING
BANGLADESH UNIVERSITY OF ENGINEERING AND TECHNOLOGY


DHAKA, BANGLADESH, JULY, 1996



#90103#

DECLARATION

I do hereby declare that this work has been done by me and neither this thesis nor any part thereof has been submitted for the award of any degree or diploma except for publication.



Dr. Mohammad Ali Choudhury

Supervisor

Dated: July 01, 1996



Mahbubur Rahman

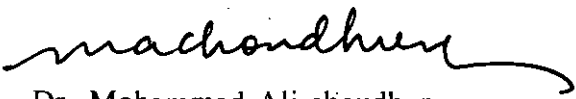
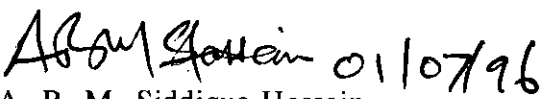

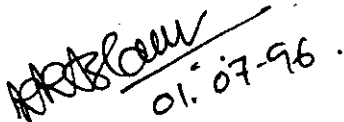
Candidate and the student

Dated: July 01, 1996

APPROVAL

The thesis titled, 'Analysis of an Electronic Phase Shift Circuit for starting a Single Phase Induction Motor', submitted by Mahbubur Rahman, Roll number 901356p, Session 1988-1989 to the Department of EEE, BUET has been accepted as satisfactory for the partial fulfilment of the requirement for the degree of Master of Science in Electrical and Electronic Engineering. The thesis defence of the candidate was held on July 01, 1996. Thesis title was approved by CASR in meeting 111, dated 18.10.93, Resolution 18 and the Board of Examiners was approved in CASR meeting 123, dated 17.06.96, Resolution 37.

BOARD OF EXAMINERS

1. 
Dr. Mohammad Ali Choudhury
Associate Professor
Department of Electrical and Electronic Engineering
BUET, Dhaka. Chairman
(Supervisor)
2. 
Dr. A. B. M. Siddique Hossain
Professor and Head of the
Department of Electrical and Electronic Engineering
BUET, Dhaka. Member
(Ex-officio)
3. 
Dr. Enamul Basher
Professor
Department of Electrical and Electronic Engineering
BUET, Dhaka. Member
(Internal)
4. 
Dr. Kazi Khairul Islam
Associate Professor
Department of Electrical and Electronic Engineering
BIT, Rajshahi, Bangladesh. Member
(External)

ACKNOWLEDGEMENT

I wish to express my deep sense gratitude to Dr. Mohammad Ali Choudhury, Associate Professor, Department of Electrical and Electronic Engineering, BUET, Dhaka for his guidance and kind supervision, constant encouragement and valuable suggestion in bringing this work to completion.

I am thankful to Dr. A. B. M. Siddique Hossain, Professor and Head of the Department of Electrical and Electronic Engineering, BUET, Dhaka, Dr. Saiful Islam and Dr. Syed Fazal-i-Rahman, Professors and Former Heads of the Department of Electrical and Electronic Engineering, BUET, Dhaka for their kind help and co-operation during this work.

I express my thanks to Dr. Shahidul Islam Khan, Professor, Department of Electrical and Electronic Engineering, BUET, Dhaka and all of my well wishers for their encouragement, support and valuable advice.

Finally, I would like to offer my thanks to all teachers and staff of the Department of Electrical and Electronic Engineering, BUET, Dhaka.

CONTENTS

	Page
Declaration	i
Approval	ii
Acknowledgement	iii
Contents	iv
List of symbols	vi
List of figures	vii
List of tables	xiii
Abstract	xiv
CHAPTER 1 : INTRODUCTION	
1.1 Introduction	1
1.2 Review of pulse width modulation techniques	1
1.3 Cycloconverter and phase shifting	8
1.4 Sine PWM technique in cycloconverter	13
1.5 Objective of the present work	17
1.6 Out line of the thesis	17
CHAPTER 2 : ANALYSIS OF PHASE SHIFT CIRCUIT WAVEFORMS	
2.1 Introduction	18
2.2.1 Single phase static phase shift circuit	19
2.2.2 Waveform analysis of single phase static phase shift circuit	24
2.3 Modulated static single phase, phase shift circuit	27
2.4 Analysis of sine pulse width modulated waves	28
2.5 Analysis of single pulse modulated phase shift circuit waveform	33

	Page
2.6	Observation 36
CHAPTER 3 : PRACTICAL IMPLEMENTATION	
3.1	Introduction 50
3.2	Practical converter circuit 50
3.3	Practical modulator circuit 50
3.4	Practical logic circuit 53
3.5	Experimental result 57
3.6	Observation 57
CHAPTER 4 : SUMMARY AND CONCLUSION	
	62
References	64
Appendix 1 : Waveforms and spectrum of sine PWM	69
Appendix II : Waveforms and spectrum of PWM phase shift circuit	88
Appendix III : Program in MATLAB	107

LIST OF SYMBOLS

A_c	Maximum magnitude of the carrier triangular wave
A_r	Maximum magnitude of the reference wave
a_n, b_n, c_n	Fourier coefficients
f_c	Carrier frequency
f_o	Output frequency
$f(t)$	Modulated or unmodulated function
$g(t, t_o, t_i)$	Gate function starting at t_o and ending at t_i
N	Number of pulses per half cycle
m	Modulating index
m_f	Frequency modulation ratio
$m(t)$	Modulated wave
$s(t)$	Switching function
T	Period of the sine wave
T_s	Period of the switching wave
v_i	Input wave
v_o	Output wave
v_s	Phase shifted wave
v_{ms}	Modulated phase shifted wave
δ_i	Pulse width of the i th pulse
Θ_i	Location of mid position of the i th pulse
α	Firing angle

LIST OF FIGURES

		Page
Fig. 1.1	Single pulse width modulation	3
Fig. 1.2	Multiple pulse width modulation	3
Fig. 1.3	Sinusoidal pulse width modulation	5
Fig. 1.4	Delta pulse width modulation	7
Fig. 1.5	Basic single phase cycloconverter	9
Fig. 1.6	Operation of 'P' converter while 'N' converter is off	10
Fig. 1.7	Operation of 'N' converter while 'P' converter is off	11
Fig. 1.8	Typical supply and the output waveform of a single phase cycloconverter	12
Fig. 1.9	Phase shifted waveform obtained from switching a sine wave by a static converter	14
Fig. 1.10	Sinusoidal pulse width modulation	15
Fig. 1.11	PWM waveform generation for a single phase cycloconverter	16
Fig. 2.1	Phase shift circuit topology I & II	19
Fig. 2.2	Phase shift circuit topology III	20
Fig. 2.3	Phase shift circuit topology IV	21
Fig. 2.4	Phase shift circuit topology V	22
Fig. 2.5	Output after 1st quarter cycle	23
Fig. 2.6	Output after 3rd quarter cycle	23
Fig. 2.7	Output of full cycle operation	23
Fig. 2.8	Sine wave	25
Fig. 2.9	Switching wave	25

		Page
Fig. 2.10	Sine wave & switching wave	25
Fig. 2.11	Modulated output of the phase shift circuit	29
Fig. 2.12	Analysis of the waveform	34
Fig. 2.13	Waveform of SPWM at modulating index $m = .5$ and carrier frequency $f_c = 450$ Hz	38
Fig. 2.14	Waveform of SPWM at modulating index $m = .5$ and carrier frequency $f_c = 850$ Hz	39
Fig. 2.15	Waveform of SPWM at modulating index $m = .7$ and carrier frequency $f_c = 850$ Hz	40
Fig. 2.16	Waveform of SPWM at modulating index $m = .9$ and carrier frequency $f_c = 850$ Hz	41
Fig. 2.17	Waveform of SPWM at modulating index $m = 1.1$ and carrier frequency $f_c = 850$ Hz	42
Fig. 2.18	Waveform of SPWM at modulating index $m = 1.3$ and carrier frequency $f_c = 850$ Hz	43
Fig. 2.19	Modulated waveform of phase shift circuit at modulating index $m = .5$ and number of pulse/ quarter cycle $N = 9$	44
Fig. 2.20	Modulated waveform of phase shift circuit at modulating index $m = .5$ and number of pulse/ quarter cycle $N = 17$	45
Fig. 2.21	Modulated waveform of phase shift circuit at modulating index $m = .7$ and number of pulse/ quarter cycle $N = 17$	46
Fig. 2.22	Modulated waveform of phase shift circuit at modulating index $m = .9$ and number of pulse/ quarter cycle $N = 17$	47
Fig. 2.24	Modulated waveform of phase shift circuit at modulating	

	Page
	index $m = 1.1$ and number of pulse/ quarter cycle $N = 17$ 48
Fig. 2.24	Modulated waveform of phase shift circuit at modulating index $m = 1.3$ and number of pulse/ quarter cycle $N = 17$ 49
Fig. 3.1	Practical converter circuit 51
Fig. 3.2	Practical modulator circuit 52
Fig. 3.3	Practical logic circuit 54
Fig. 3.4	Generation of switching signals 55
Fig. 3.5	Output of practical phase shift circuit 56
Fig. 3.6	a) Rectifier output and modulator switching signal 58 b) Modulated output 58
Fig. 3.7	a) Switching signals of MOSFETs 59 b) output of the single phase , phase shift circuit 59
Fig. 3.8	Output of the single phase , phase shift circuit at $f_c = 1$ Khz and $f_c = 1.5$ Khz 60
Fig. 3.9	Output of the single phase , phase shift circuit at $f_c = 2.5$ Khz 61
Fig. A.1.1	Waveform of SPWM at modulating index $m = .5$ and carrier frequency $f_c = 550$ Hz 69
Fig. A.1.2	Waveform of SPWM at modulating index $m = .5$ and carrier frequency $f_c = 650$ Hz 70
Fig. A.1.3	Waveform of SPWM at modulating index $m = .5$ and carrier frequency $f_c = 750$ Hz 71
Fig. A.1.4	Waveform of SPWM at modulating index $m = .7$ and carrier frequency $f_c = 450$ Hz 72

		Page
Fig. A.1.5	Waveform of SPWM at modulating index $m = .7$ and carrier frequency $f_c = 550$ Hz	73
Fig. A.1.6	Waveform of SPWM at modulating index $m = .7$ and carrier frequency $f_c = 650$ Hz	74
Fig. A.1.7	Waveform of SPWM at modulating index $m = .7$ and carrier frequency $f_c = 750$ Hz	75
Fig. A.1.8	Waveform of SPWM at modulating index $m = .9$ and carrier frequency $f_c = 450$ Hz	76
Fig. A.1.9	Waveform of SPWM at modulating index $m = .9$ and carrier frequency $f_c = 550$ Hz	77
Fig. A.1.10	Waveform of SPWM at modulating index $m = .9$ and carrier frequency $f_c = 650$ Hz	78
Fig. A.1.11	Waveform of SPWM at modulating index $m = .9$ and carrier frequency $f_c = 750$ Hz	79
Fig. A.1.12	Waveform of SPWM at modulating index $m = 1.1$ and carrier frequency $f_c = 450$ Hz	80
Fig. A.1.13	Waveform of SPWM at modulating index $m = 1.1$ and carrier frequency $f_c = 550$ Hz	81
Fig. A.1.14	Waveform of SPWM at modulating index $m = 1.1$ and carrier frequency $f_c = 650$ Hz	82
Fig. A.1.15	Waveform of SPWM at modulating index $m = 1.1$ and carrier frequency $f_c = 750$ Hz	83
Fig. A.1.16	Waveform of SPWM at modulating index $m = 1.3$ and carrier frequency $f_c = 450$ Hz	84

		Page.
Fig. A.1.17	Waveform of SPWM at modulating index $m = 1.3$ and carrier frequency $f_c = 550$ Hz	85
Fig. A.1.18	Waveform of SPWM at modulating index $m = 1.3$ and carrier frequency $f_c = 650$ Hz	86
Fig. A.1.19	Waveform of SPWM at modulating index $m = 1.3$ and carrier frequency $f_c = 750$ Hz	87
Fig. A.2.1	Modulated waveform of phase shift circuit at modulating index $m = .5$ and number of pulse/ quarter cycle $N = 11$	88
Fig. A.2.2	Modulated waveform of phase shift circuit at modulating index $m = .5$ and number of pulse/ quarter cycle $N = 13$	89
Fig. A.2.3	Modulated waveform of phase shift circuit at modulating index $m = .5$ and number of pulse/ quarter cycle $N = 15$	90
Fig. A.2.4	Modulated waveform of phase shift circuit at modulating index $m = .7$ and number of pulse/ quarter cycle $N = 9$	91
Fig. A.2.5	Modulated waveform of phase shift circuit at modulating index $m = .7$ and number of pulse/ quarter cycle $N = 11$	92
Fig. A.2.6	Modulated waveform of phase shift circuit at modulating index $m = .7$ and number of pulse/ quarter cycle $N = 13$	93
Fig. A.2.7	Modulated waveform of phase shift circuit at modulating index $m = .7$ and number of pulse/ quarter cycle $N = 15$	94
Fig. A.2.8	Modulated waveform of phase shift circuit at modulating index $m = .9$ and number of pulse/ quarter cycle $N = 9$	95
Fig. A.2.9	Modulated waveform of phase shift circuit at modulating index $m = .9$ and number of pulse/ quarter cycle $N = 11$	96

		Page
Fig. A.2.10	Modulated waveform of phase shift circuit at modulating index $m = .9$ and number of pulse/ quarter cycle $N = 13$	97
Fig. A.2.11	Modulated waveform of phase shift circuit at modulating index $m = .9$ and number of pulse/ quarter cycle $N = 15$	98
Fig. A.2.12	Modulated waveform of phase shift circuit at modulating index $m = 1.1$ and number of pulse/ quarter cycle $N = 9$	99
Fig. A.2.13	Modulated waveform of phase shift circuit at modulating index $m = 1.1$ and number of pulse/ quarter cycle $N = 11$	100
Fig. A.2.14	Modulated waveform of phase shift circuit at modulating index $m = 1.1$ and number of pulse/ quarter cycle $N = 13$	101
Fig. A.2.15	Modulated waveform of phase shift circuit at modulating index $m = 1.1$ and number of pulse/ quarter cycle $N = 15$	102
Fig. A.2.16	Modulated waveform of phase shift circuit at modulating index $m = 1.3$ and number of pulse/ quarter cycle $N = 9$	103
Fig. A.2.17	Modulated waveform of phase shift circuit at modulating index $m = 1.3$ and number of pulse/ quarter cycle $N = 11$	104
Fig. A.2.18	Modulated waveform of phase shift circuit at modulating index $m = 1.3$ and number of pulse/ quarter cycle $N = 13$	105
Fig. A.2.19	Modulated waveform of phase shift circuit at modulating index $m = 1.3$ and number of pulse/ quarter cycle $N = 15$	106

LIST OF TABLES

Table 2.1	Harmonic contents of phase shift output waveform	27
-----------	--	----

ABSTRACT

Fractional horse power single phase induction motors have no starting torque of their own. As a result, these motors are started by auxiliary methods. Now-a-days, single phase induction motors having large horse power rating are also in use in rural areas and in industries. These large horse power single phase induction motors require medium size capacitors for their start and running purpose. In this thesis static cycloconverter and inverter topologies have been proposed to perform the function of capacitors. Static converters are used for conversion of ac and dc power to ac and dc having frequency, magnitude and phase other than supply voltage. Several of the conventional static converters can replace the starting and running capacitors of single phase induction motors. When sinusoidal supply is switched at every quarter cycle, switched waveform shifted by 90° can be obtained. This waveform may be utilized in the starting purposes of large hp single phase motors. This would replace the bulky capacitors otherwise required for starting these motors and may also serve the purpose of power factor and other type of controls of the motors. The quarter cycle switched waveform though fulfils the required phase shift, pulse width modulated switching is proposed in the thesis for better harmonic performance of output waveform. Analysis and implementation of the PWM phase shift circuit has been carried out and reported in this thesis to justify the feasibility of using these circuits in the practical field. It has been found by analysis that over modulated sine PWM switched static cycloconverters provide necessary phase shift for motor start and at the same time keep the low order harmonics of the phase shift circuit output voltage within acceptable limit. Motor operation by the proposed circuits has not been studied in detail in this thesis and left for future investigation.

CHAPTER 1

INTRODUCTION



1.1 INTRODUCTION

Fractional horse power single phase induction motors have no starting torque of their own. As a result, these motors are usually started by auxiliary methods [1]. One of the conventional method of starting is to use split phase winding with provision of connecting capacitors. The size of the capacitors increase with the increase of motor horse power and supply voltage. In Bangladesh large horse power induction motors are being used in rural areas and in industrial application. In the proposed research an attempt will be made to fabricate a static cycloconverter circuit to replace the starting capacitor of single phase induction motors. Static cycloconverters are basically converters which are used in variable frequency AC-AC conversion. The output of the converters is nonsinusoidal. Fundamental component of the output voltage of such converters is in phase with the input supply voltage but have different frequency. Our effort will to be develop a switching technique for single phase cycloconverters so that the fundamental of the output voltage will have same frequency with formidable phase shift. This can be used to replace the starting capacitors of single phase induction motors.

1.2 REVIEW OF PULSE WIDTH MODULATION TECHNIQUES

The output of normal inverters are non sinusoidal (square wave, semi square wave) in nature and contain harmonics. The harmonic contents are detrimental to the applications in terms of losses. They are also detrimental to the utility power supply in-terms of line harmonic injection and requires large output filter to eliminate low order harmonics. This can be improved by employing a PWM inverter to reduce the input/output filter size. In PWM switching the output voltage and frequency can be changed according to the need by varying the gating pulse of a particular converter. Switches are operated at higher frequencies. High frequency switching causes the dominant harmonic to occur

at higher frequency which is odd integer multiple of the fundamental frequency and reduce the output filter size. PWM inverters are capable of controlling voltage, frequency and harmonic contents in a single stage [2-6, 12-13].

In the pulse width modulation technique the switches of the power converter are operated at higher frequencies according to a particular pattern so as to produce pulses of varying widths at the output of the inverter. The earliest modulation technique applied to inverter operation are single pulse modulation and the multiple pulse modulation [2, 14-16]. In single pulse modulation control, there is only one pulse per half cycle of the reference wave and the width of the pulse is varied to control the inverter output voltage or power. Figure 1.1 shows the generation of gating signals and output of a full bridge inverter. The gating signals are generated by comparing a rectangular reference wave of amplitude A_r with a triangular carrier wave of amplitude A_c . The frequency of the reference signal determines the fundamental frequency of the output voltage. By varying A_r from 0 to A_c the pulse width δ can be varied from 0° to 180° . The dominant harmonic is the third and the distortion factor increases significantly at the low output voltage [6-7, 17-18]. The low order harmonic contents can be reduced by using several pulses in each half cycle of output voltage. The generation of gating signals of multiple pulse PWM for turning ON and OFF the inverter switches are shown in figure 1.2. The frequency of the reference signal sets the output frequency f_o and the carrier frequency f_c determines the number of pulses per half cycle, N . The order of harmonics is the same as that of single pulse modulation. The distortion factor is reduced significantly compared to that of single pulse modulation. However, due to large number of switching per half cycle switching loss would increase. With large values of N the amplitudes of the lower harmonics would be lower but the amplitudes of the higher order harmonics would increase. These techniques are capable of providing inverter voltages with low harmonic contents.

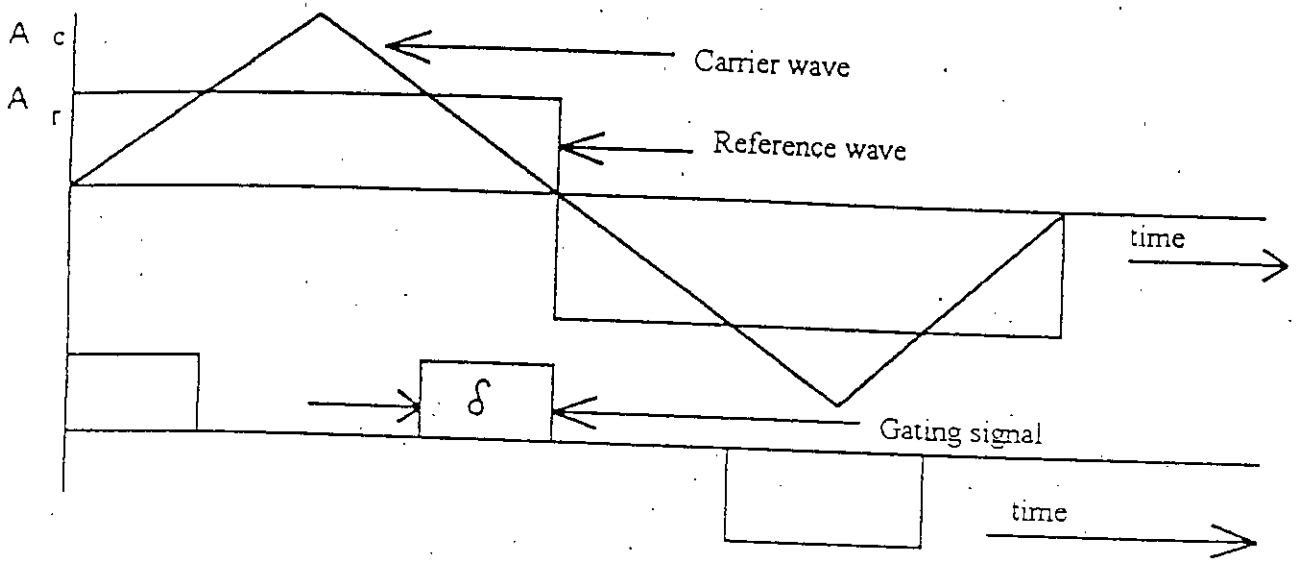


Fig. 1.1 Single pulse-width modulation

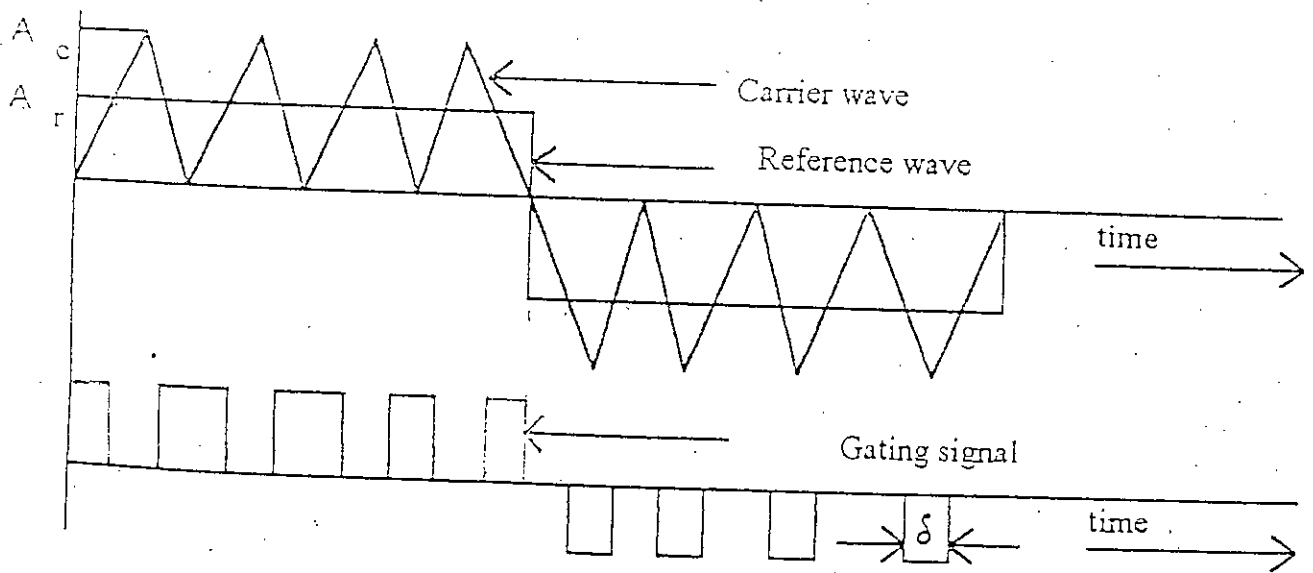


Fig. 1.2 Multiple pulse-width modulation

Among several PWM techniques, sinusoidal pulse width modulation (SPWM) is common. At the beginning two different types, namely the synchronous and asynchronous sine pulse width modulation schemes were used for switching power converters [12, 19-20]. In sine pulse width modulation, instead of maintaining the width of each pulse same (as in the case of multiple pulse modulation) the width of each pulse is varied in proportion to the amplitude of a sine wave evaluated at the centre of the same pulse. The distortion factor and lower order harmonics are reduced significantly [7-12, 17, 21-22]. The gating signals as shown in figure 1.3, are generated by comparing an isoscele triangular carrier wave with the sine wave signal. The crossover points determine the points of commutation. Except in low frequency range the carrier is synchronized with the modulating signal, and an odd integer (multiple of three, five etc.) ratio is maintained to improve the harmonic content. The fundamental output voltage can be varied by variation of the modulation index [12, 16-17, 23-24]. It can be shown that if the modulating index is less than unity. Only carrier frequency harmonic with the fundamental frequency related side bands appear at the output. The voltage of the inverter can be increased by changing modulation index until maximum voltage is obtained in square wave mode. The distortion factor is less compared to that of multiple pulse modulation. This type of modulation eliminates all the harmonics less than or equal to $2(N-1)$. The output voltage of an inverter contains harmonics. The PWM pushes the harmonics into a higher frequency range around the frequency f_c and its multiples, that is, around harmonics m_f , $2m_f$, $3m_f$ and so on.

In order to overcome the drawbacks of sine pulse width modulation in drive applications, variable ratio PWM scheme was introduced. Three distinct sinusoidal pulse width modulation scheme are in use for inverters [3-5, 7-15, 25-26]. They are the 1) Natural sampled 2) Symmetric regular sampled and 3) Asymmetric regular sampled PWM. In regular sampling method sine wave was replaced by a sampled or stepped sine wave. The stepped sine wave is not a sampled approximation to the sine

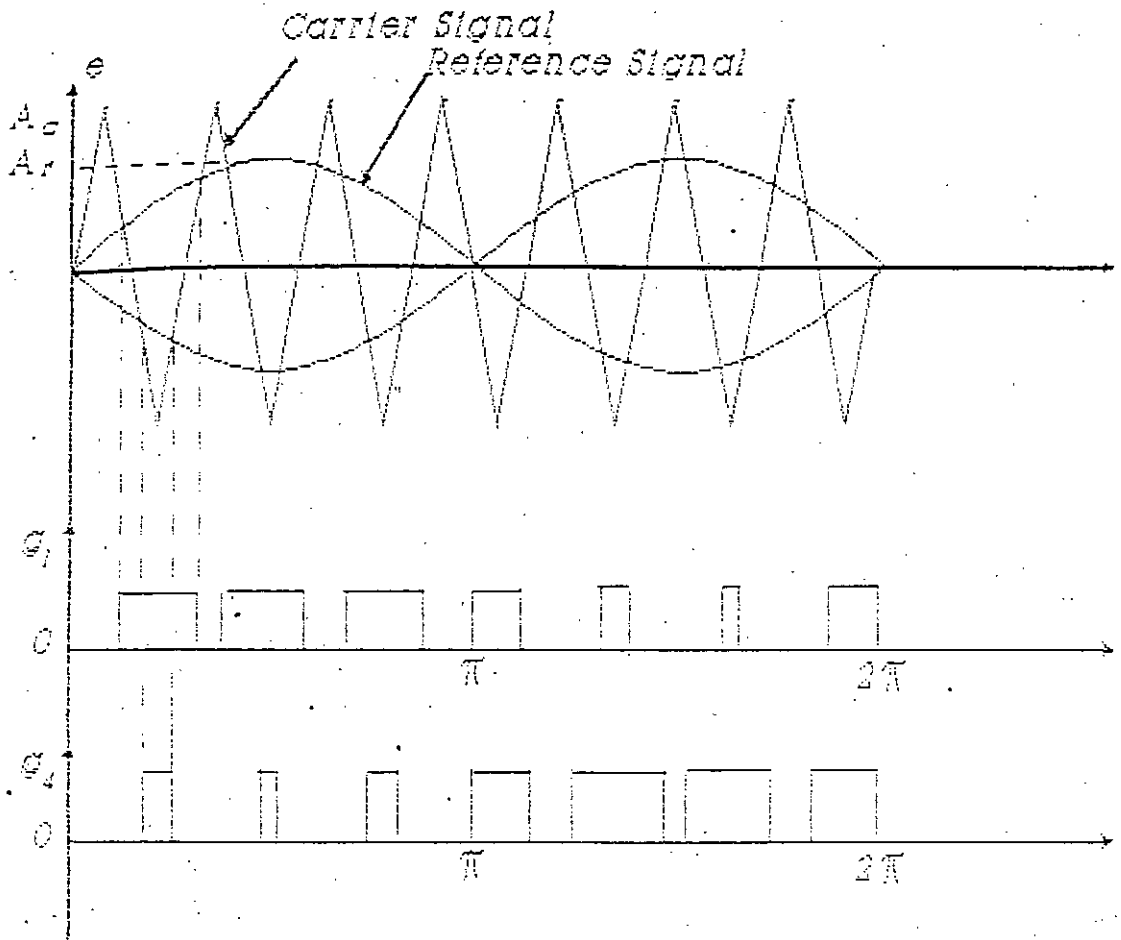


Fig. 1.3 Sinusoidal Pulse Width Modulation

wave. It is divided in specified intervals, say 20° ; each interval being controlled individually to control the magnitude of the fundamental component and to eliminate specific harmonics. This type of control gives low distortion but higher fundamental amplitude compared to that of normal PWM control. On the other hand the optimized PWM waveform do not follow well defined modulation process [25-26]. This PWM approach is based on certain performance criteria [21, 23]. As a result of the developments of microprocessor technology in recent year, the implementation of optimized pulse width modulation for switching inverters have become feasible [5, 26-27]. The technique of selected harmonic elimination, PWM has received wide attention recently. In this method the notches are created at predetermined angles of the square wave which permits voltage control as well as elimination of selected harmonics. The notch angle can be programmed so that the rms ripple current for a specified load condition is minimum.

There is another PWM scheme where the feedback current tracks the reference current wave within a hysteresis band. Two types of PWM strategies have been reported recently for inverter operation. They are bang-bang sample PWM technique and the delta modulation technique. The principle of bang-bang sampling is based on the motor output current hysteresis comparison with a reference waveform to generate the modulated waveform [26-27]. In recent years delta modulation has been finding its way for generating switching waveforms for converters [20, 25, 28]. In delta modulation a triangular wave is allowed to oscillate within a defined window above and below the reference sine wave A_r . The inverter switching function which is identical to the output voltage V_o is generated from the vertices of the triangular wave A_c as shown in figure 1.4. It is also known as hysteresis modulation. If the frequency of the modulating wave is changed keeping the slope of the triangular wave constant, the number of the pulses and the pulse width of the modulated wave would change. The delta modulation can control the ratio of the voltage to frequency of an inverter which is a desirable feature in ac motor control.

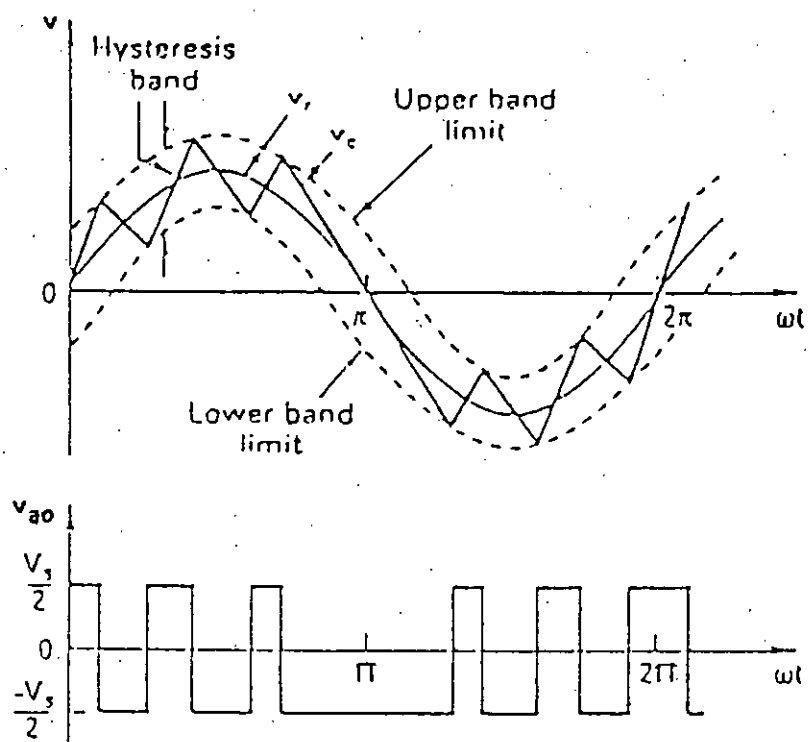


Fig. 1.4 Delta Pulse Width Modulation

1.3 CYCLOCONVERTER AND PHASE SHIFTING

Cycloconverters are the static power converters employed for the purpose of ac-ac energy transfer. It provides output of a variable frequency that is lower than or equal to the angular frequency of the source.

Figure 1.5 shows a single phase cycloconverter employing two controlled rectifiers. One rectifier handles only positive pulses, known as positive group or 'P' converter and the other handles negative pulses, known as negative or 'N' converters. Each converter supply the load for 50% of the total cycloconverter period.

During 'P' converter operation, the gating signals required for the switching devices of the converter are shown in figure 1.6. It is noted that when the switching devices of P-converter are turned ON and OFF, the switching devices of the N-converter are completely OFF. When half of the period of the cycloconverter is over all the P-converter switches are made OFF and N-converter switches are activated by the gating signals as shown in figure 1.7. As a result negative voltage is applied to the load via N-converter. Hence by alternate operation of the P-converter and N-converter an ac of desired frequency can be obtained at load side. The frequency of the cycloconverter is determined by the total duration of P and N-converters ON/OFF time. The gating signals of a phase controlled cycloconverter switches and the resultant output waveforms are shown in figure 1.8.

This type of cycloconverter are naturally commuted. If force commutation technique is used only one converter would perform the same job.

The converter can also be switched in such a manner that the output line voltage consists of a series

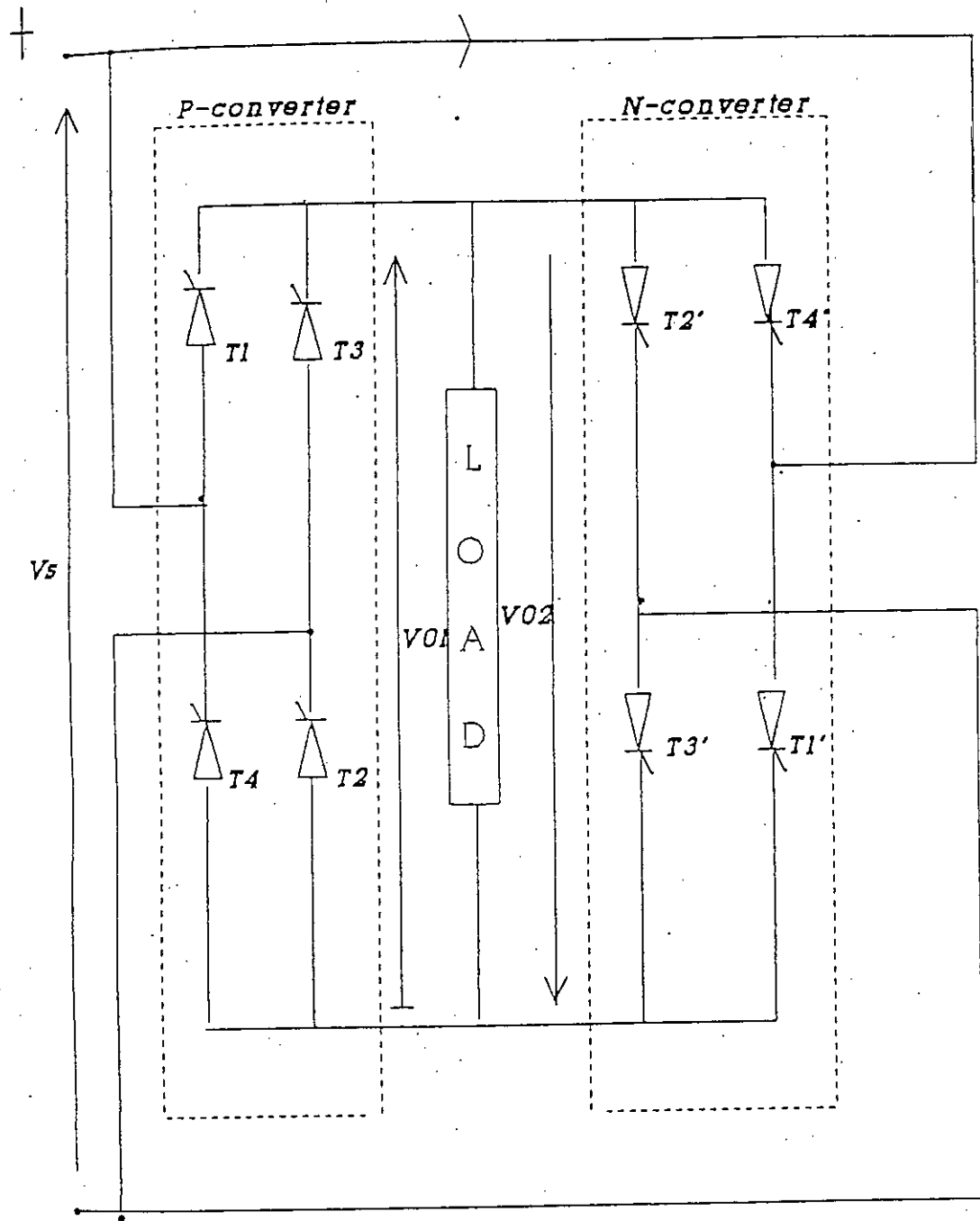


Fig. 1.5 Basic single phase cycloconverter

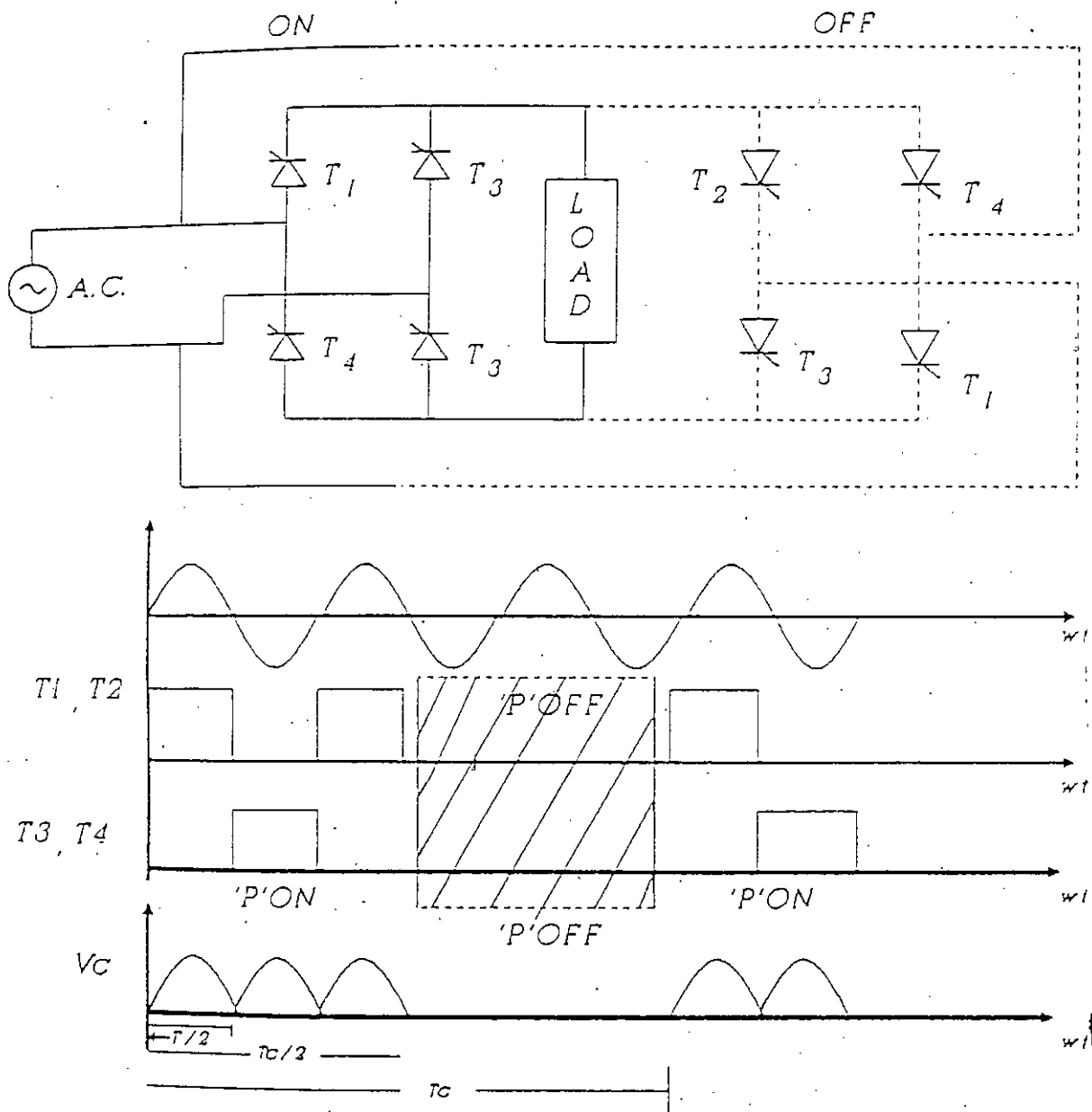


Fig. 1.6 Operation of the 'P' Converter while 'N' converter is off
 1) 'P' Converter on, 'N' Converter off
 2) Input Sine Wave
 3) Gating Signals of Switch T_1 & T_2 of 'P' Converter
 4) Gating Signals of Switch T_3 & T_4 of 'p' Converter
 5) V_c Cycloconverter Output when 'P' Converter is on
 T = Period of Sine Wave
 T_c = Period of Cycloconverter Output

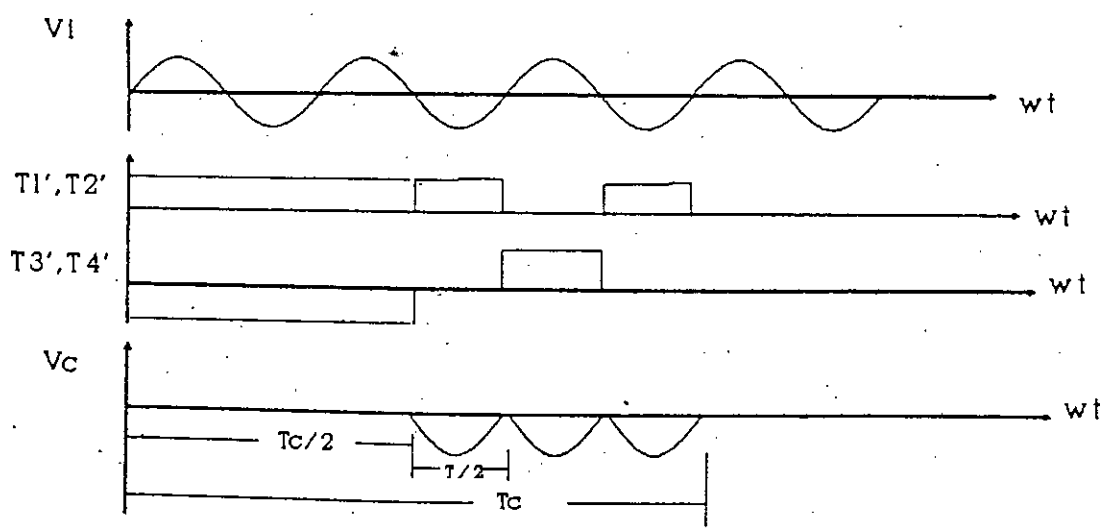
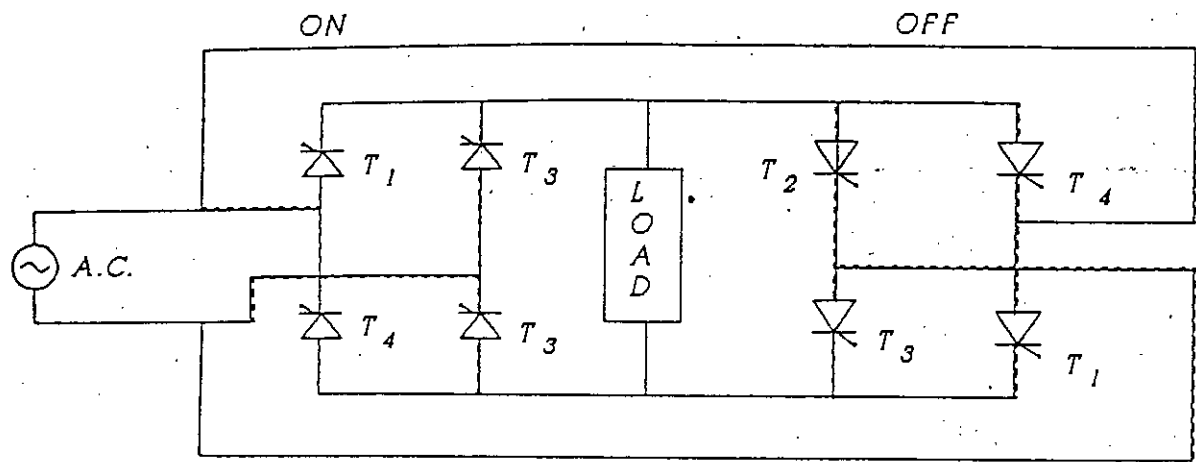


Fig. 1.7 Operation of the 'n' converter while 'p' converter is OFF.

- 1) 'n' converter ON, 'P' converter OFF
 - 2) Input sine wave
 - 3) Gating signals of switch T1'&t2' of 'n' converter
 - 4) Gating signals of switch T3'&T4 of 'n' converter
 - 5) Vc cycloconverter output when 'n' converter is ON
- T= Period of supply sinewave
Tc= period of cycloconverter output

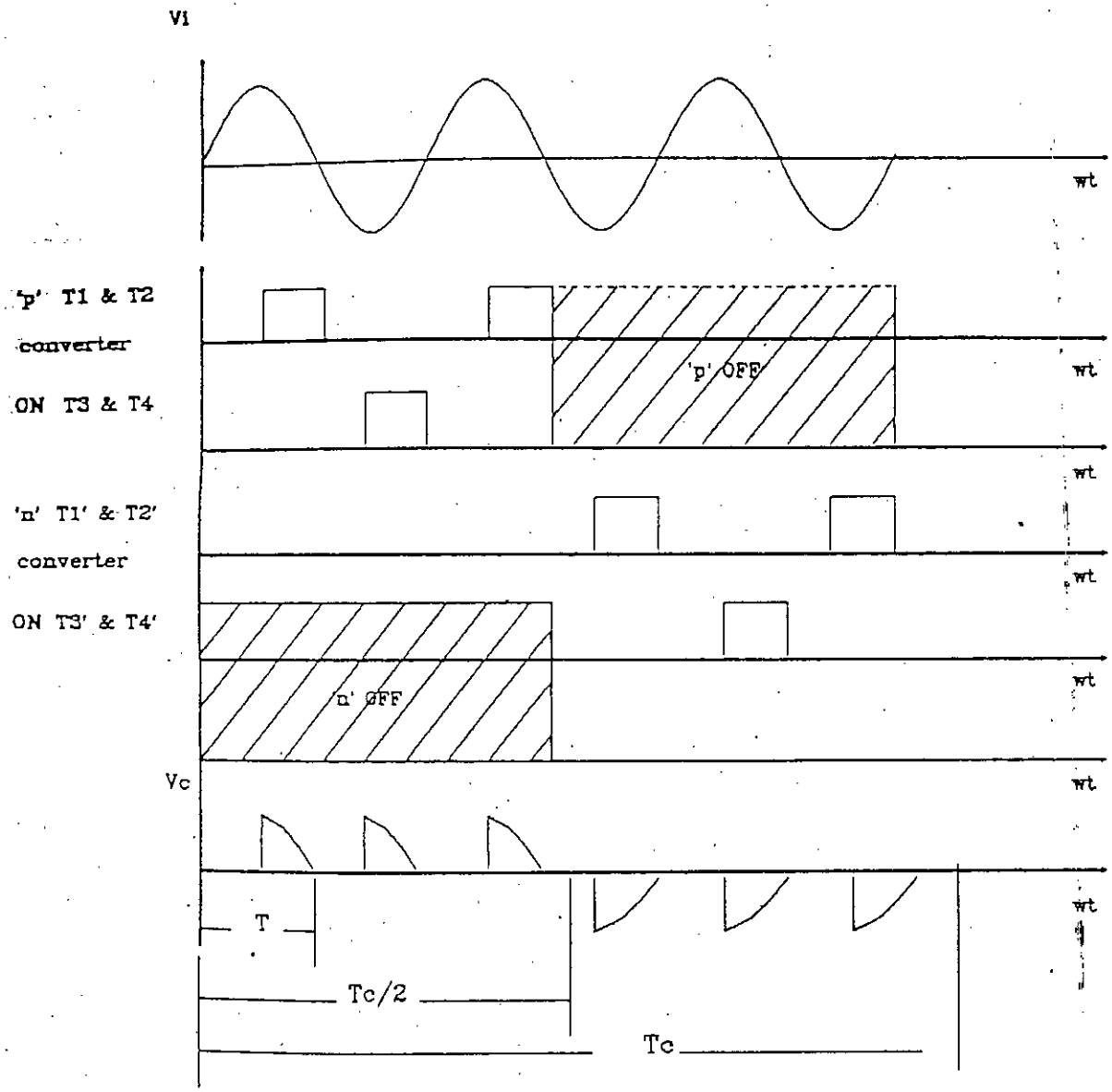


Fig. 1.8 Typical supply and the output waveforms of a single phase cycloconverter

- i) input sine wave
- ii) gating signals of T1 & T2 of 'p' converter
- iii) gating signals of T3 & T4 of 'p' converter
- iv) gating signals of T1 & T2 of 'n' converter
- v) gating signals of T3 & T4 of 'n' converter

of pulse. The pulses in the series can be arranged in such a way that the average output voltage leads to a cosine wave. This causes the phase shifting (90°) of a input sine wave. Figure 1.9 shows the phase shifted output of a sine wave

1.4 SINE PWM TECHNIQUE IN CYCLOCONVERTER

One of the major disadvantage of normal cycloconverter is its high harmonic content. Moreover, the dual control of both voltage and frequency often become inconvenient.

Among the three modulation processes used in converter control the sine pulse width modulation of Figure 1.10 is the most versatile one. In this method the switching waveform's pulse width's are sinusoidal function of each cycle. Good performance of this modulation technique depends precisely on the capability of the electronic circuitry to define accurately the switching instants of the power converters in order to cause the output of the controller to be a train of pulses with a time average that approximate a sinusoid.

Figure 1.11 illustrates the technique of SPWM waveform generation for a single phase cycloconverter. In this process the reference rectified sine wave is compared with a high frequency carrier triangular wave to produce the switching instants at the crossover of the two waveforms. The resultant waveform can be obtained by switching of input wave for desired duration to obtain the final gating signal for device switching. Output waveform's harmonic content, switching frequency and the magnitude of the output voltage can be controlled by variation of either the carrier wave frequency or the magnitude. These changes result in change in switching frequency and the pulse widths. This variation is usually measured in terms of modulation index which can be defined as the ratio of the magnitude of modulating wave to that of the carrier wave.

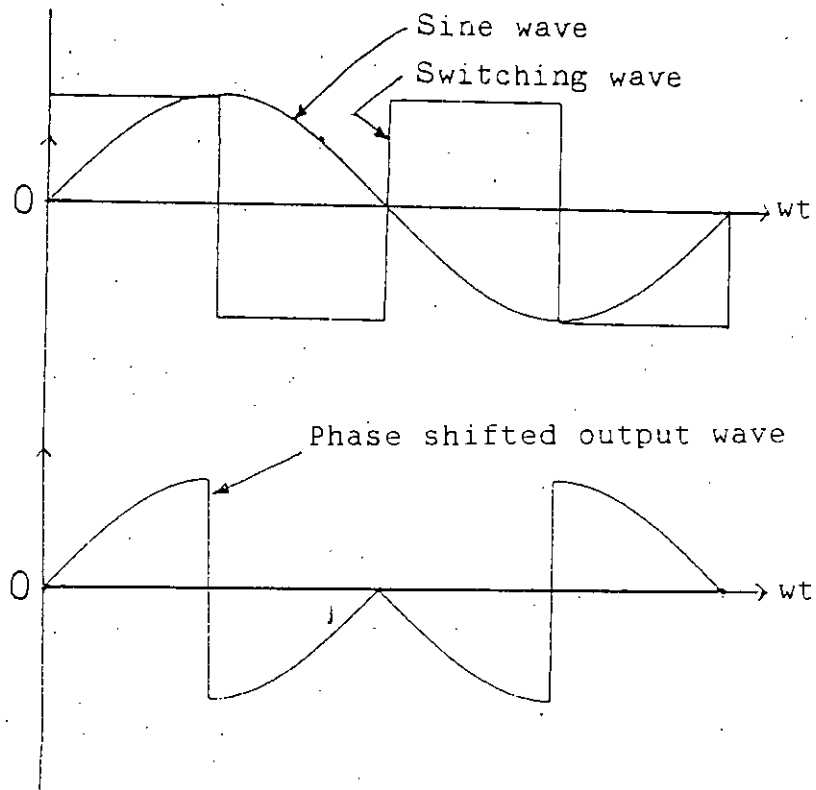


Fig. 1.9 Phase Shifted Waveform Obtained From Switching a Sine Wave By a Static Converter.

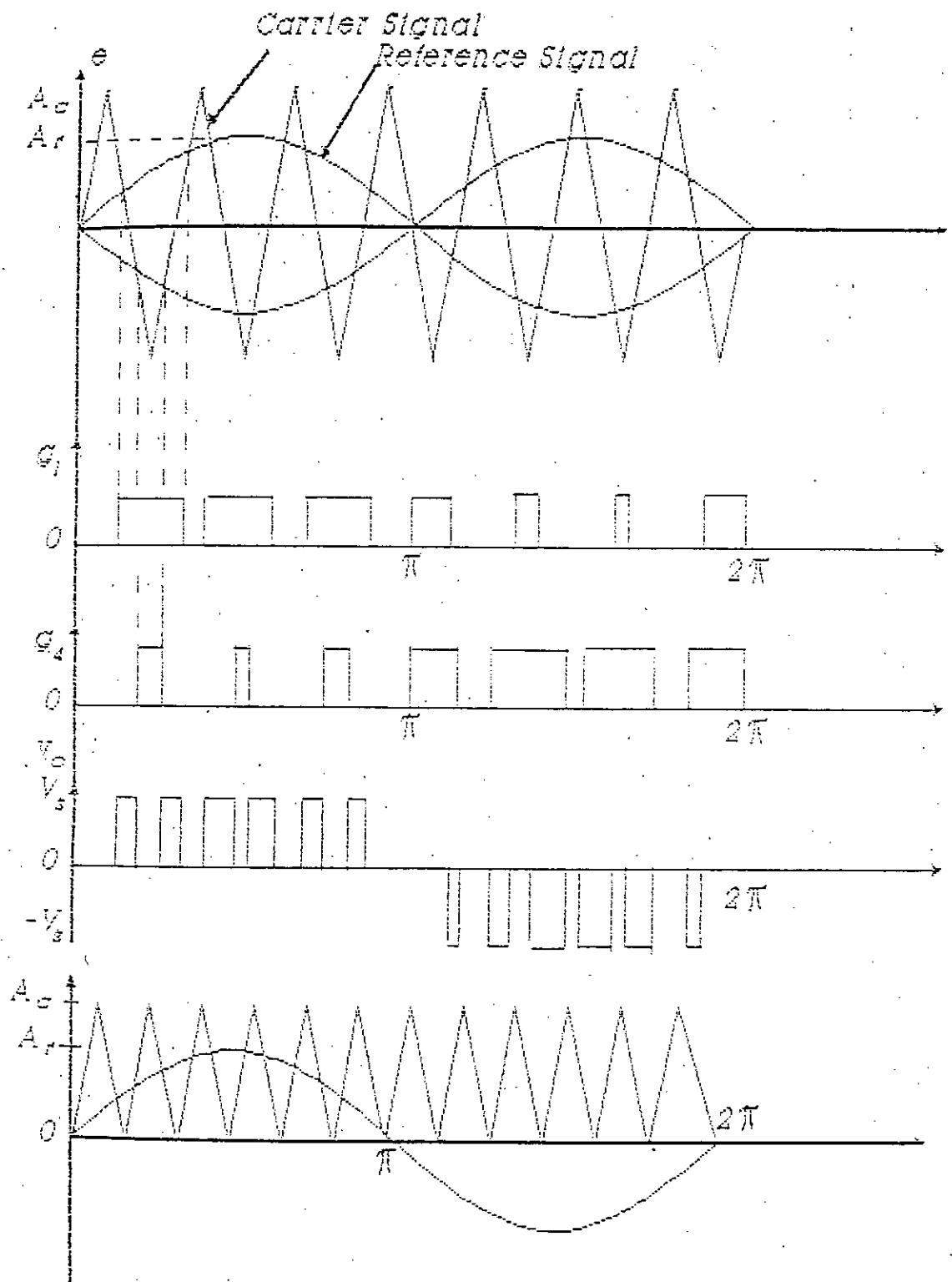


Fig. 1.10 Sinusoidal Pulse Width Modulation

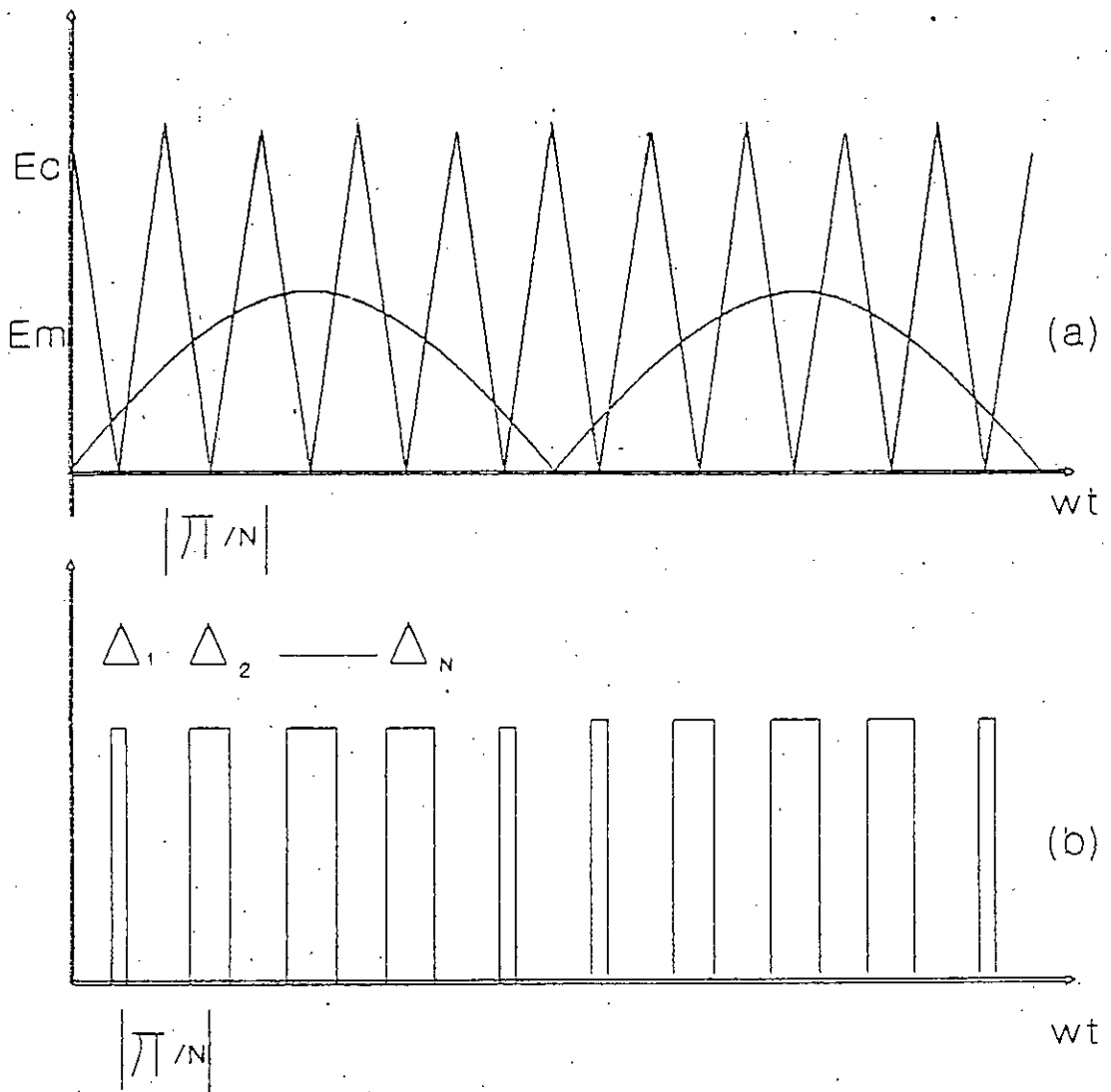


Fig. 1.11 PWM waveform generation for a single phase cycloconverter

a) Comparison between rectified sine wave with carrier triangular wave

b) Modulated wave

1.5 OBJECTIVE OF THE PRESENT WORK

Analysis and design of phase shift circuit is the main focus of this work. Several topologies of cycloconverter will be studied to develop an appropriate static phase shift circuit. PWM switching strategy will be explored to choose an appropriate switching signal for static switches of the static phase shift circuit.

Analysis will be carried out to find a suitable pulse width modulated switching strategy for the phase shift circuit. The result of the analysis will be used in the design and construction of logic circuit to build a practical phase shift circuit.

Implementation of the phase shift circuit and experimental verification of the theoretical result will be carried out in this research to substantiate the result and claims.

1.6 OUT LINE OF THE THESIS

In chapter one, an overall introduction of the work is presented. Review of some basic concepts i.e modulation technique are included in this chapter. Operation of cycloconverter is also included.

In chapter two, operation of a phase shift circuit and analysis of waveforms of phase shift circuit have been undertaken. Analysis of waveforms in time domain and spectrums in frequency domain are included in this chapter. The variation in waveforms and spectrum with the possible variation of modulation index and carrier frequency have been discussed with special emphasis on voltage variation and dominant harmonics.

Chapter three deals with the practical implementation of the proposed work. It describes the practical circuits and related specification of the devices and components which are being used to implement the circuits. It also includes the output waveforms of the practical circuit.

Chapter four contains the conclusion and recommendation of the thesis.

CHAPTER 2

ANALYSIS OF PHASE SHIFT CIRCUIT WAVE FORMS

2.1 INTRODUCTION

This chapter deals with the description of single phase, phase shift circuit and analysis of output wave forms of single phase, phase shift circuit. For the sine pulse width modulated phase shift circuit, determination of switching points from the various condition of modulation is necessary. Effort has been made in this chapter to find the switching points using simple mathematics and few acceptable assumption. Harmonic analysis of the waveform has been performed by discrete Fourier transform. Discrete Fourier Transform (DFT) software are readily available these days. A commercial software (MATLAB) [8] has been used for evaluation of DFT of output waveform of single phase SPWM phase shift circuit

The result thus obtain are used to decide which combination of modulation index and carrier frequency can practically be used to obtain high performance output voltage waveform.

2.2.1 SINGLE PHASE STATIC PHASE SHIFT CIRCUIT

The phase shift circuit means the output waveform of this circuit will be 90° apart from the input waveform of the circuit.

Five topologies of proposed phase shift circuit are shown in figure 2.1 to 2.4 . The gating signals of the static devices of the converters for each topology are shown in the corresponding figure, which can be used to switch supply voltage at every quarter cycle. In the figure 2.2, when switch S_1 (A,D) and S_2 (A,D) are closed for a first quarter cycle, the output waveform of Figure 2.5 is obtained, and when switch S_3 (B,C) and S_4 (B,C) are closed for next two quarter cycle the output is obtained as shown in Figure 2.6. After a full cycle switching the output waveform will look like as shown in Figure 2.7.

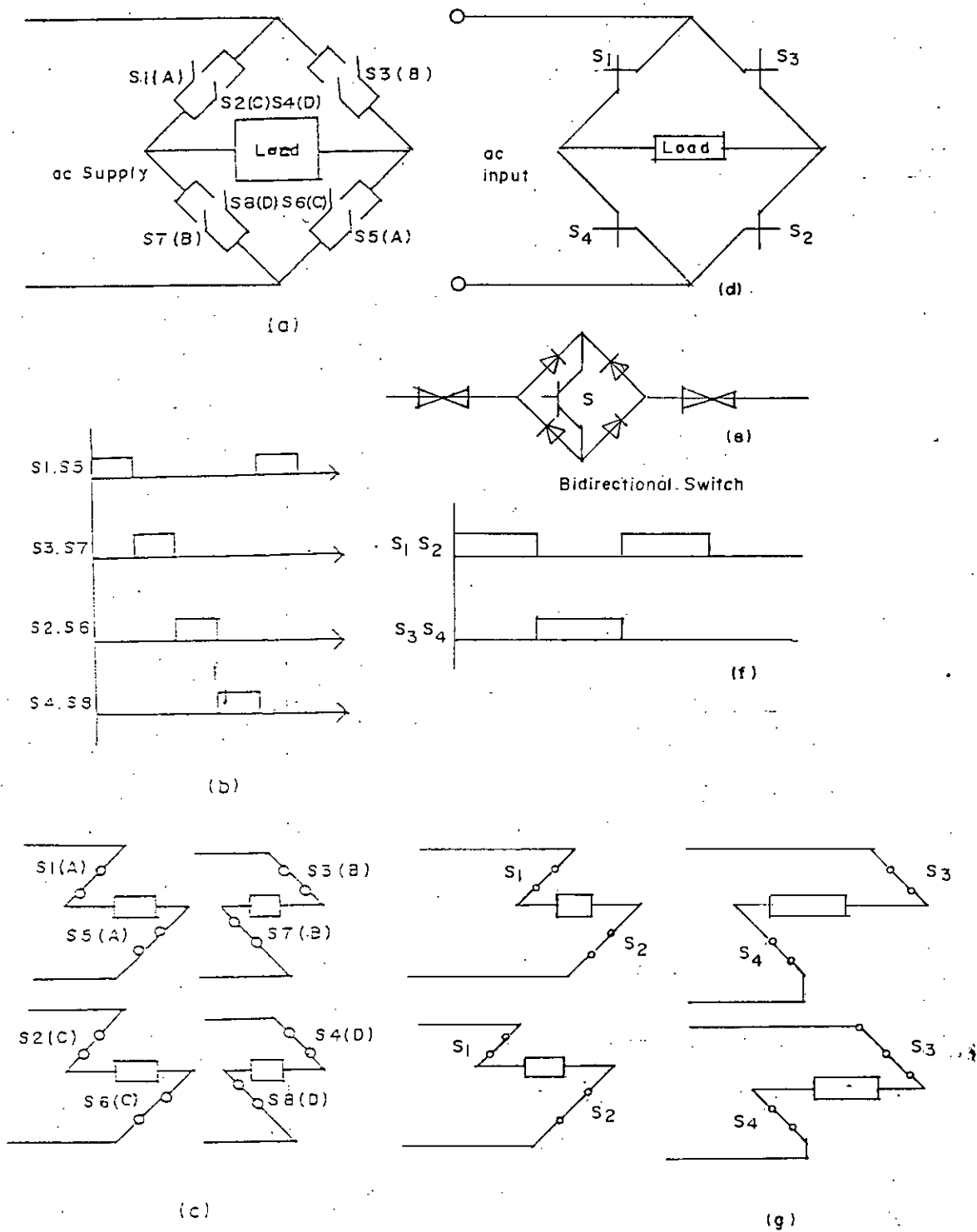
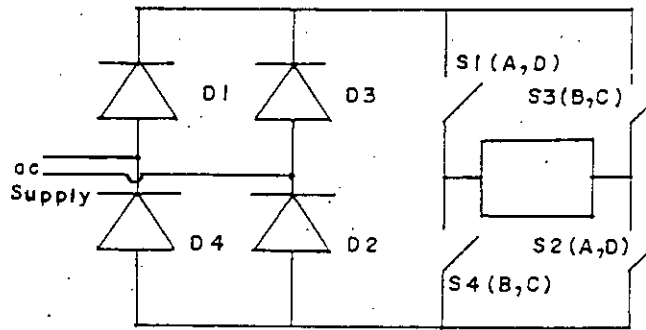
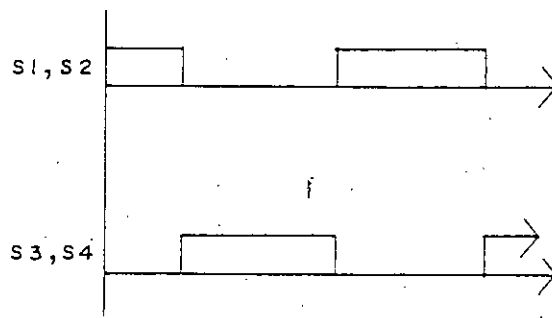


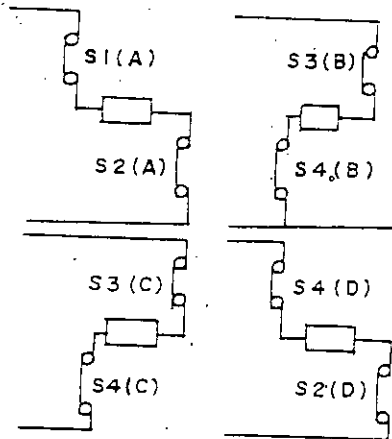
Fig. 2.1 Pasche Shift Circuit Topology I & II
 a & d The Topology
 b & f The Gatting Sgnals
 c & g Different Paths



(a)

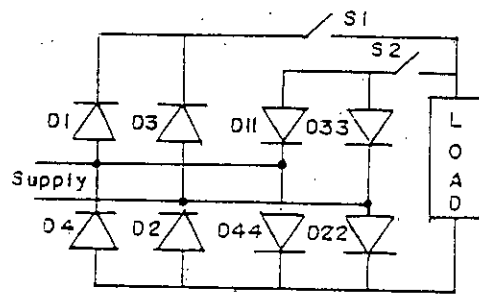


(b)

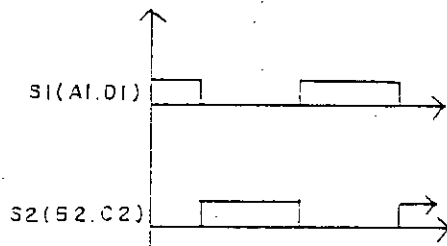


(c)

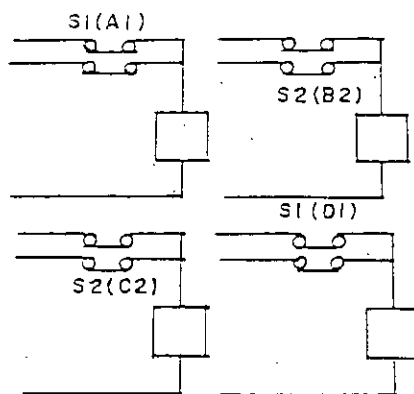
Fig. 2.2 Pashe Shift Circuit Topology III
 a). The Topology
 b). The Gating Signals
 c). Different Paths



(a)

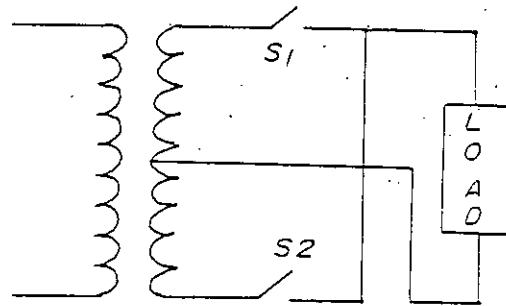


(b)

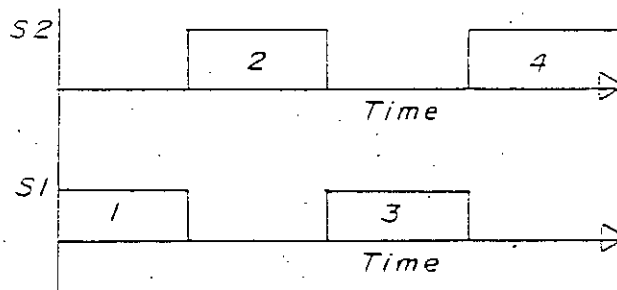


(c)

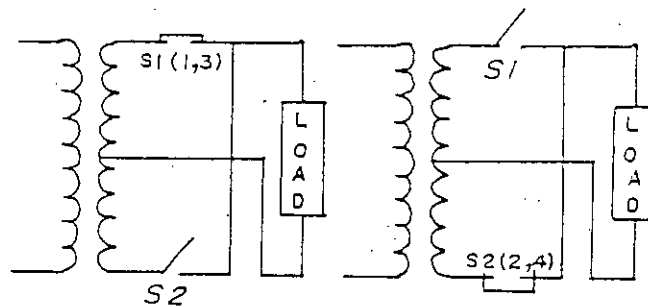
Fig. 2.3 Pasche Shift Circuit Topology IV
 a). The Topology
 b). The Gating Signals
 c). Different Paths



(a)



(b)



(c)

Fig. 2.4 Pashe Shift Circuit Topology V
 a). The Topology
 b). The Gating Signals
 c). Different Paths

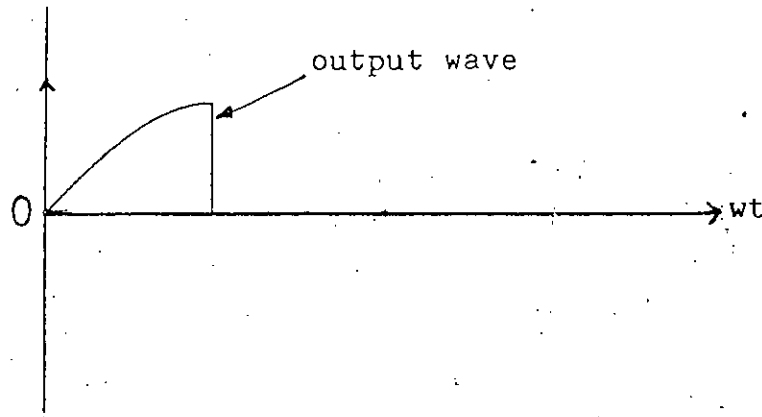


Fig. 2.5 Output after 1st Quarter Cycle

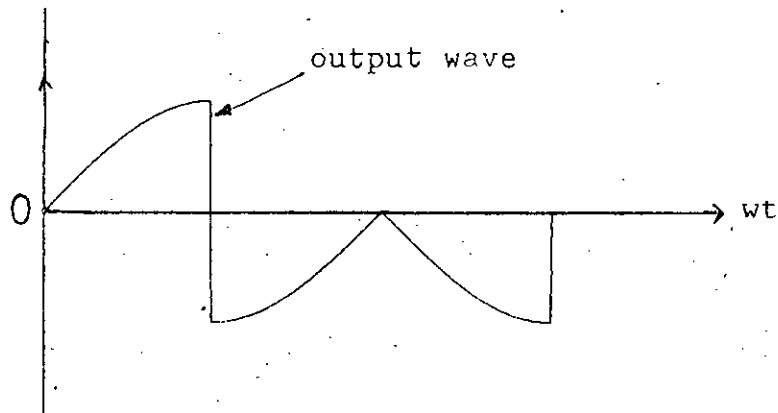


Fig. 2.6 Output after 3rd Quarter Cycle

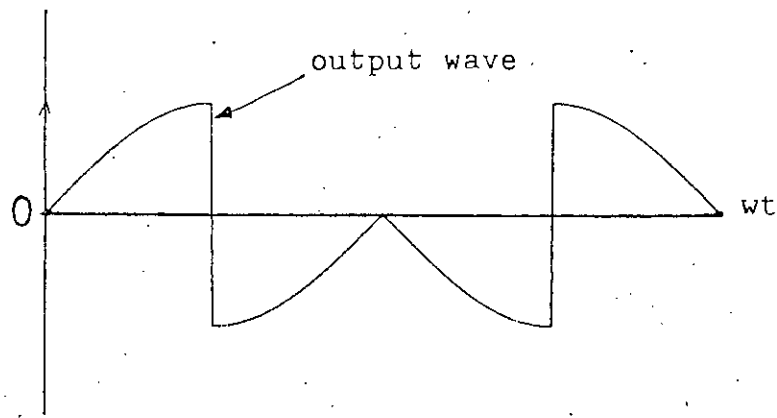


Fig. 2.7 Output of Full Cycle Operation.

For circuits of Figure 2.1, 2.3 and 2.4 the conduction of switches as gating signals are applied are shown in respective figures to give same output waveform. In Figure 2.1 the switching devices can be replaced by bidirectional switches to reduce the number of switching elements. The gating circuit of such a circuit is shown in Figure 2.1(f).

The output waveform in figure 2.7 is 90° phase shifted from the input waveform and can be used for starting single phase induction motors.

2.2.2 WAVEFORM ANALYSIS OF SINGLE PHASE STATIC PHASE SHIFT CIRCUIT

Figure 2.7 shows the output waveform of a single phase, phase shift circuit, which is a product of two waveforms shown in figure 2.8 and figure 2.9.

We can find out the $s(t)$ by Fourier series, T_s is the period of $s(t)$ and it's a odd function. So the Fourier coefficient;

$$\begin{aligned}
 b_n &= \frac{4}{T_s} \int_0^{\frac{T_s}{2}} s(t) \sin \frac{2n\pi t}{T_s} dt \\
 &= \frac{4}{T_s} \int_0^{\frac{T_s}{2}} \sin \frac{2n\pi t}{T_s} dt \quad (\text{Magnitude of } s(t) \text{ consider as unity}) \\
 &= \frac{4}{T_s} \cdot \left[-\frac{T_s}{2n\pi} \cos \frac{2n\pi t}{T_s} \right]_0^{\frac{T_s}{2}} \\
 &= \frac{2}{n\pi} [1 - \cos n\pi] = \frac{4}{n\pi} \quad \text{where } n = 1, 3, 5, \dots
 \end{aligned}$$

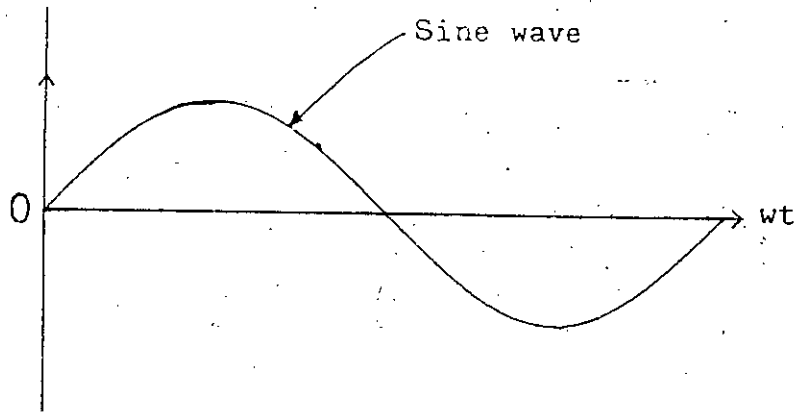


Fig. 2.8 Sine Wave

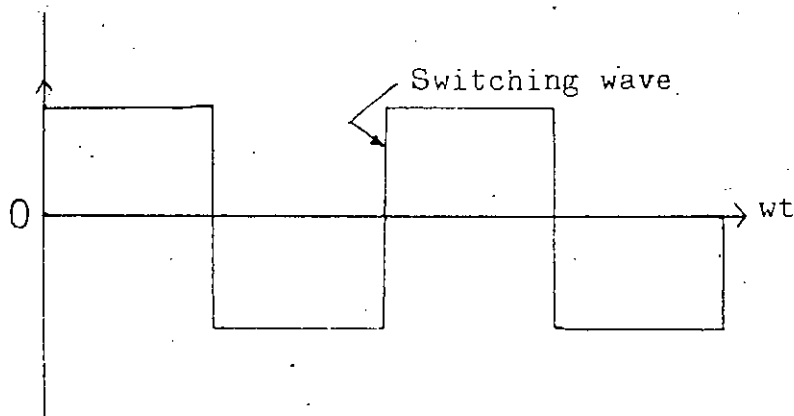


Fig. 2.9 Switching Wave

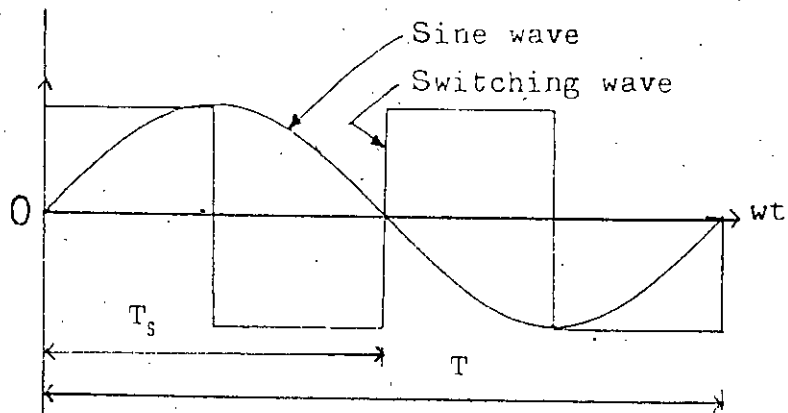


Fig. 2.10 Sine Wave and Switching wave

$$s(t) = \frac{4}{\pi} \sum_{n=1,3,5,\dots}^{\infty} \frac{\sin n\omega_s t}{n} \quad \text{where } \omega_s = 2\pi f_s = 2\omega$$

$$= \frac{4}{\pi} \sum_{n=1,3,5,\dots}^{\infty} \frac{\sin 2n\omega t}{n}$$

$$f(t) = V_m \sin \omega t$$

The phase shift output voltage

$$v_o = f(t)s(t) = \frac{4V_m}{\pi} \sum_{n=1,3,5,\dots}^{\infty} \frac{\sin \omega t \sin 2n\omega t}{n}$$

$$= \frac{2V_m}{\pi} \sum_{n=1,3,5,\dots}^{\infty} \frac{2\sin \omega t \sin 2n\omega t}{n}$$

$$= \frac{2V_m}{\pi} \sum_{n=1,3,5,\dots}^{\infty} \frac{\cos (2n - 1)\omega t - \cos (2n + 1)\omega t}{n}$$

$$= \frac{2V_m}{\pi} (\cos \omega t - \cos 3\omega t + \frac{1}{3} \cos 5\omega t - \frac{1}{3} \cos 7\omega t + \frac{1}{5} \cos 9\omega t - \dots)$$

It is evident from the above expression that the low order harmonics of the phase shift circuit converter output is considerably high. The third harmonic is equal to the magnitude of the fundamental component and other harmonics are also high.

Harmonics contents are tabulated in table 2.1.

Order of harmonics	Harmonics contents in p.u	Order of harmonics	Harmonics contents in p.u
1	0.637	15	-0.090
3	-0.637	17	0.070
5	0.212	19	-0.070
7	-0.212	21	0.057
9	0.127	23	-0.057
11	-0.127	25	0.047
13	0.090	27	-0.047

Table 2.1 Harmonic contents of phase shift output waveform.

To reduce low order harmonics from the output waveform PWM switching technique is to be applied.

2.3 MODULATED STATIC SINGLE PHASE, PHASE SHIFT CIRCUIT

To reduce low order harmonic from the output waveform, PWM switching of converters is used. To obtain Fourier series of the modulated output waveform, it is necessary to determine switching points and different switching functions [2] so as to define output waveform in terms of switching points and switching function . The following steps were used in defining the modulated output waveforms in terms of switching points and switching functions.

$s_i(t)$ = switching Function

$$= g(t, t_0, t_1) - g(t, t_1, t_2) + g(t, t_2, t_3)$$

Where

$g(t, t_0, t_1)$ = gate function starting at 0 and ending at $t_1 = \pi/2$

$g(t, t_1, t_2)$ = gate function starting at $\pi/2$ and ending at $t_2 = 3\pi/2$

$g(t, t_2, t_3)$ = gate function starting at $3\pi/2$ and ending at $t_3 = 2\pi$

$m(t)$ = modulated waveform obtained by the comparison of modulating sine wave with a carrier triangular wave.

$$m(t) = \sum_{i=1,2,3}^N g(t, t_{2i-1}, t_{2i})$$

where

$g(t, t_{2i-1}, t_{2i})$ = gate function starting at t_i and ending at t_{i+1} . t_i and t_{i+1} are switching points of the modulated wave.

If $v_i = V_m \sin\theta$ is the input sine wave to the static converter, phase shifted waveform v_s and modulated phase shifted waveform v_{ms} can be obtained as

$$v_s = v_i s_1(t) \text{ and } v_{ms} = v_s m(t)$$

The modulated phase shifted waveform can then be processed by package programs [8] to obtain the fourier spectrum. A typical result of the above mentioned method is shown in figure 2.11.

2.4 ANALYSIS OF SINE PULSE WIDTH MODULATED WAVES

To analyze the sine pulse width modulated waves, it is important to find the switching point of the modulating wave so that the waveforms can be defined in terms of switching point. The modulated wave switching points are determined by the fact that whenever the carrier triangular wave crosses

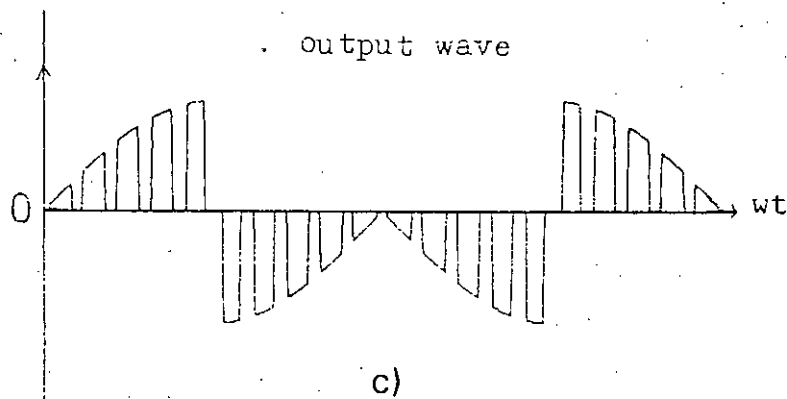
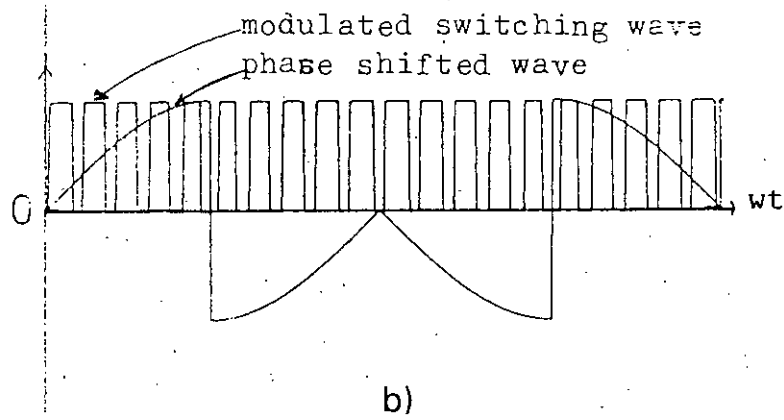
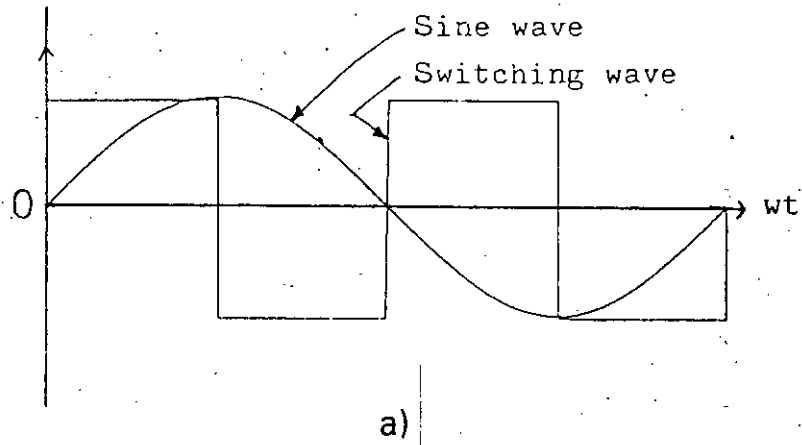


Fig. 2.11 Modulated Output of the Phase Shift circuit
 a) sine wave and switching wave
 b) modulate switching wave and phase shifted wave
 c) modulated phase shifted wave

the reference rectified sine modulating wave, a pulse is produced and its duration is as long as the carrier wave's magnitude remains higher than the modulating wave.

Let

N = number of modulating pulses for each half cycle

δ_i = pulse width of the i th pulse

= π/N = distance between successive pulses

A_r = maximum magnitude of modulating rectified sine wave

A_c = maximum magnitude of the carrier triangular wave

θ_i = mid location of i th pulse

$m = A_r/A_c$ = modulating index

The modulating process ensures the following

$$\delta_i \propto e$$

$$\delta_i \propto \frac{1}{A_c}$$

Where e is the modulating wave and α is the sine of proportionality

$$e = A_r \sin \theta_i$$

$$= mA_c \sin \theta_i$$

$$\text{but } \theta_i = \frac{2i - 1}{N} \pi$$

$$e = mA_c \sin \frac{2i - 1}{N} \pi$$

From the condition $\delta_i \propto e$ and $\delta_i \propto 1/A_c$ we can write

$$\delta_i = K \frac{e}{A_c}$$

Which can be written as

$$\begin{aligned} \delta_i &= \frac{KA_r}{A_c} \sin \frac{2i - 1}{N} \pi \\ &= Km \sin \frac{2i - 1}{N} \pi \end{aligned}$$

which shows, when number of pulses are kept constant pulse widths vary with modulation index. When modulating index is kept constant, pulse widths vary as a sinusoidal function of pulse number N. Once the pulse widths of all the pulses in the half cycle can be found by the above the expression, the waveform can be represented in terms of the pulse widths. For example, the pulse position can be written as;

$$\frac{\pi}{N} - \frac{\delta_1}{2} \text{ is the first rising edge}$$

$$\frac{\pi}{N} + \frac{\delta_1}{2} \text{ is the first falling edge}$$

$$\frac{3\pi}{2N} - \frac{\delta_2}{2} \text{ is the 2nd rising edge}$$

$\frac{3\pi}{2N} + \frac{\delta_2}{2}$ is the 2nd falling edge

In general the i th rising edge is

$$\theta_{i,r} = \frac{2i - 1}{2N} \pi - \frac{\delta_i}{2}$$

and the i th falling edge is

$$\theta_{i,d} = \frac{2i - 1}{2N} \pi + \frac{\delta_i}{2}$$

These expressions can also be obtained in time domain and can be used for waveform construction and Fourier series or Fourier transform analysis.

In the derivation involving interaction between sinusoidal and triangular wave, the proportionality constant K is given by π/N [29]

In this thesis, however, the modulated signal was simulated by using two sinusoidal waves i.e triangular wave is considered as sine wave. Let the modulating signal be expressed as;

$$f_m(t) = A_r \sin \omega_m t$$

and the carrier signal be expressed as;

$$f_c(t) = A_c \sin N\omega_m t \quad \text{where } f_c = Nf_m$$

To find out the cross over points of the above two signals, we have to solve the equation;

$$f_m(t) - f_c(t) = 0$$

$$A_r \sin \omega_m t - A_c \sin N\omega_m t = 0$$

$$\sin \omega_m t = \frac{A_r}{A_c} \sin N\omega_m t$$

$$\sin 2\pi f_m t = \frac{1}{m} \sin 2\pi N f_m t$$

For $m = A_r/A_c$ and $f_c = Nf_m =$ certain value will give switching point t_1, t_2, \dots and we have solved this equation for up to $t = T/4$.

The switching points were found by this equation solved in a commercially available software package known as MATLAB [8].

2.5 ANALYSIS OF SINGLE PULSE MODULATED PHASE SHIFT CIRCUIT WAVEFORM

Analysis of the single pulse modulated single phase static phase shift circuit waveform shown in figure 2.12 is as below,

Fourier coefficient

$$b_n = \frac{2}{T_s} \int_0^{T_s} s(t) \sin \frac{2n\pi}{T_s} t dt$$

$$= \frac{2}{T_s} \int_{\alpha}^{\frac{T_s}{2} - \alpha} \sin \frac{2n\pi}{T_s} t dt - \frac{2}{T_s} \int_{\frac{T_s}{2} + \alpha}^{T_s} \sin \frac{2n\pi}{T_s} t dt$$

$$= -\frac{2}{T_s} \cdot \frac{T_s}{2n\pi} \left[\cos \frac{2n\pi}{T_s} t \right]_{\alpha}^{\frac{T_s}{2} - \alpha} + \frac{2}{T_s} \cdot \frac{T_s}{2n\pi} \left[\cos \frac{2n\pi}{T_s} t \right]_{\frac{T_s}{2} + \alpha}^{T_s}$$

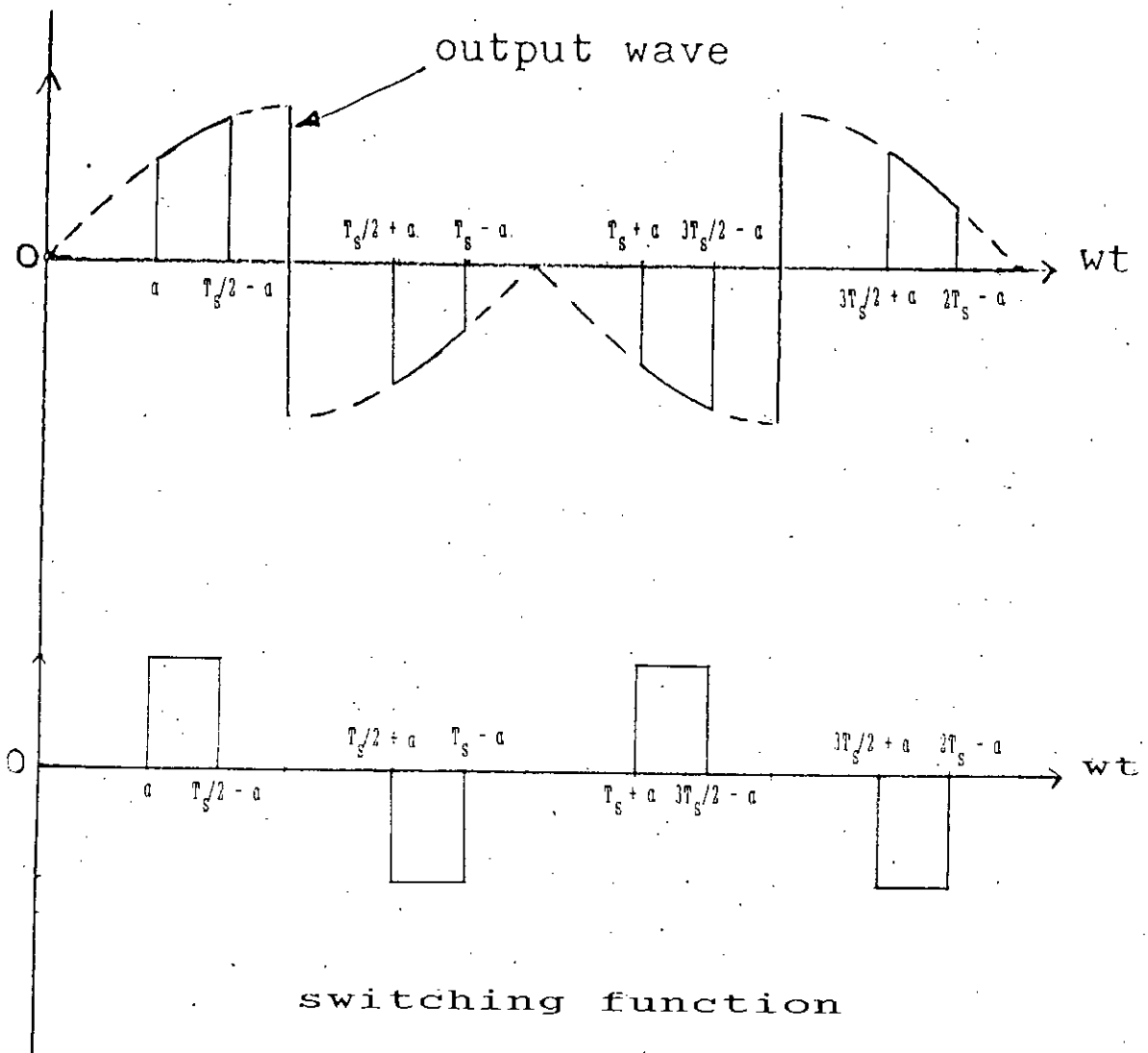


Fig. 2.12 Analysis of the Waveform

$$\begin{aligned}
&= -\frac{1}{n\pi} \left[\cos \frac{2n\pi}{T_s} t \right]_{\alpha}^{\frac{T_s}{2} - \alpha} + \frac{1}{n\pi} \left[\cos \frac{2n\pi}{T_s} t \right]_{\frac{T_s}{2} + \alpha}^{T_s - \alpha} \\
&= \frac{1}{n\pi} \left[\cos \frac{2n\pi}{T_s} \alpha - \cos \left(n\pi - \frac{2n\pi}{T_s} \alpha \right) \right] + \frac{1}{n\pi} \left[\cos \left(2n\pi - \frac{2n\pi}{T_s} \alpha \right) \right. \\
&\quad \left. - \cos \left(n\pi + \frac{2n\pi}{T_s} \alpha \right) \right] \\
&= \frac{1}{n\pi} \left[\cos \frac{2n\pi}{T_s} \alpha - \cos n\pi \cos \frac{2n\pi}{T_s} \alpha - \sin n\pi \sin \frac{2n\pi}{T_s} \alpha \right] \\
&\quad + \frac{1}{n\pi} \left[\cos \frac{2n\pi}{T_s} \alpha - \cos n\pi \cos \frac{2n\pi}{T_s} \alpha - \sin n\pi \sin \frac{2n\pi}{T_s} \alpha \right] \\
&= \frac{1}{n\pi} \left[2 \cos \frac{2n\pi}{T_s} \alpha - 2 \cos n\pi \cos \frac{2n\pi}{T_s} \alpha \right] \\
&= \frac{2}{n\pi} \left[\cos n\omega_s \alpha (1 - \cos n\pi) \right] \\
&= \frac{4}{n\pi} \cos n\omega_s \alpha \quad \text{where } n = 1, 3, 5, \dots
\end{aligned}$$

Switching function $s(t)$ can be express as:

$$\begin{aligned}
s(t) &= \sum_{n=1, 2, 3, \dots}^{\infty} \frac{4}{n\pi} \cos n\omega_s \alpha \sin n\omega_s t \\
&= \sum_{n=1, 2, 3, \dots}^{\infty} \frac{4}{n\pi} \cos 2n\omega \alpha \sin 2n\omega t \quad \text{where } \omega_s = 2\omega
\end{aligned}$$

So the modulated static phase shifted output would be

$$\begin{aligned}
 v_{mo}(t) &= \sum_{n=1, 2, 3..}^{\alpha} \frac{4}{n\pi} \cos 2n\alpha_T \sin 2n\theta \sin \theta \quad \text{where } \omega\alpha = \alpha_T, \omega t = \theta \\
 &= \sum_{n=1, 2, 3..}^{\alpha} \frac{4}{n\pi} \cos 2n\alpha_T \cdot \frac{1}{2} [\cos (2n - 1)\theta - \cos (2n + 1)\theta] \\
 &= \frac{2}{\pi} \cos 2\omega\alpha \cos \theta - \frac{2}{\pi} \cos 2\omega\alpha \cos 3\theta + \frac{2}{3\pi} \cos 6\omega\alpha \cos 5\theta - \dots
 \end{aligned}$$

Which shows that third harmonic does not reduce and other harmonic also considerably high.

Computations have been done by using MATLAB software for different modulation index and carrier frequency for sine PWM switched phase shift circuit which are shown in the following pages

2.6 OBSERVATIONS

A series of Fourier analysis of sine pulse width modulated wave and the single phase, phase shift circuit output voltage has been done. In the analysis modulating index m was varied from .5 to 1.3 and carrier frequency f_c was varied from 450 Hz to 850 Hz. From Figure 2.13 & 2.14 it is evident that dominant harmonics of sine PWM wave shift to higher frequency near carrier frequency, whereas, From Figure 2.17 to figure 2.18 indicates that fundamental voltage of sine PWM increases with increase of modulation index. This observation is as expected and the variation of carrier frequency and the modulation index are presented in details in the form of Figures in Appendix-I.

Some results are expected for the phase shifted modulated output waveforms. The behaviour of the modulated phase shifted waveforms were obtained as shown in Figure 2.19 to 2.24. Harmonics near

carrier frequency shift with the change of carrier frequency as evident in Figure 2.20 and 2.21 and the magnitude of the fundamental wave increases with the increase of modulation index. Though low order harmonics, specially the 3rd, 5th, 7th etc are lower than the output wave of unmodulated phase shift circuit, their magnitudes are still comparatively high. This situation improves if over modulation is applied to the modulation circuit and the effect of over modulation is evident in Figure 2.23 and 2.24.

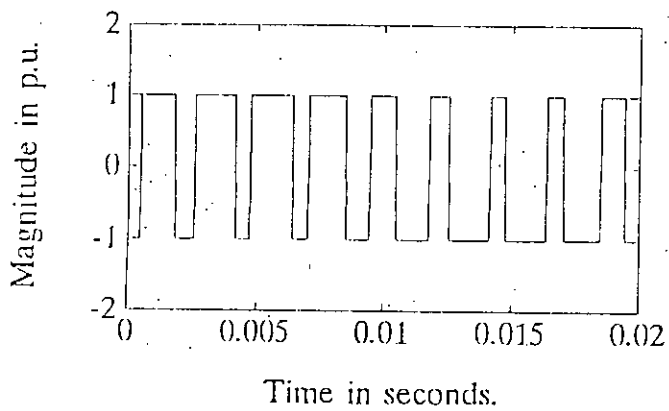
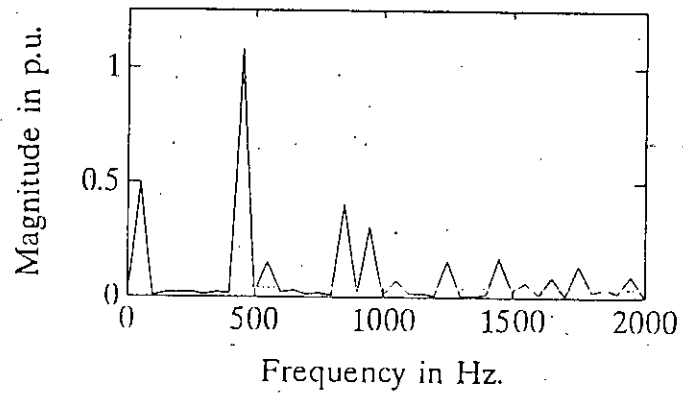
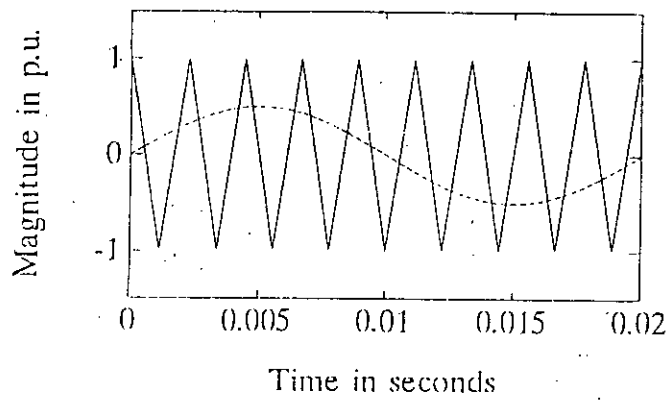


Fig. 2.13 Waveform of SPWM at Modulation Index $m = .5$
 and Carrier Frequency $f_c = 450$ Hz
 a) Reference and Carrier Wave
 b) Frequency Spectrum
 c) Switching Function

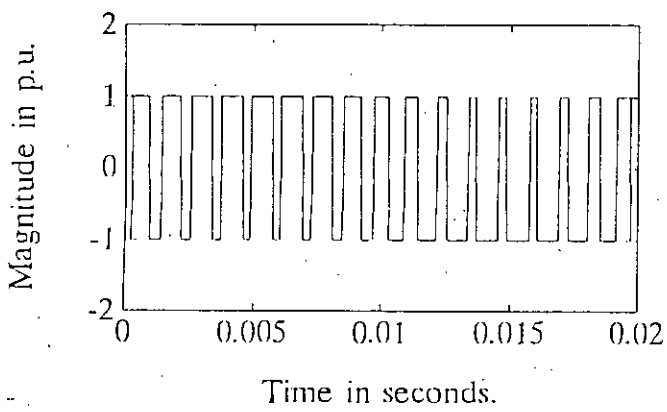
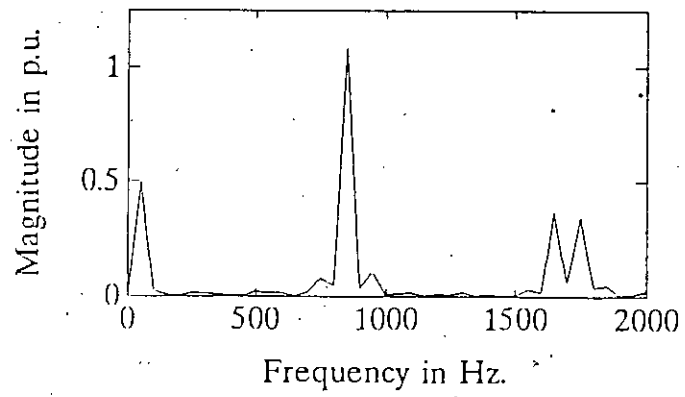
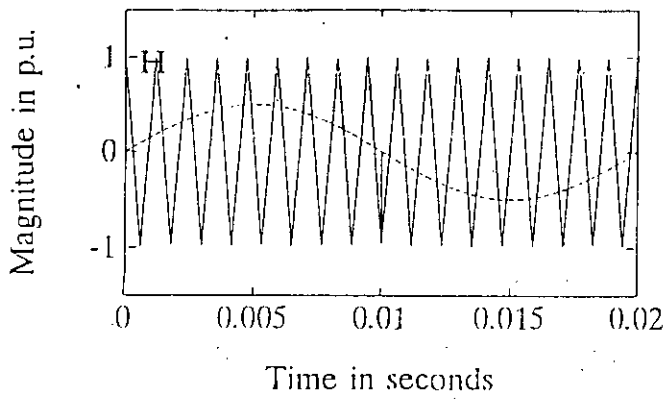


Fig. 2.14 Waveform of SPWM at Modulation Index $m = .5$ and Carrier Frequency $f_c = 850$ Hz
 a) Reference and Carrier Wave
 b) Frequency Spectrum
 c) Switching Function.

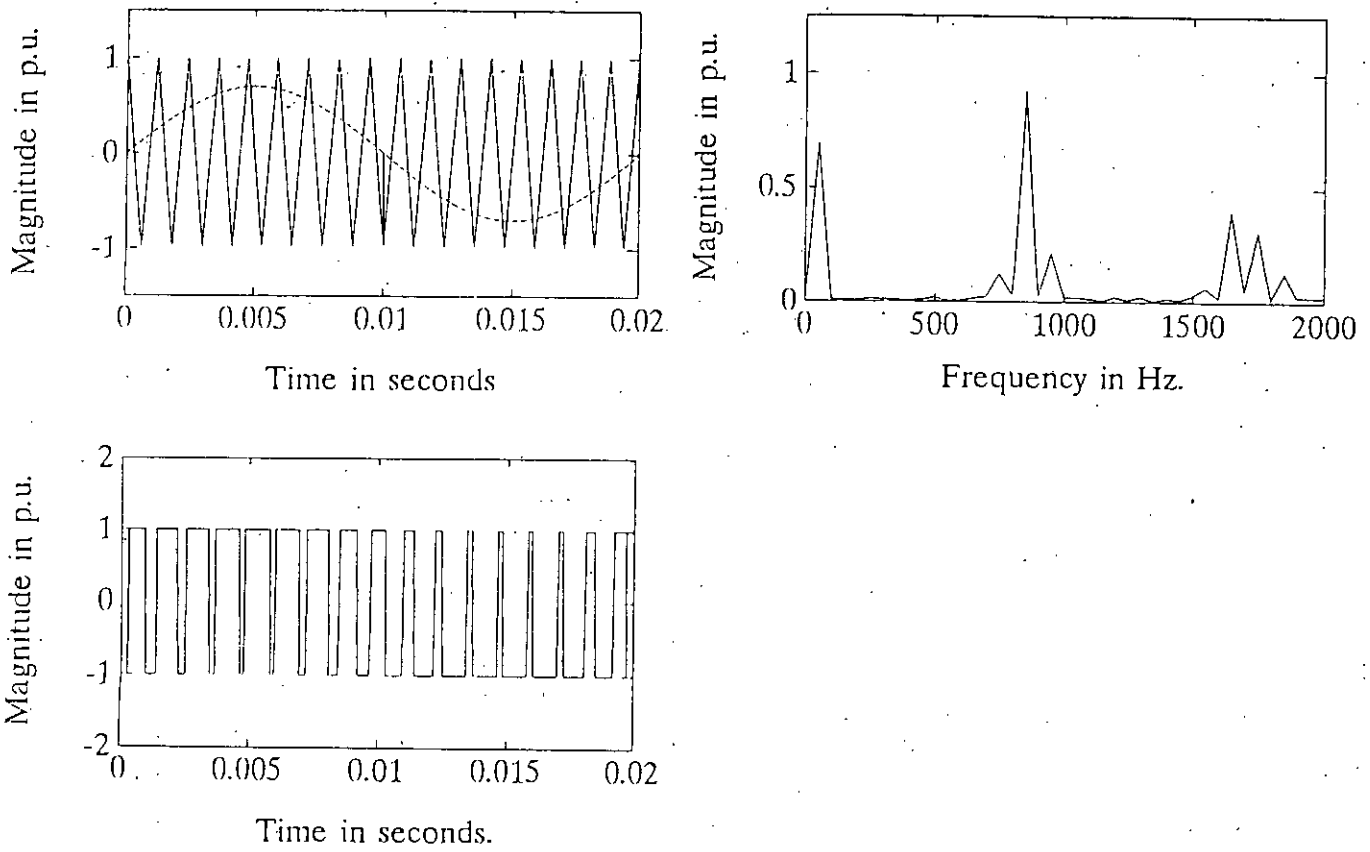


Fig. 2.15 Waveform of SPWM at Modulation Index $m = .7$ and Carrier Frequency $f_c = 850$ Hz
 a) Reference and Carrier Wave
 b) Frequency Spectrum
 c) Switching Function

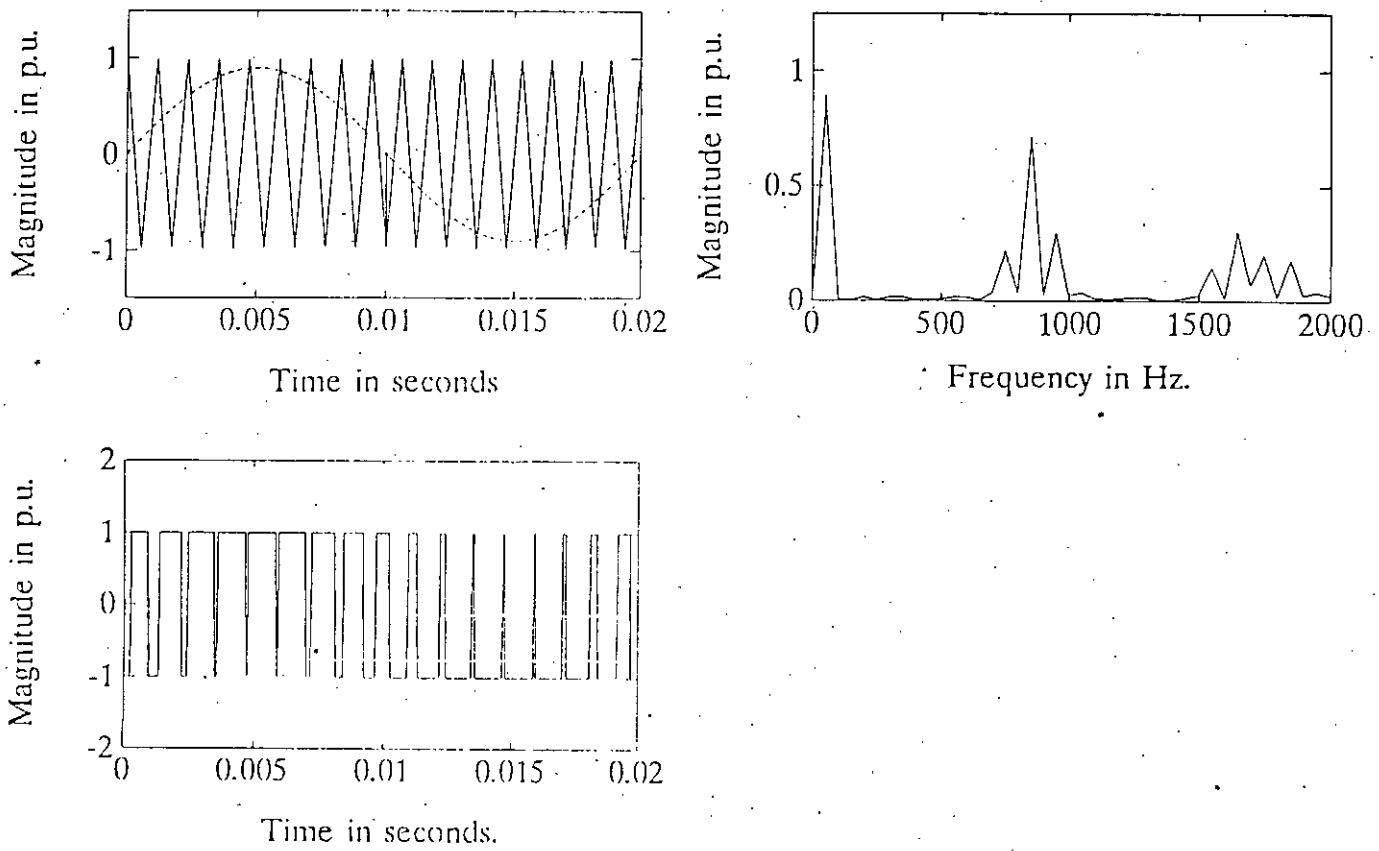


Fig. 2.16 Waveform of SPWM at Modulation Index $m = .9$ and Carrier Frequency $f_c = 850$ Hz
 a) Reference and Carrier Wave
 b) Frequency Spectrum
 c) Switching Function

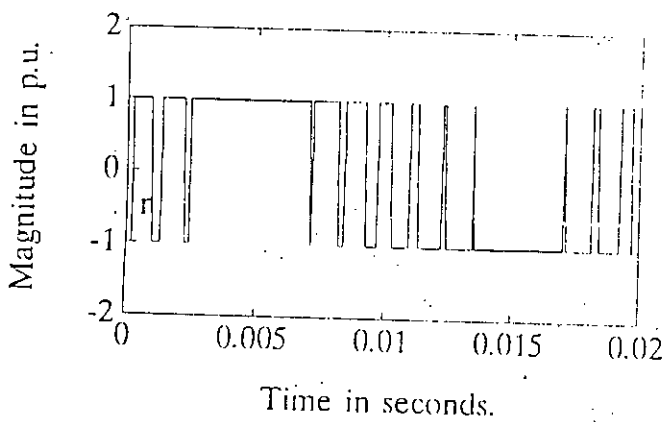
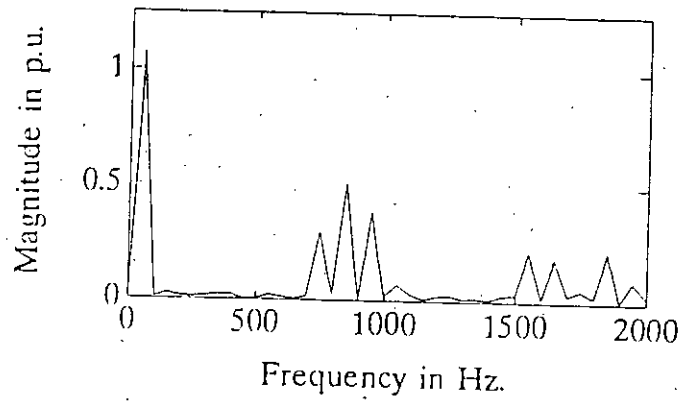
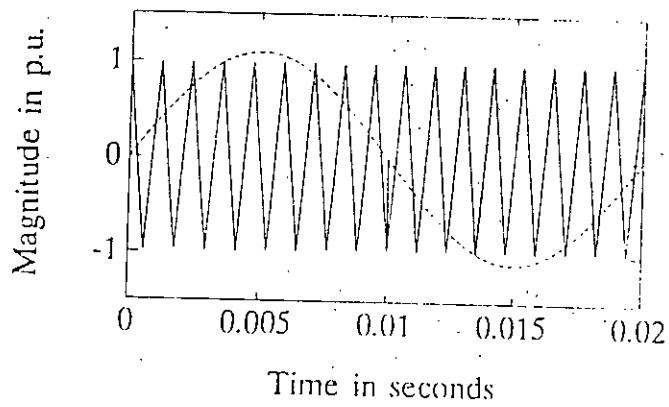


Fig. 2.17 Waveform of SPWM at Modulation Index $m = 1.1$ and Carrier Frequency $f_c = 850$ Hz
 a) Reference and Carrier Wave
 b) Frequency Spectrum
 c) Switching Function

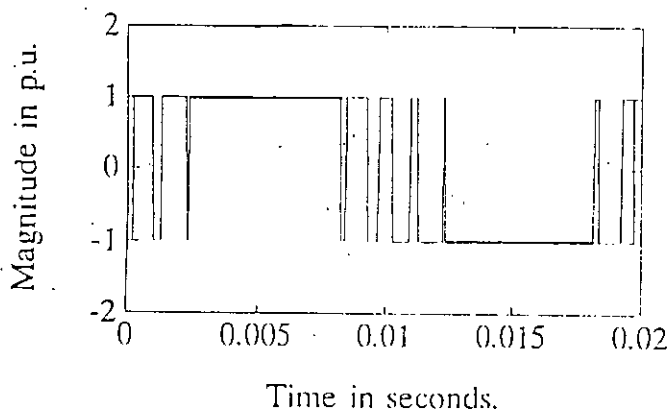
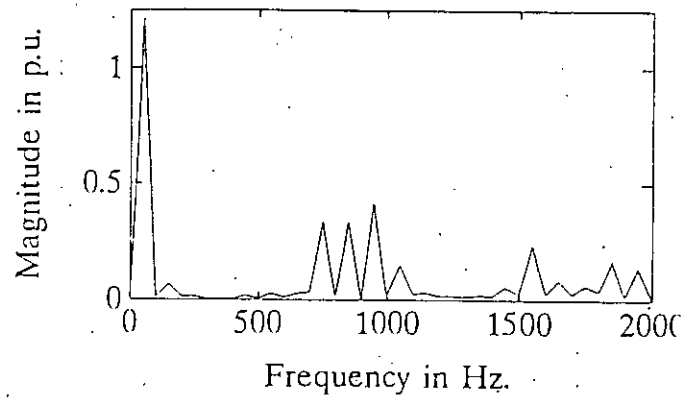
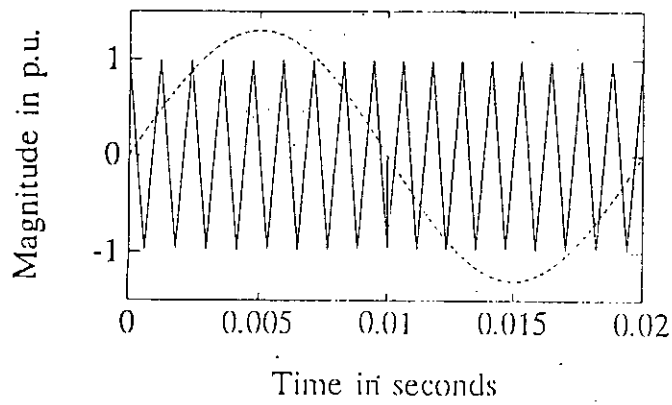


Fig. 2.18 Waveform of SPWM at Modulation Index $m = 1.3$ and Carrier Frequency $f_c = 850$ Hz
 a) Reference and Carrier Wave
 b) Frequency Spectrum
 c) Switching Function

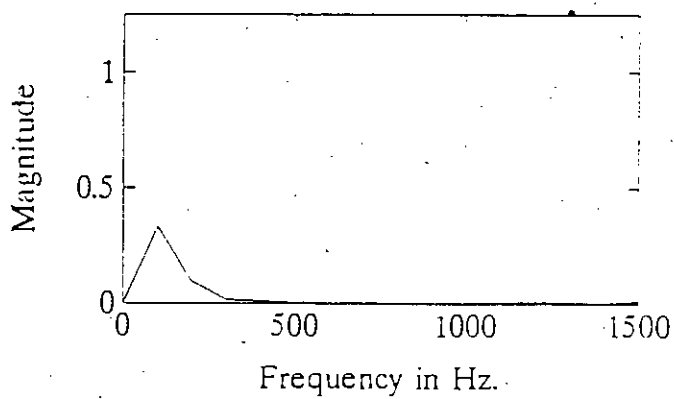
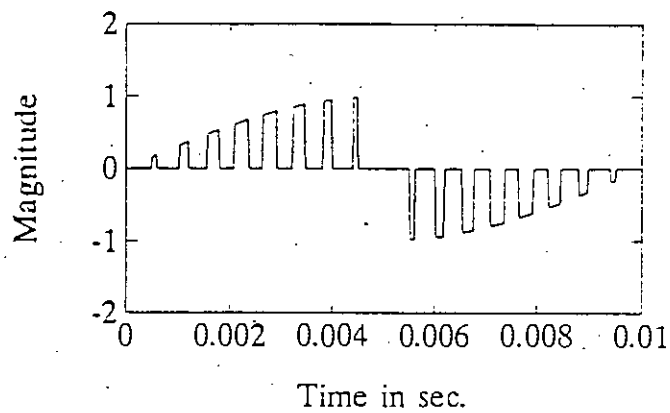


Fig. 2.19 Modulated Waveform of Phase Shift Circuit at Modulation Index $m = .5$ and Number of Pulse/Quarter Cycle $N = 9$
 a) Modulated Output
 b) Frequency Spectrum

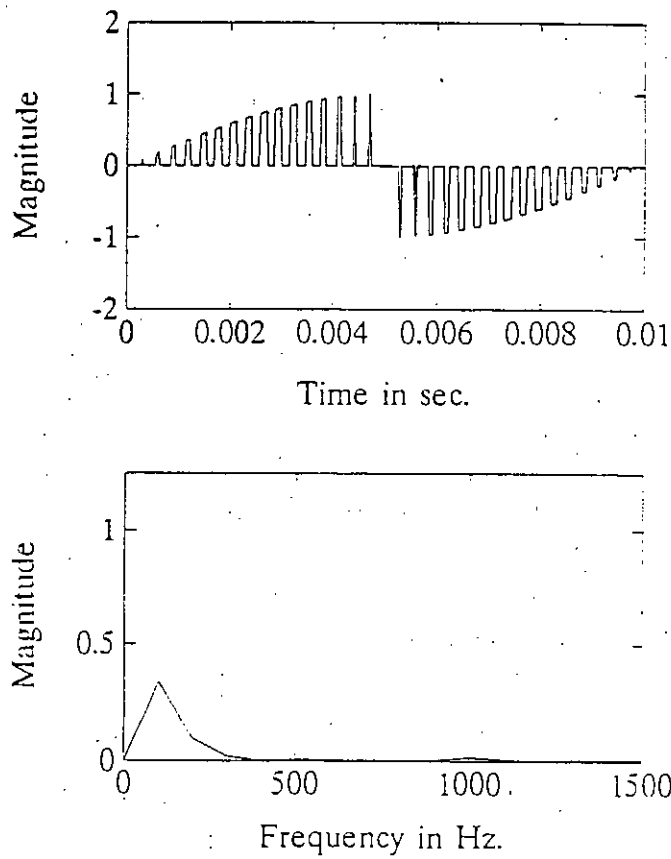


Fig. 2.20 Modulated Waveform of Phase Shift Circuit at Modulation Index $m = .5$ and Number of Pulse/Quarter Cycle $N = 17$
 a) Modulated Output
 b) Frequency Spectrum

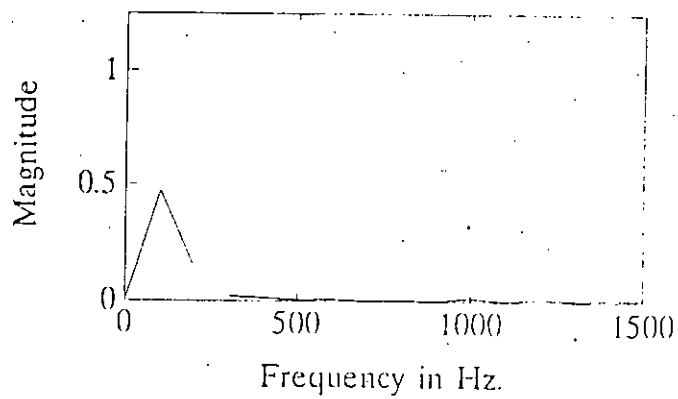
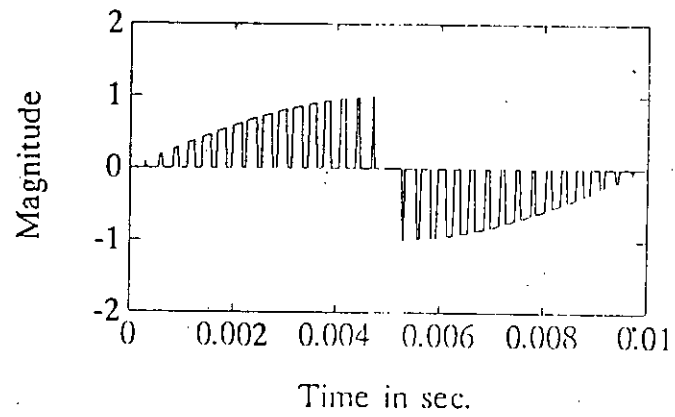


Fig. 2.21 Modulated Waveform of Phase Shift Circuit at Modulation Index $m = .7$ and Number of Pulse/Quarter Cycle $N = 17$
 a) Modulated Output
 b) Frequency Spectrum

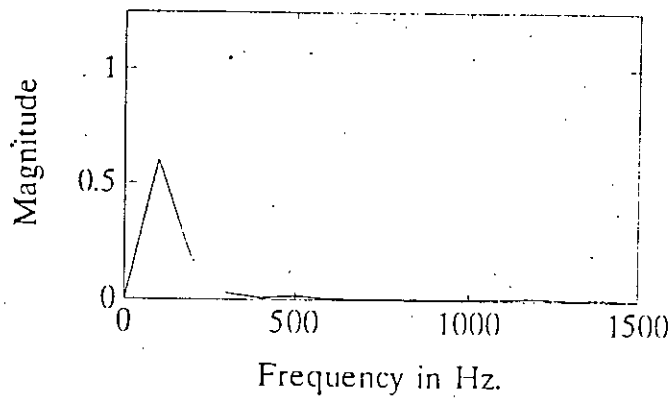
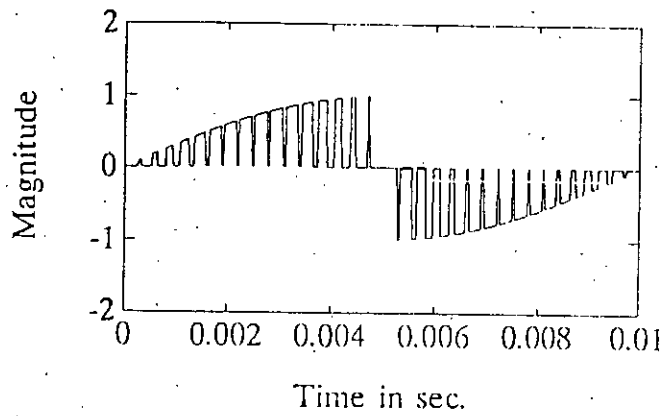


Fig. 2.22 Modulated Waveform of Phase Shift Circuit at Modulation Index $m = .9$ and Number of Pulse/Quarter Cycle $N = 17$
 a) Modulated Output
 b) Frequency Spectrum

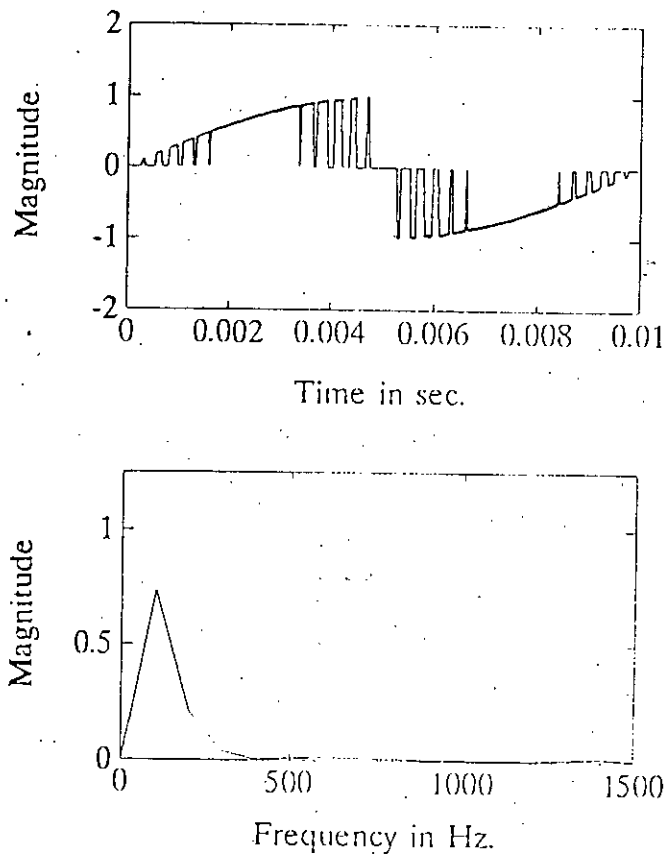


Fig. 2.23 Modulated Waveform of Phase Shift Circuit at Modulation Index $m = 1.1$ and Number of Pulse/Quarter Cycle $N = 17$
 a) Modulated Output
 b) Frequency Spectrum

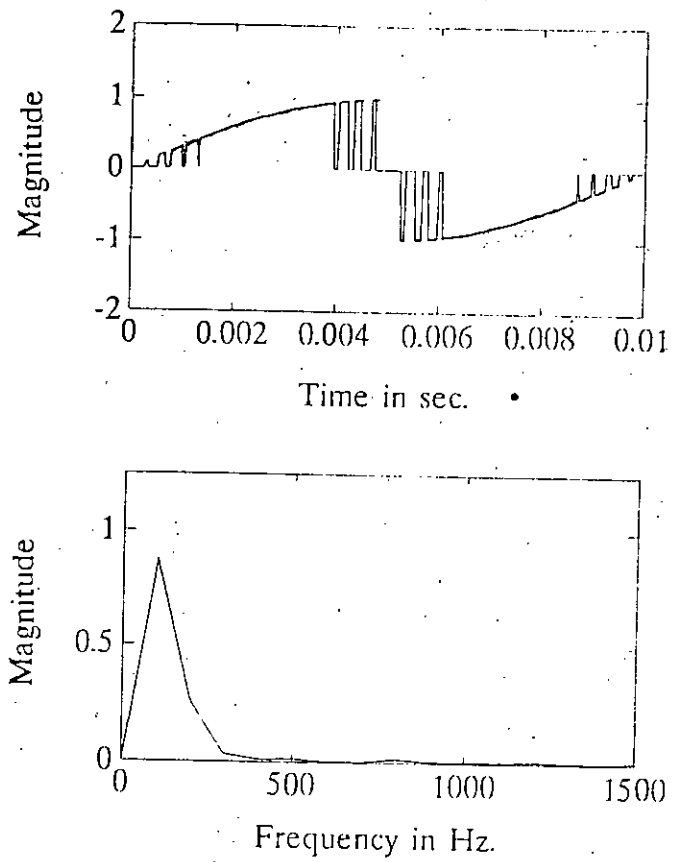


Fig. 2.24 Modulated Waveform of Phase Shift Circuit at Modulation Index $m = 1.3$ and Number of Pulse/Quarter Cycle $N = 17$
 a) Modulated Output
 b) Frequency Spectrum

CHAPTER 3

PRACTICAL IMPLEMENTATION

3.1 INTRODUCTION

To demonstrate the practicability of the single phase, phase shift circuit, an experiment was set up and successful operation of the single phase, phase shift circuit was performed. In this chapter details of the experimental circuits are discussed with the results obtained from the operation of the phase shift circuit.

3.2 PRACTICAL CONVERTER CIRCUIT

The practical converter is shown in figure 3.1. The circuit consists of a bridge rectifier, four MOSFET (IRF840), four optocoupler connected to the gate of the MOSFETs and a load resistor of 2 kilo ohms, 5 watt rating.

Pulsating unidirectional AC voltage comes from the bridge rectifier and the MOSFET switches were switched every 90° through isolation optocoupler (4N25) to obtain desired output at the load. To isolate the gates of the MOSFETs, three power supply units having separate grounds were used.

3.3 PRACTICAL MODULATOR CIRCUIT

The modulator circuit consist of a 566 timer based triangular wave generator, a rectifier with a step down transformer, a comparator operational amplifier LM741 and a MOSFET switch with an optocoupler at the gate and two buffer stage or isolation stage. To avoid loading effect of the different parts of the modulator circuit, a number of isolation stage comprising high input impedance buffers were used. Operational amplifier LM741 circuit served this purpose. This configuration provides a high impedance in one side and low impedance in the other side. Figure 3.2 shows the

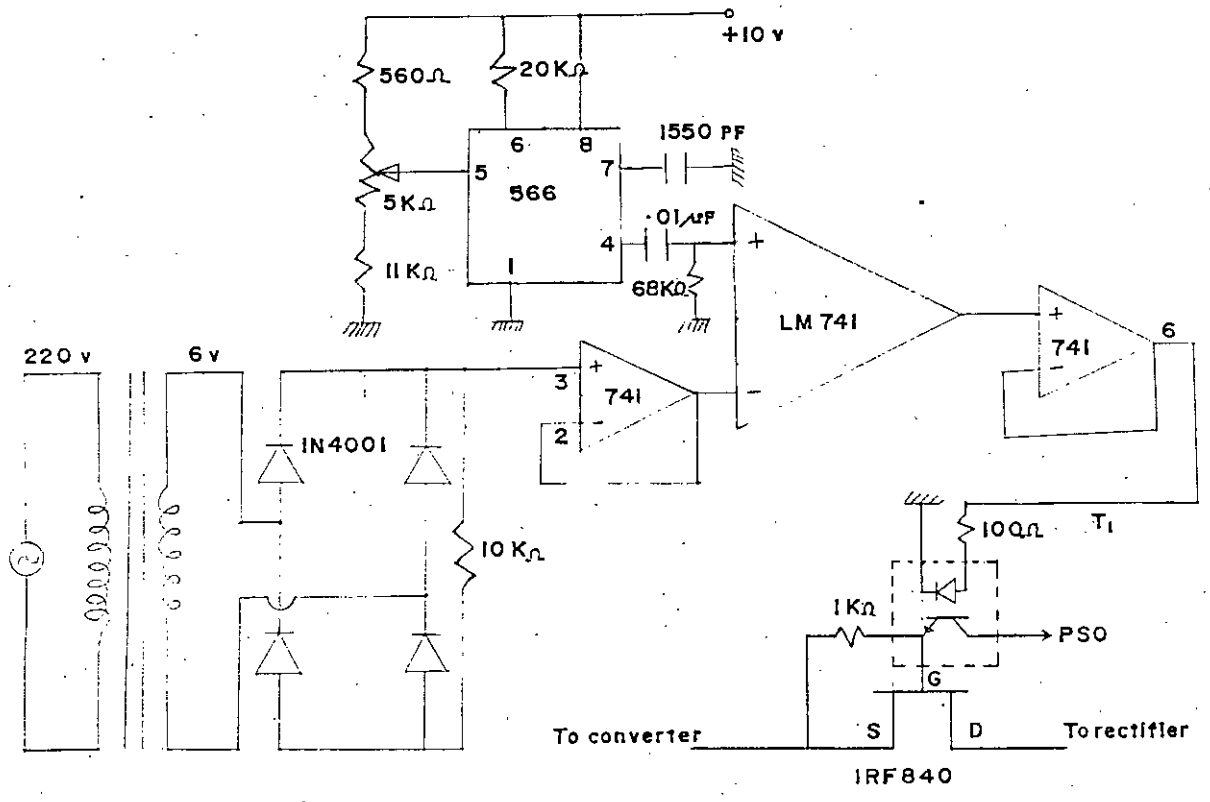


Fig. 3.2 Practical Modulator Circuit

practical modulator circuit with proper rating of the components.

The triangular and rectified unidirectional sine waves were compared in the comparator, the output is a modulated wave of varying pulse widths having constant magnitude. This pulse width modulated signal is used as a switching signal to switch the full wave rectified signal, to obtain a pulse width modulated rectified wave.

3.4 PRACTICAL LOGIC CIRCUIT

The logic circuit was design for generating two switching signals T_2 and T_3 . The circuit was design such that there was a 60 micro second delay between pulses of T_2 and T_3 to avoid short circuit due to simultaneous triggering of switches on the same leg of bridge circuit. The logic circuit comprised of an integrator, a Schmitt trigger, a comparator, AND and NOT gates and a diode clipper. The figure 3.3 show the practical logic circuit with it's ratings.

Figures 3.4 and 3.5 show the output of the different stages of the logic circuit, a sine wave was passed through an integrator and output was a cosine wave. The cosine wave was compared with zero reference in the comparator and the output was square wave 'a'. After clipping the negative portion of 'a' by a diode clipper square wave 'A' was obtained. Square wave 'C' was obtain by the NOT operation of 'A' by using one of the NOT gates of CMOS hexinverter 4049.

Square wave 'D' was generated by passing a cosine wave through Schmitt trigger and a diode clipper, 60 micro second difference between the down edge of 'A' and rising edge of 'D' was fixed by designing the resistance value of Schmitt trigger. Wave 'B' was produced by passing signal 'D' through a NOT gate of hexinverter buffer chip 4049.

The switching signals T_2 and T_3 were found by AND operation of 'A' with 'B' and 'C' with 'D' using quad AND chip 4081.

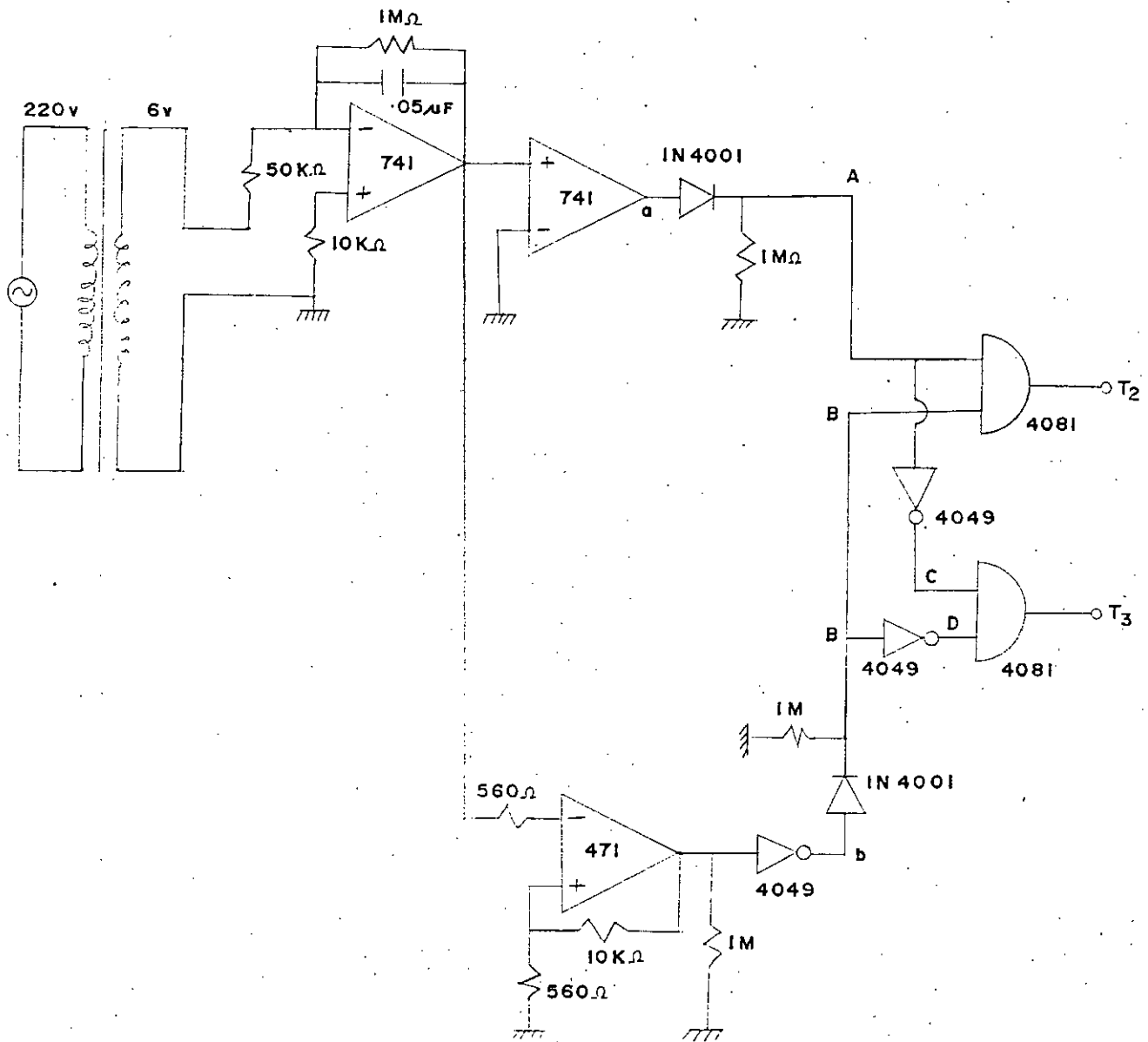


Fig. 3.3 Practical Logic Circuit

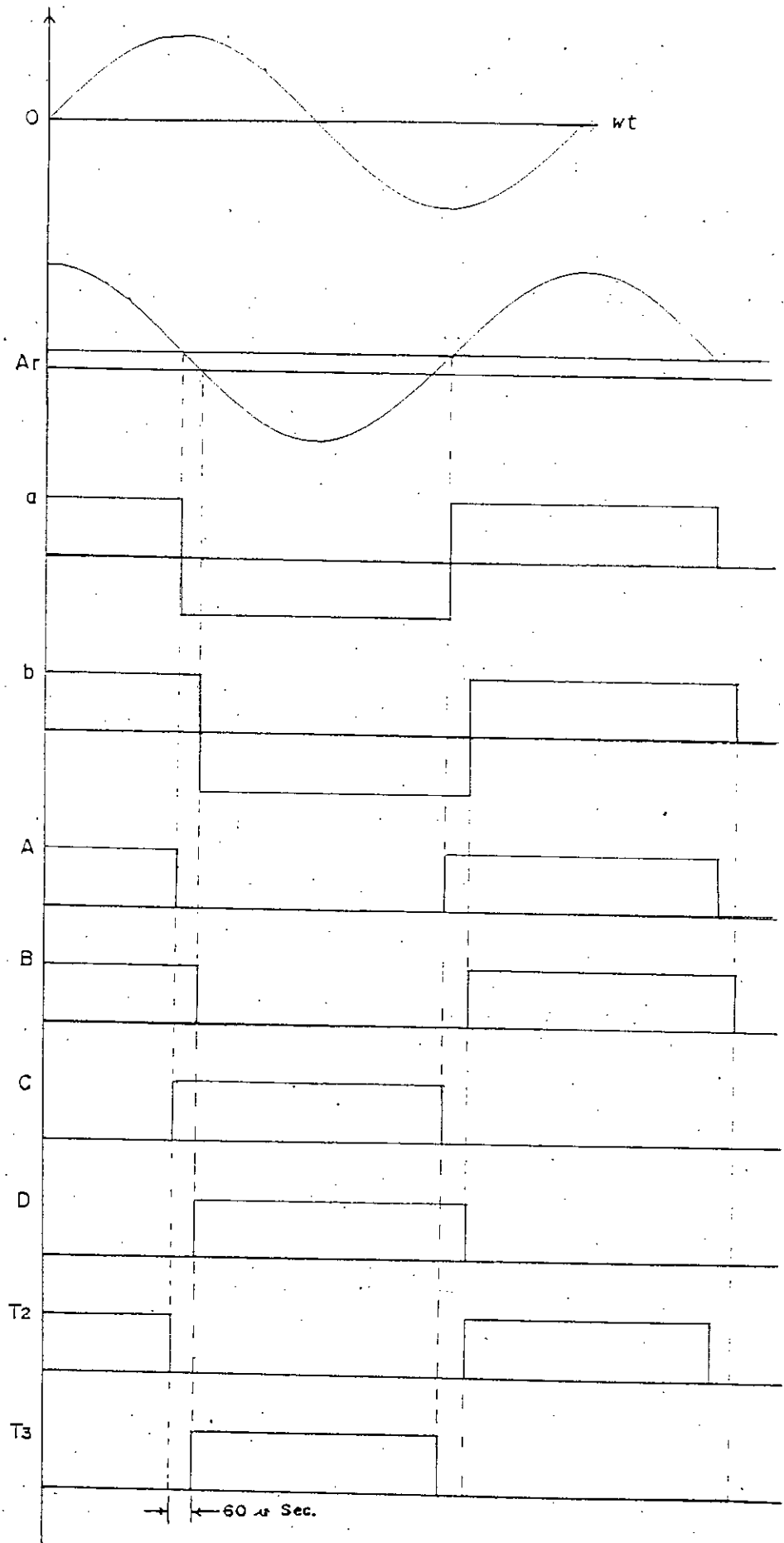


Fig. 3.4 Generation of Switching Signals

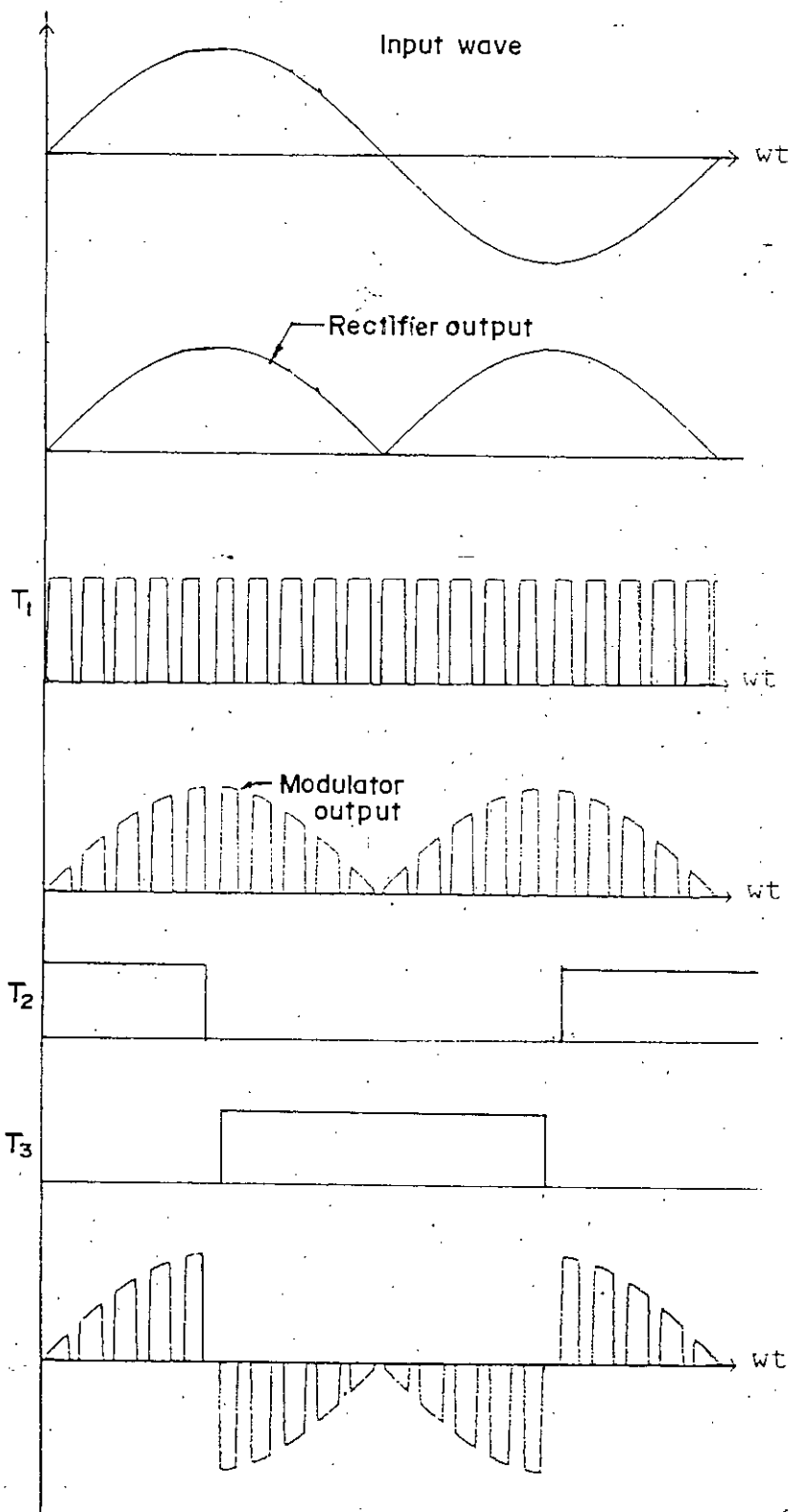


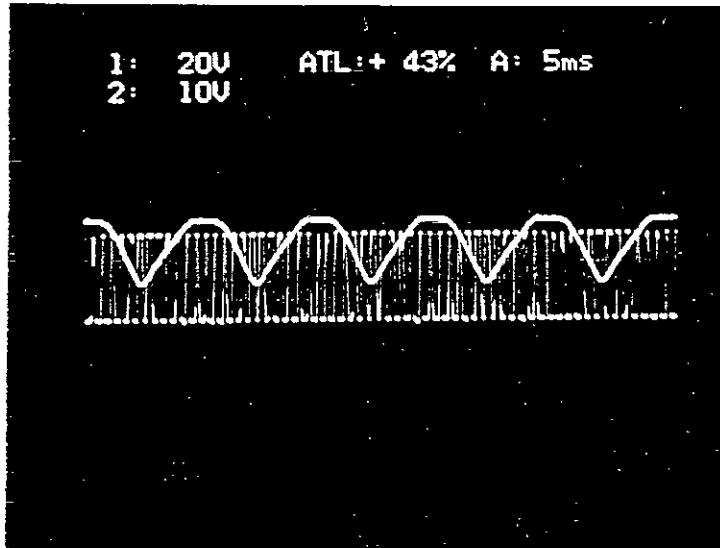
Fig. 3.5 Output of Practical Phase Shift Circuit

3.5 EXPERIMENTAL RESULTS

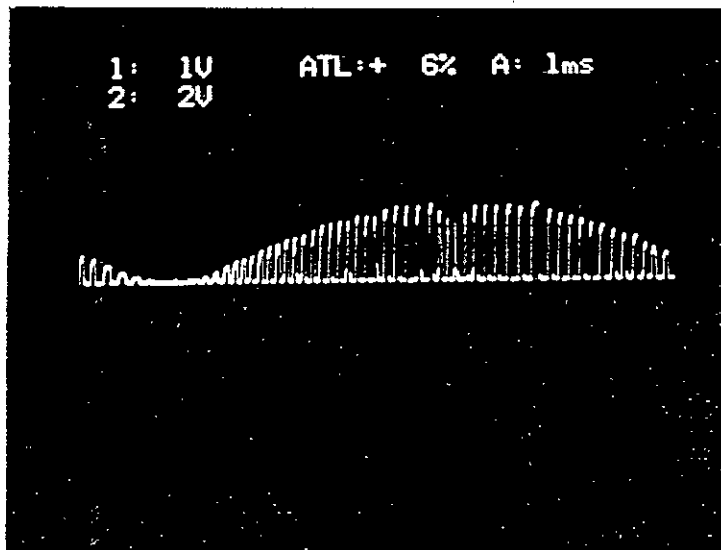
Representative experimental results of the practical implementation are shown in figures 3.6 to 3.9. Figure 3.6 (a) shows the rectified output of the power circuit and modulated switching signal for the switch after rectifier in the power circuit of the phase shift circuit. Figure 3.6 (b) is the modulated rectified output obtained by switching the rectifier circuit. Figure 3.7 (a) shows the gating signals of bridge circuit of the phase shift circuit acting as an inverter. The switching devices used in the power circuit are MOSFETs IRF 840 of 800 V, 8 A rating. Figure 3.7 (b) shows the modulated phase shift circuit output obtained by switching the rectified modulated wave of Figure 3.5 (b) by the inverter circuit. Figures 3.8 and 3.9 show the output of the of the phase shift circuit for different carrier frequencies resulting the change of switching frequency of the modulated output. Figure 3.8 is the output for carrier frequencies of 1 and 1.5 KHZ. whereas, Figure 3.9 is the output for carrier frequency of 2.5 KHZ.

3.6 OBSERVATION

The experimental part of this research work only demonstrates the successful operation of modulated single phase, phase shift circuit. The experimental output shows quite compliance with the simulated theoretical waveform. It is observed that as the carrier frequency f_c is increased, the number of switching points are increased. Spikes noticed in the photograph of the output waveforms, are inherent characteristics of the static switches during turn ON and turn Off processes. The unmodulated and the modulated phase shift circuit waveforms have been used to run a single phase motor without another starting mechanism. However, detail study was not carried out to monitor and analyze the performance of the motor supplied from such phase shift circuit during this research.

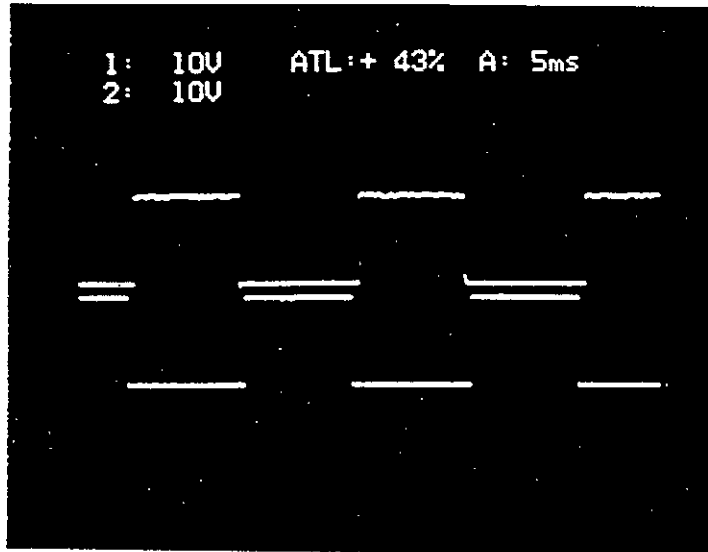


a)

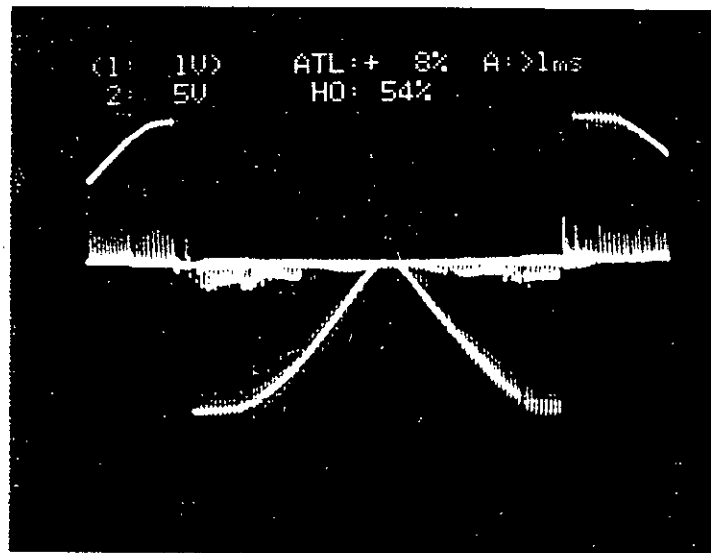


b)

Fig. 3.6 a) Rectifier Output and Modulator Switching Signal
b) Modulated Output

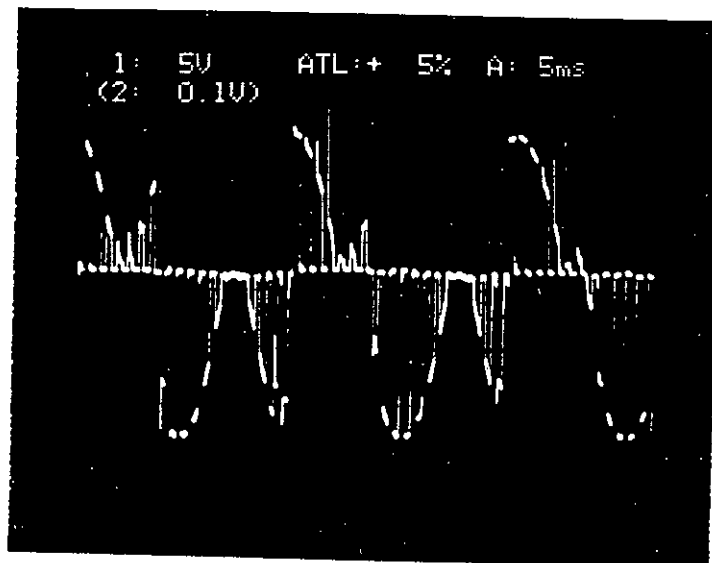


a)

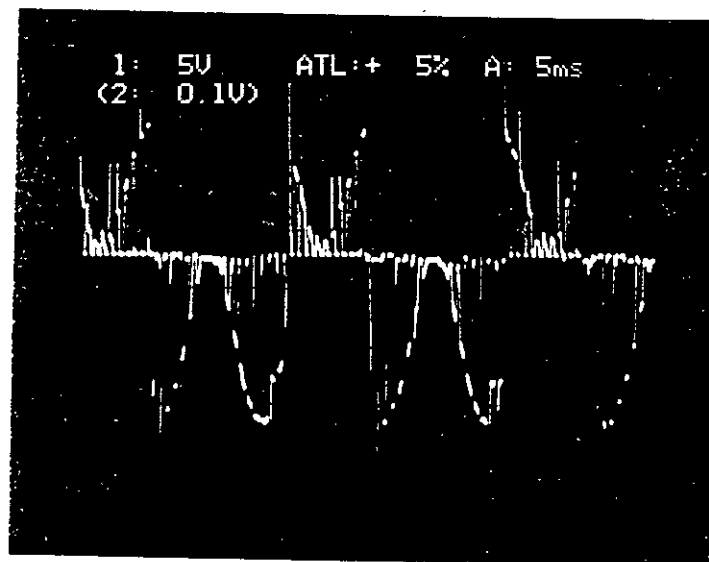


b)

Fig. 3.7 a) Switching Signals of MOSFETs
 b) Output of The Single Phase Phase Shift Circuit



a)



b)

Fig. 3.8 Output of The Single Phase Phase Shift Circuit

a) At $f_c = 1 \text{ kHz}$

b) At $f_c = 1.5 \text{ kHz}$

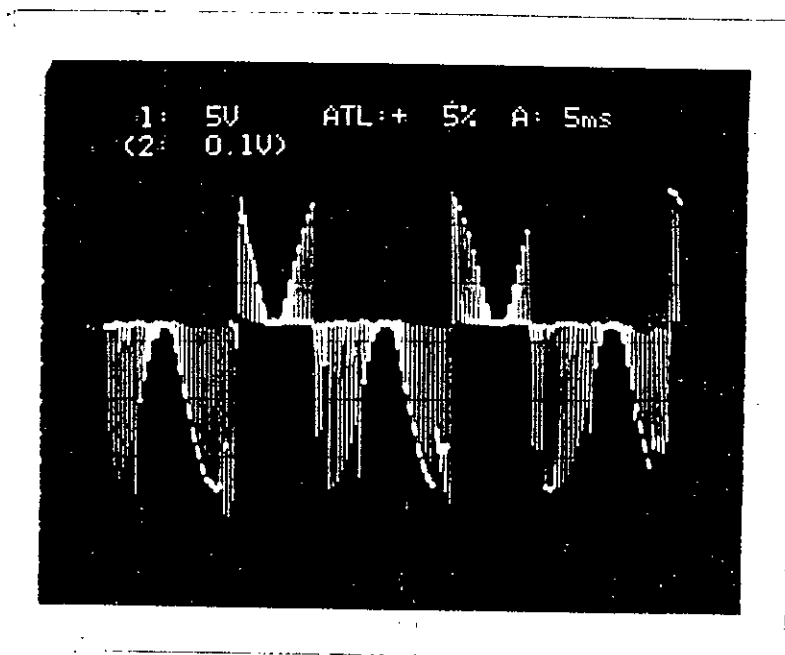


Fig. 3.9 Output of The Single Phase Phase Shift Circuit
At $f_c = 2.5 \text{ kHz}$

CHAPTER 4
SUMMARY AND CONCLUSIONS

Analysis and design of a phase shift circuit to provide considerable phase shift of the supply voltage in a single phase motor has been the main focus of this research work. Several topologies of static cycloconverters and cycloinverters have been studied to develop an appropriate static phase shift circuit. Quarter cycle switching of supply sinusoidal voltage provides an easy method of obtaining an output having phase shift of 90° from the input. However, such an output contains significant amount of low order harmonics (third harmonics equal to that of fundamental voltage) which is detrimental in terms of harmonics losses and unwanted torque production in a motor causing reduction of efficiency of the motor and causing acoustic problems. To overcome these problems it was decided to implement sine pulse width modulated switching of the phase shift circuit.

Sine pulse width modulated switching allows simultaneous voltage and frequency control of static cycloconverters and inverters and also maintains input power factor of the converter near to unity. Analysis was carried out to find the proper modulation parameters to obtain small low order harmonics and high fundamental voltage at the output of the phase shift circuit. It was found that over modulation (having modulation index $A_r/A_c > 1.0$) would provide the above features in the phase shift converter circuit.

Analysis of the phase shift circuit waveforms was carried out using commercially available MATLAB software on the simulated waveforms. Simulation of the waveforms have been done by taking product of the input sine wave with appropriate switching function. The switching function in the case of normal phase shift circuit is a square wave synchronized with input sine wave having double frequency of the input sine wave. In the case of modulating switching the switching function was constructed by gate functions defined by the switching points generated from the intersection of a sine modulating wave and a high frequency triangular wave. The solution of the modulated

switching function is obtained by simple equations proposed in a recent thesis [29]. Harmonic analysis was carried out on the waveforms by Fast Fourier Transform by commercial software MATLAB.

A practical circuit was built to demonstrate the feasibility of the results of this thesis. A MOSFET power inverter and chopper circuit were used for this purpose. The low voltage switching signal were obtained from a comparator circuit comparing stepped down supply voltage with a carrier triangular wave generated by an oscillator circuit, whereas, the inverter gating signals were obtained by a logic circuit designed for this purpose. Finally practical operation of the circuit has been carried out to observe its typical operation. A fractional horsepower induction motor has been operated by this circuit without any other starting mechanism. However, a detail study of the running condition of the motor was not carried out and it is hoped that such detailed study will be carried out in future investigation.

90103

REFERENCES

- [1] Matsh, Leander, W., 'Electromagnetic and Electromechanical Machines.', Harper and Row Publishers, New York, USA 2nd Edition, 1977, pp. 166-170.
- [2] M. H. Rashid, 'Power Electronics Circuit Device and Application', Prentic Hall Inc., 1993, pp 166-170, 356-378, 484-487, 497-504,
- [3] S. Vadivel, G. Bhuvaneswari, and G. Siridhara Rao, " A Unified Approach to the Real-time Implementation of Microprocessor- based PWM Waveforms", IEEE Transaction on Power Electronics, Vol.6, No.4, Oct.1991, pp. 565-574
- [4] S. R. Bowes and M. J. Mount, " Microprocessor control of PWM Inverters", IEEE Proc., Vol.128, Pt. B, Nov. 1981, pp. 123-127
- [5] F. C. Zaeg, R. Martinez, S. Keplinger and A. Seiser, " Dynamically Optimal Switching Patterns for PWM Inverter Drives", IEEE Transaction, Ind. Appl. Vol21, No.4, Jul/Aug. 1985, pp. 320-326
- [6] M. Varnovistsky, 'A Microcomputer-based Control Signal Generator for Three Phase Switching PWM Inverter', IEEE Trans. Ind. Appl. Vol. 1A-19, No. 2, March/April 1983, pp. 187-194.
- [7] R. G. Hoft, T. Khuwatsamrit and R. McLaren, "Microprocessor Application for Power

- Electronics in the North America", Microelectron. Power Electron. Electr. Drives Conf., Darmstadt, W Germany, 1982, pp, 29-42.
- [8] Mathworks Ins., USA, 'Matlab Package Program.' 1991
- [9] F. Aldana, J. Piere, and C. M. Penaver." Microprocessor Control for Power Electronic Systems", Microelectron. Power Electron. Electr. Drives Conf. Rec., Darmstadt, W Germany, 1982, pp. 111-115
- [10] R. G. Hoft, R. W. McLaren, R. L. Pimmel and K. P. Gokhale, " The Impact of Microelectronics and Microprocessors on Power Electronics and Variable Speed Drives", Int.Power Elec. and Variable Speed Drives Conf. Rec., London, 1984, pp. 191-198
- [11] S. B. Dewan and A. Mirbod, " Microprocessor-based Optimum Control for Four Quadrant chopper", IEEE Trans. Ind. Appl., IA-17, Jan/Feb. 1981, pp. 34-40
- [12] D. A. Grant, M. Stevens and J. A. Houldsworth, " The effect of Word Length on the Harmonics Content of microprocessor-based PWM Waveform Generators", IEEE Trans. Ind. Appl., Vol. IA-21, Jan/Feb. 1985, pp. 218-225
- [13] S. Bolognani, G. S. Buja and D. Longo, " Hardware and performance Effective Microcomputer Control of a Three-phase PWM Inverter", Int. Power Electronic Conf. Rec., Tokyo, 1983, pp. 360-371

- [14] A. Billini, C. D Masro, G. Figalli and G. Ulivi, 'An Approach for the Implementation on a Microcomputer Control Circuit of Variable Frequency Three Phase Inverter', IEEE/IAS Annual Meeting Conf. Rec., 1981, pp. 650-655.
- [15] V. V. Athani and S. M. Deshpande, " Microprocessor control of a Three-phase Inverter in Induction motor Speed Control System", IEEE Trans. Ind. Electron. Conf. Rec., Vol IECEI-27, Nov. 1980, pp. 291-298
- [16] M. J. Case and P. Kulentic, " A Microprocessor controller for the Cycloconverter", Microelectron. Power electron. electr. Drives Conf. Rec., Darmstsd, W Germany, 1982, pp 171-181
- [17] A. Bohuss, P. Buzas and K. Ganszky, 'Microcomputer Controlled Inverter for Uninterruptible Power Supply', Microelectron Power Electr. Drives Conf. Rec., Dramstadt, Germany, 1982, pp. 203-206.
- [18] E. A. Rothwell, " The use of Microprocessor and Power Transistor in Modern Uninterruptible Power Supplies", Microelectron Power Electr. Drives Conf. Rec., 1984, pp. 413-418.
- [19] T Kutman, " Implementation of a Microprocessor-based Technique for Output Filter Optimization in UPS System', Int. Power Elec. and Variable Speed drives Conf. Rec., London, 1984, pp. 75-78
- [20] G. S. Buja and P. floroni, 'Microprocessor Control of PWM Inverter', IEEE Trans. Ind.

Electron., Vol. 1F-29, Aug. 12982, pp. 212-218.

- [21] F. Harashima and S. Kondo, " Microprocessor-based optimal Speed control System of motor Drives", IEEE/IECI Conf. Rec., 1981, pp. 252-257
- [22] U. Waschatz, " Adaptive control of Electrical Drives Employing Microprocessor", Microelectron Power Electr. Drives Conf. Rec., Darmstadt, W Germany, 1982, pp. 135-140.
- [23] Y. T. Chan, A. J. Chmiel and J. B. Plant, " A Microprocessor-based current Controller for SCR-DC Motor drives", IEEE Trans. Ind. Electr. Conf. instr., Vol IECI27, Aug.1980, pp. 543-567
- [24] S. Franze, " Programmable Counter Simplifies Measurement of feedback signal and Generation of Firing Pulses for DC Drives", Microelectron Power Electr. Drives Conf. Rec., Darmstadt, W Germany, 1982, pp. 245-248
- [25] N. K. De, S. Sinha and A. K. Chattopadhyay, " Microcomputer as a Programmable Controller for Sate feedback Control of a DC Motor Employing Thyristor Amplifier", IEEE/IAS Annual Meeting Conf. Rec., 1984, pp. 586-592
- [26] W. S. Moak and P. C. Sen, " Induction Motor Drives with a Microcomputer Control system", IEEE/IAS Annual Meeting Conf. Rec., 1983, pp. 653-662

- [27] P. Misic and V. Vukovic, " Microprocessor Control Unit for Variable speed Induction motor drives", Microelectron Power Electr. Drives Conf. Rec., Darmstadt, W Germany, 1982, pp. 321-328
- [28] A. Moschetti, " Microprocessor-based PWM System for Inverter-fed Squarrel Cage motor traction Drives", Microelectron Power Electr. Drives Conf. Rec., Darmstadt, W Germany, 1982, pp. 425-431
- [29] Md. Bashir Uddin, 'Stability Analysis of PWM Inverter Fed Synchronous Motor', 1996, Department of Electrical and Electronic Engineering, BUET, Dhaka.

APPENDIX I

WAVEFORMS AND SPECTRUM OF SINE PWM

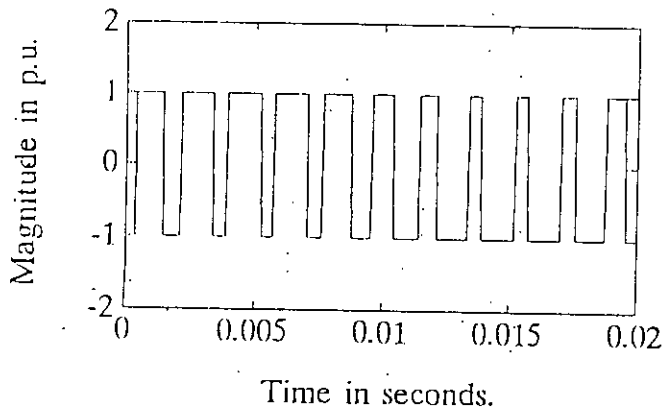
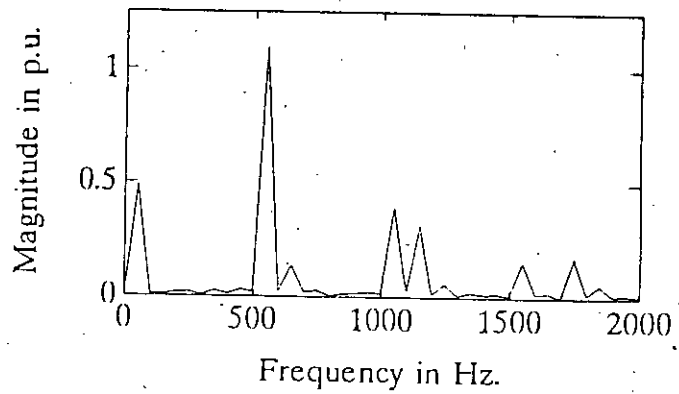
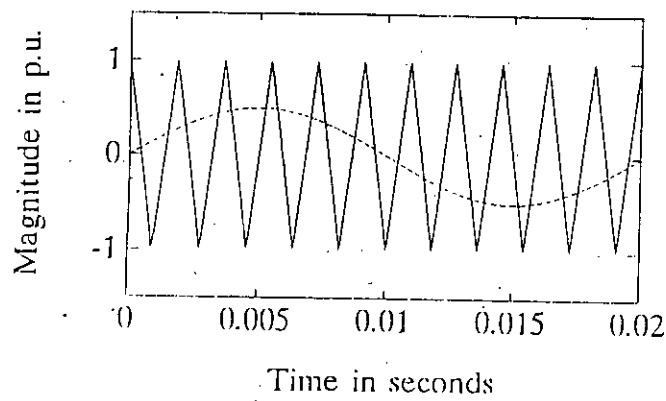


Fig. A.1.1 Waveform of SPWM at Modulation Index $m = .5$
 and Carrier Frequency $f_c = 550$ Hz
 a) Reference and Carrier Wave
 b) Frequency Spectrum
 c) Switching Function

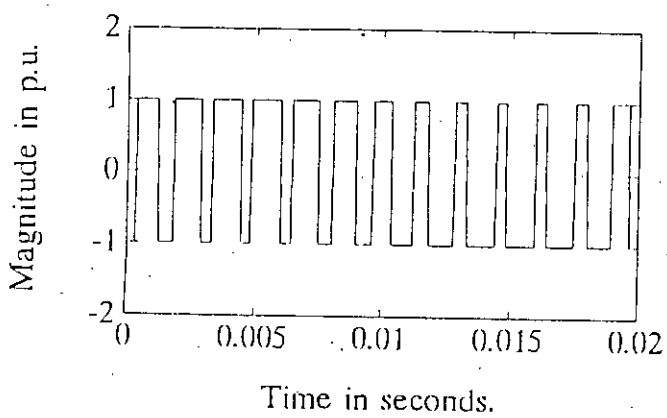
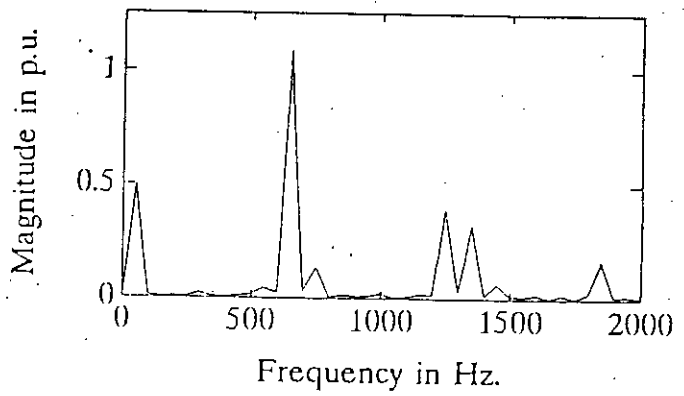
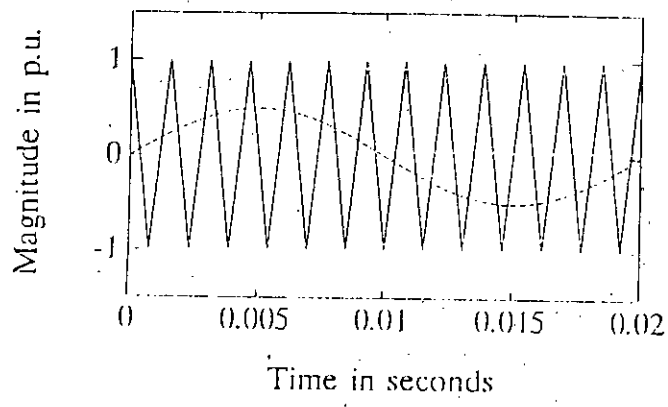


Fig. A.1.2 Waveform of SPWM at Modulation Index $m = .5$ and Carrier Frequency $f_c = 650$ Hz
 a) Reference and Carrier Wave
 b) Frequency Spectrum
 c) Switching Function

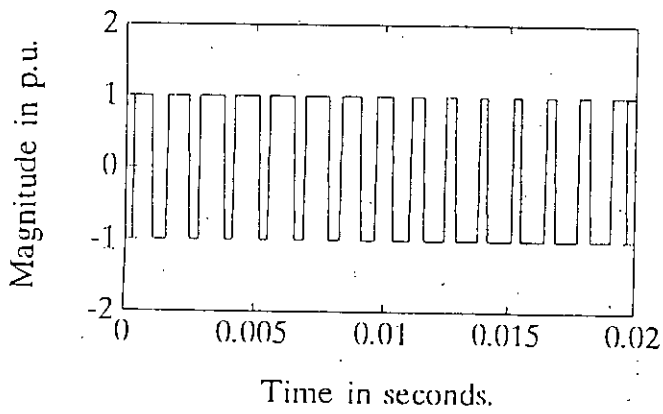
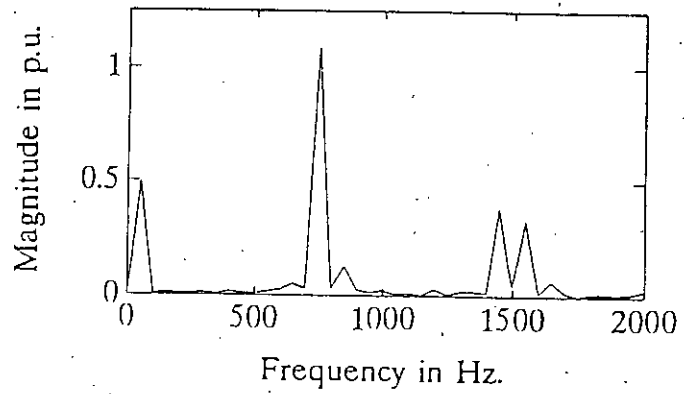
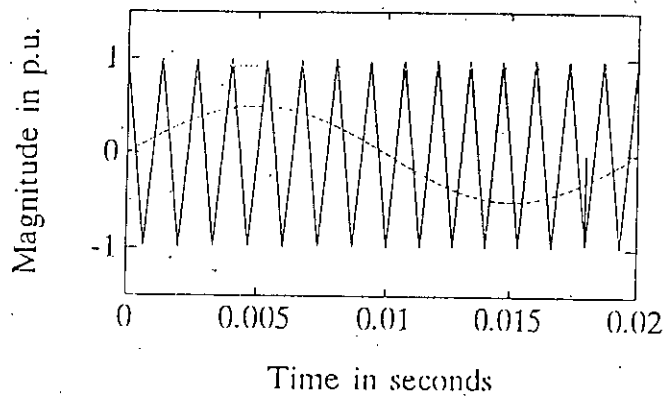


Fig. A:1.3 Waveform of SPWM at Modulation Index $m = .5$ and Carrier Frequency $f_c = 750$ Hz
 a) Reference and Carrier Wave
 b) Frequency Spectrum
 c) Switching Function

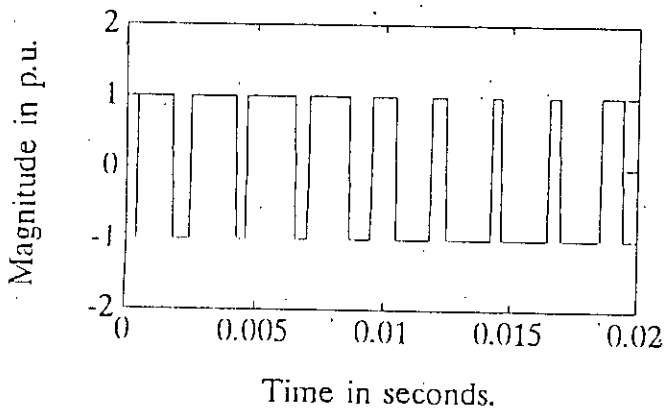
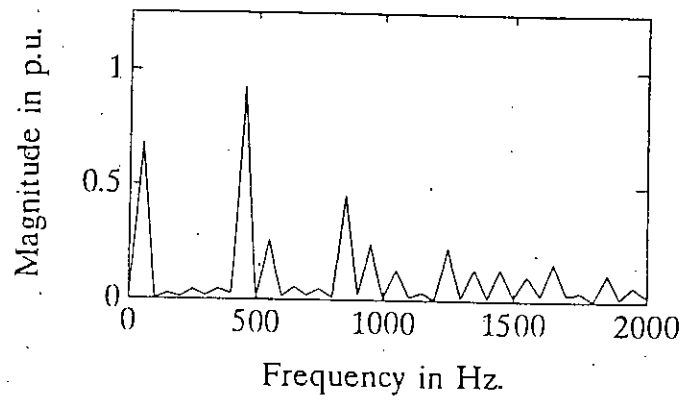
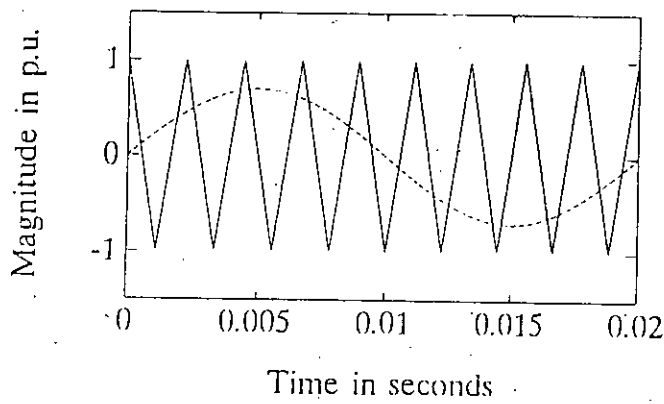


Fig. A.1.4 Waveform of SPWM at Modulation Index $m = .7$ and Carrier Frequency $f_c = 450$ Hz
 a) Reference and Carrier Wave
 b) Frequency Spectrum
 c) Switching Function

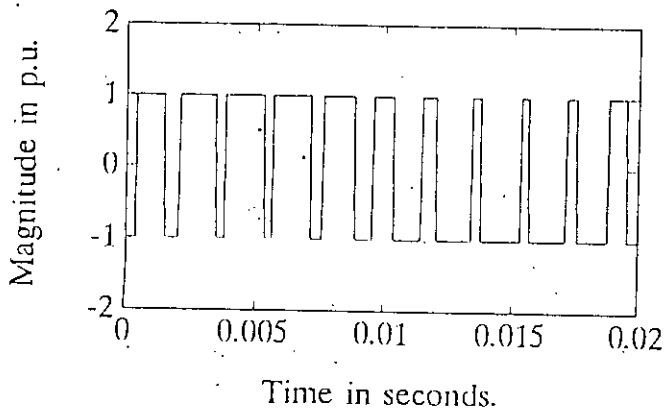
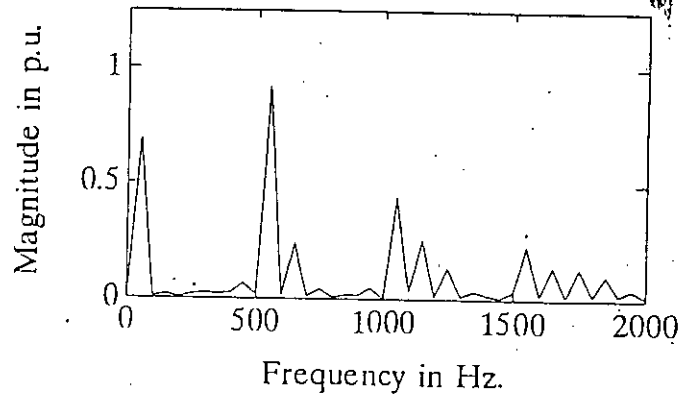
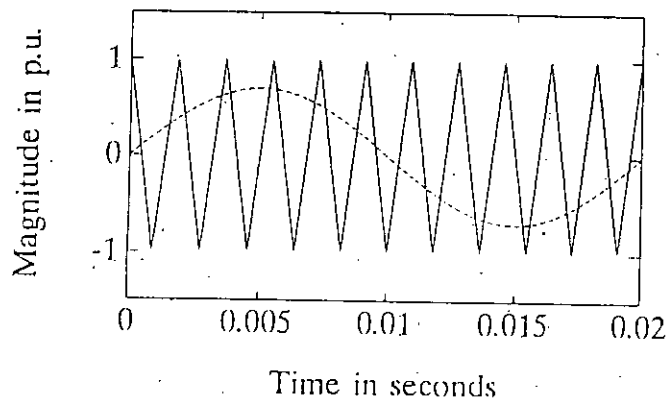


Fig. A.1.5 Waveform of SPWM at Modulation Index $m = .7$
 and Carrier Frequency $f_c = 550$ Hz
 a) Reference and Carrier Wave
 b) Frequency Spectrum
 c) Switching Function

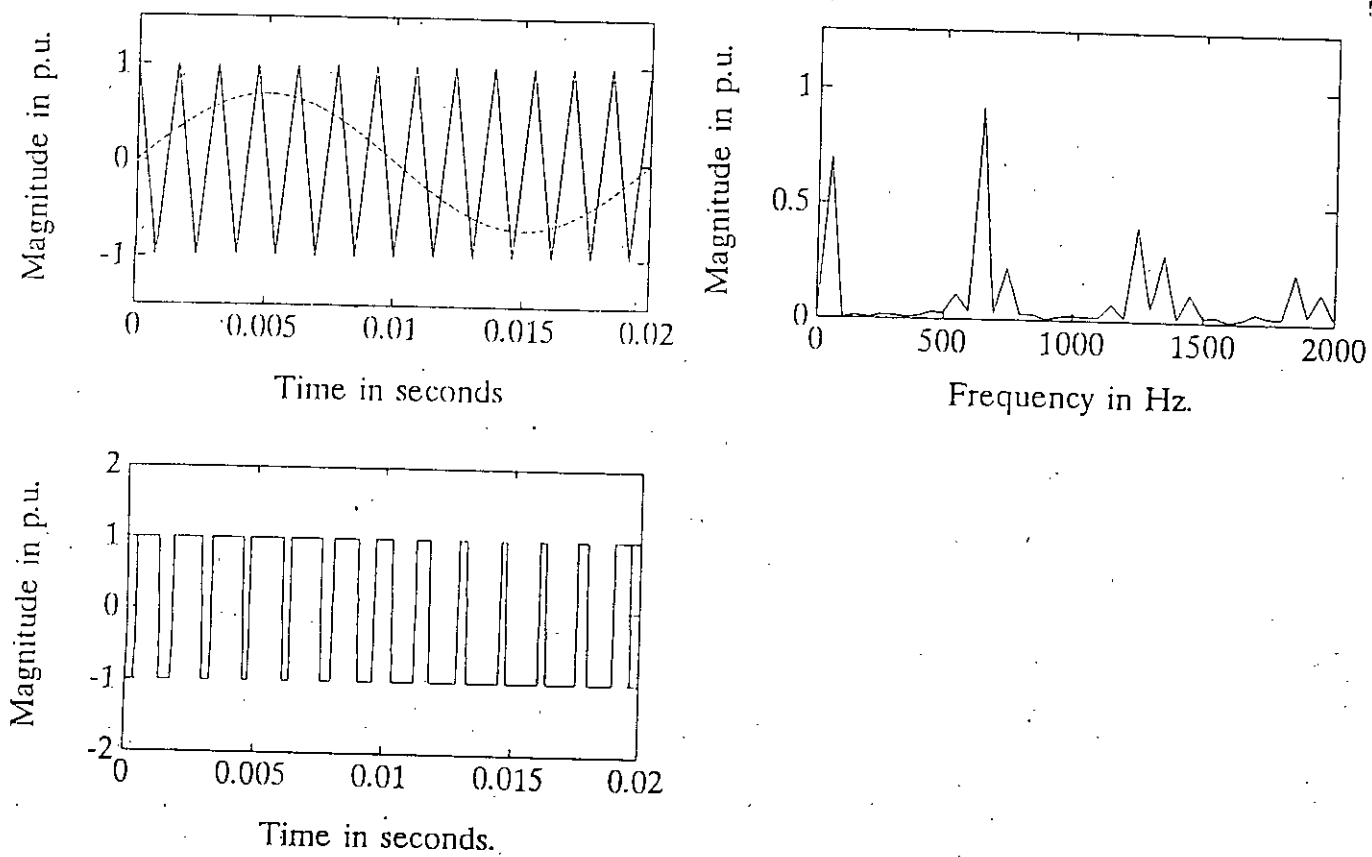


Fig. A.1.6 Waveform of SPWM at Modulation Index $m = .7$ and Carrier Frequency $f_c = 650$ Hz
 a) Reference and Carrier Wave
 b) Frequency Spectrum
 c) Switching Function

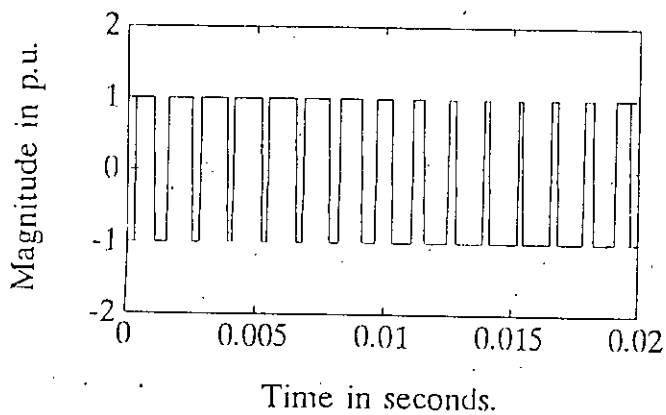
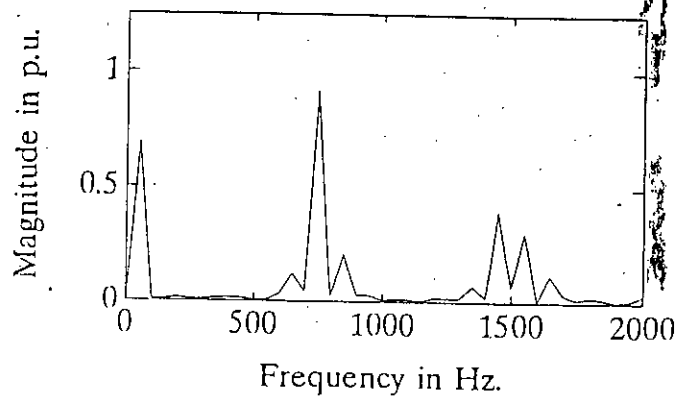
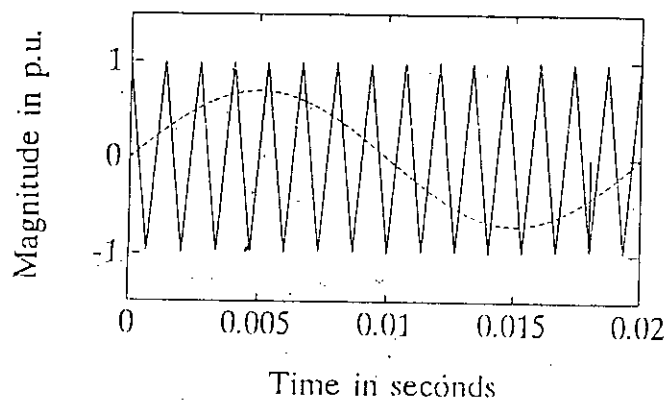


Fig. A.1.7 Waveform of SPWM at Modulation Index $m = .7$
 and Carrier Frequency $f_c = 750$ Hz
 a) Reference and Carrier Wave
 b) Frequency Spectrum
 c) Switching Function

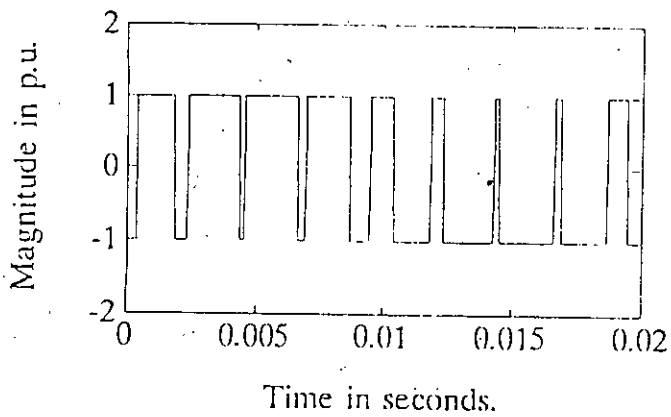
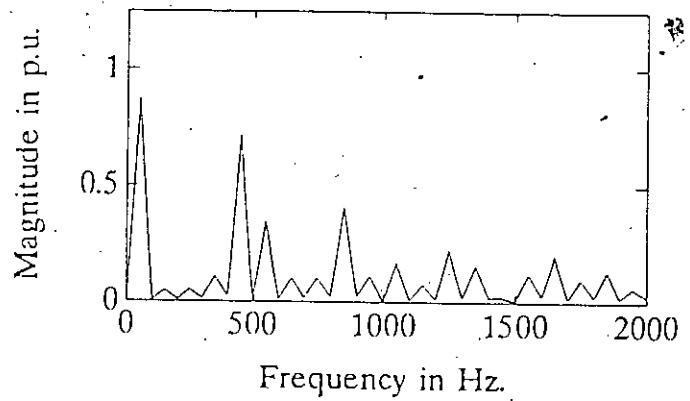
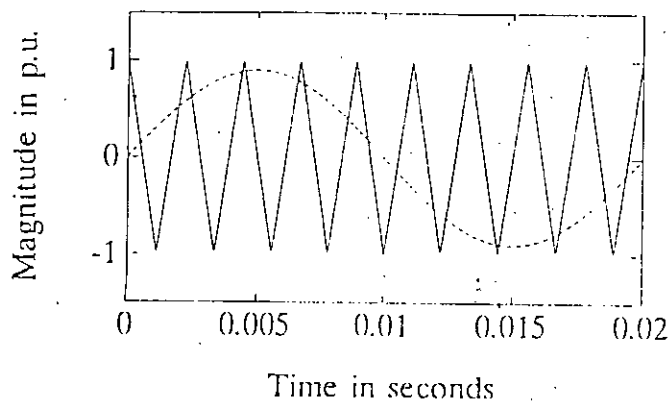


Fig. A.1.8 Waveform of SPWM at Modulation Index $m = .9$ and Carrier Frequency $f_c = 450$ Hz
 a) Reference and Carrier Wave
 b) Frequency Spectrum
 c) Switching Function

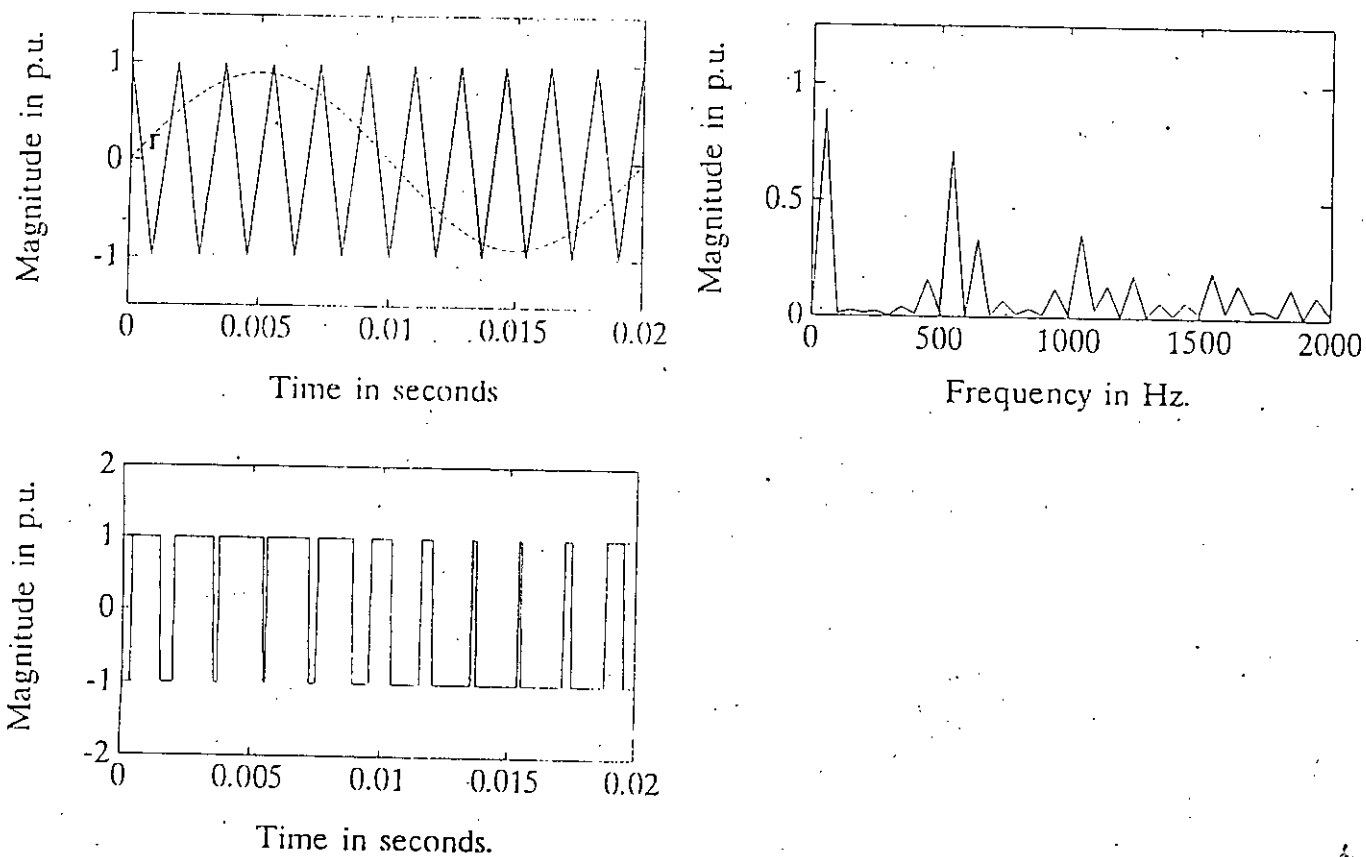


Fig. A.1.9 Waveform of SPWM at Modulation Index $m = .9$
 and Carrier Frequency $f_c = 550$ Hz
 a) Reference and Carrier Wave
 b) Frequency Spectrum
 c) Switching Function

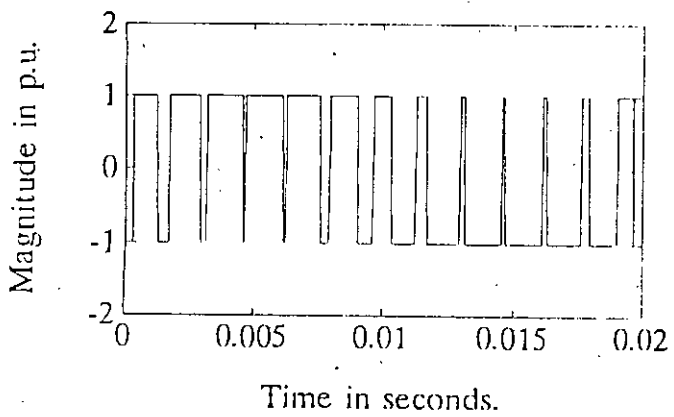
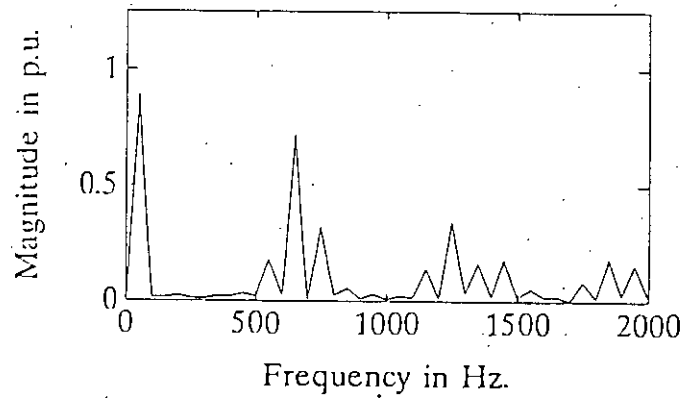
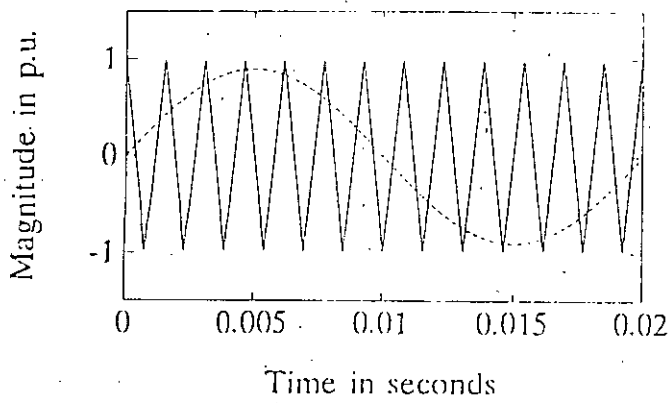


Fig. A.1.10 Waveform of SPWM at Modulation Index $m = .9$ and Carrier Frequency $f_c = 650$ Hz
 a) Reference and Carrier Wave
 b) Frequency Spectrum
 c) Switching Function

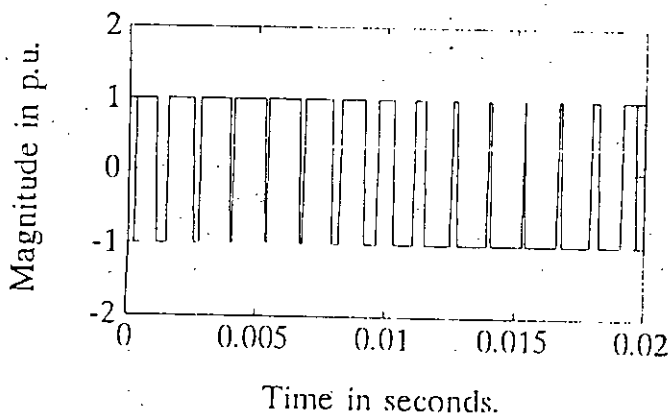
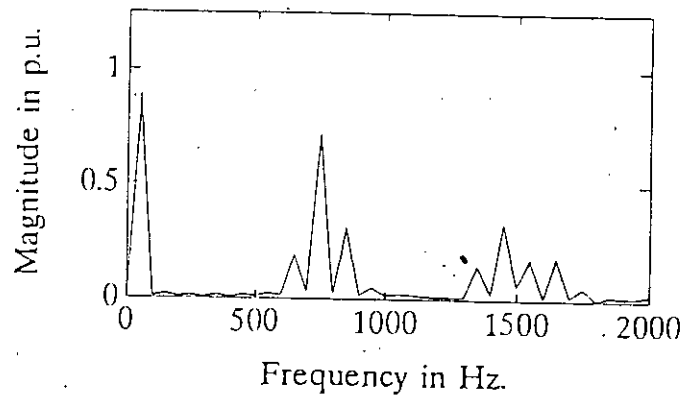
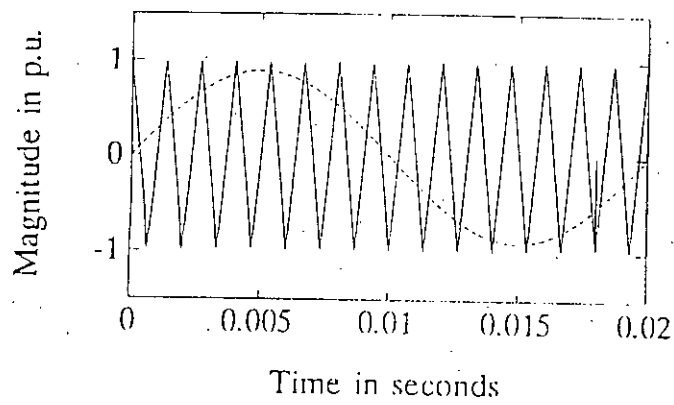


Fig. A.1.11 Waveform of SPWM at Modulation Index $m = .9$ and Carrier Frequency $f_c = 750$ Hz
 a) Reference and Carrier Wave
 b) Frequency Spectrum
 c) Switching Function

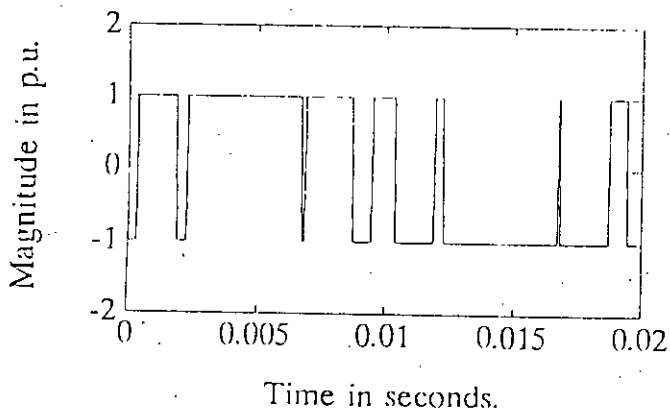
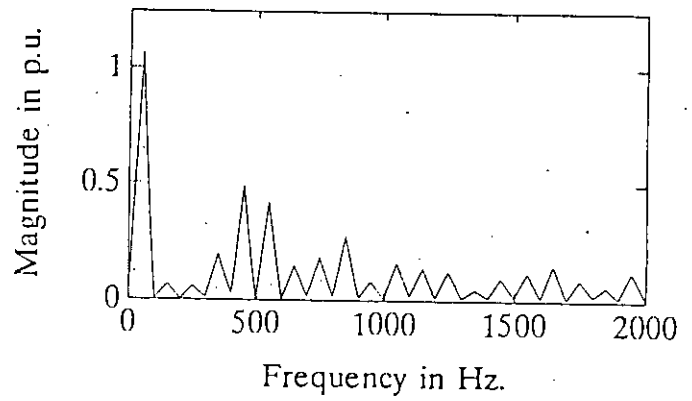
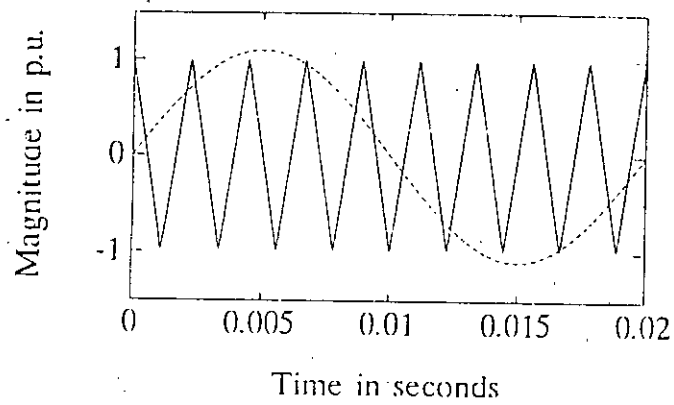


Fig. A.1.12 Waveform of SPWM at Modulation Index $m = 1.1$ and Carrier Frequency $f_c = 450$ Hz
 a) Reference and Carrier Wave
 b) Frequency Spectrum
 c) Switching Function

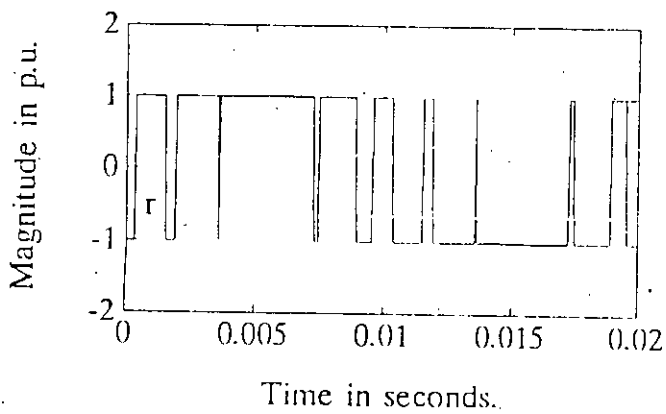
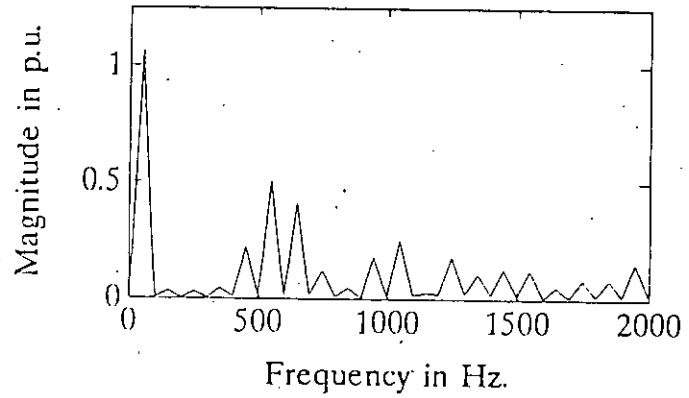
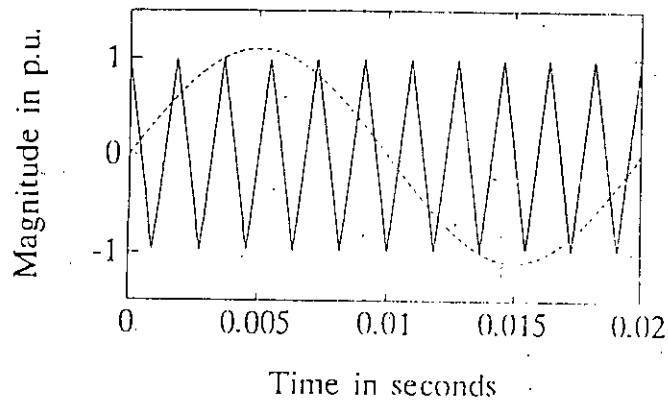


Fig. A.1.13 Waveform of SPWM at Modulation Index $m = 1.1$ and Carrier Frequency $f_c = 550$ Hz
 a) Reference and Carrier Wave
 b) Frequency Spectrum
 c) Switching Function

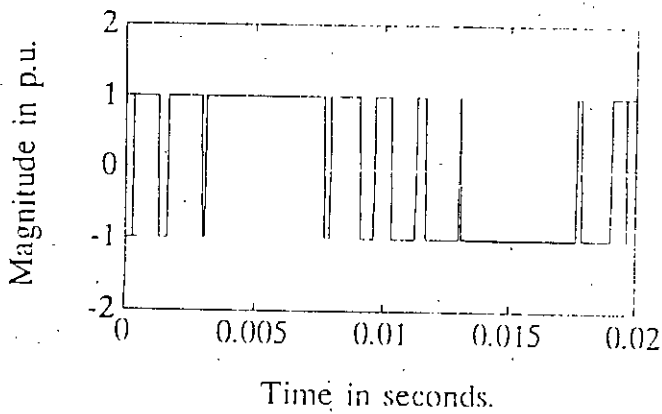
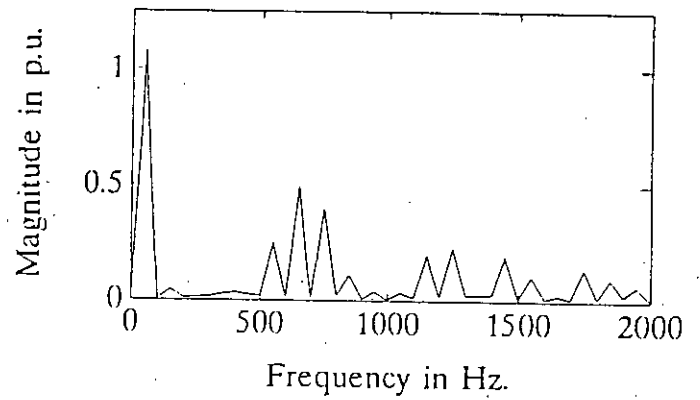
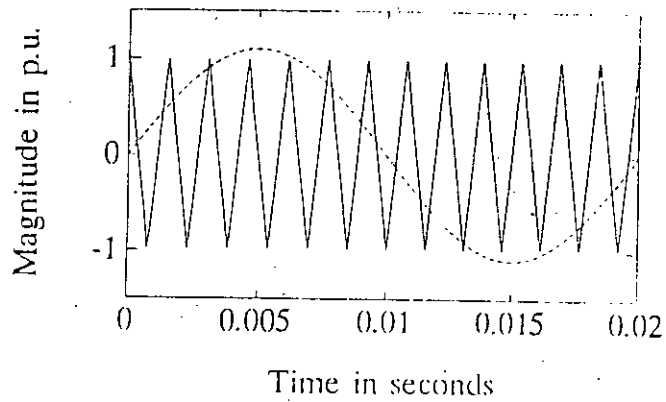


Fig. A.1.14 Waveform of SPWM at Modulation Index $m = 1.1$ and Carrier Frequency $f_c = 650$ Hz
 a) Reference and Carrier Wave
 b) Frequency Spectrum
 c) Switching Function

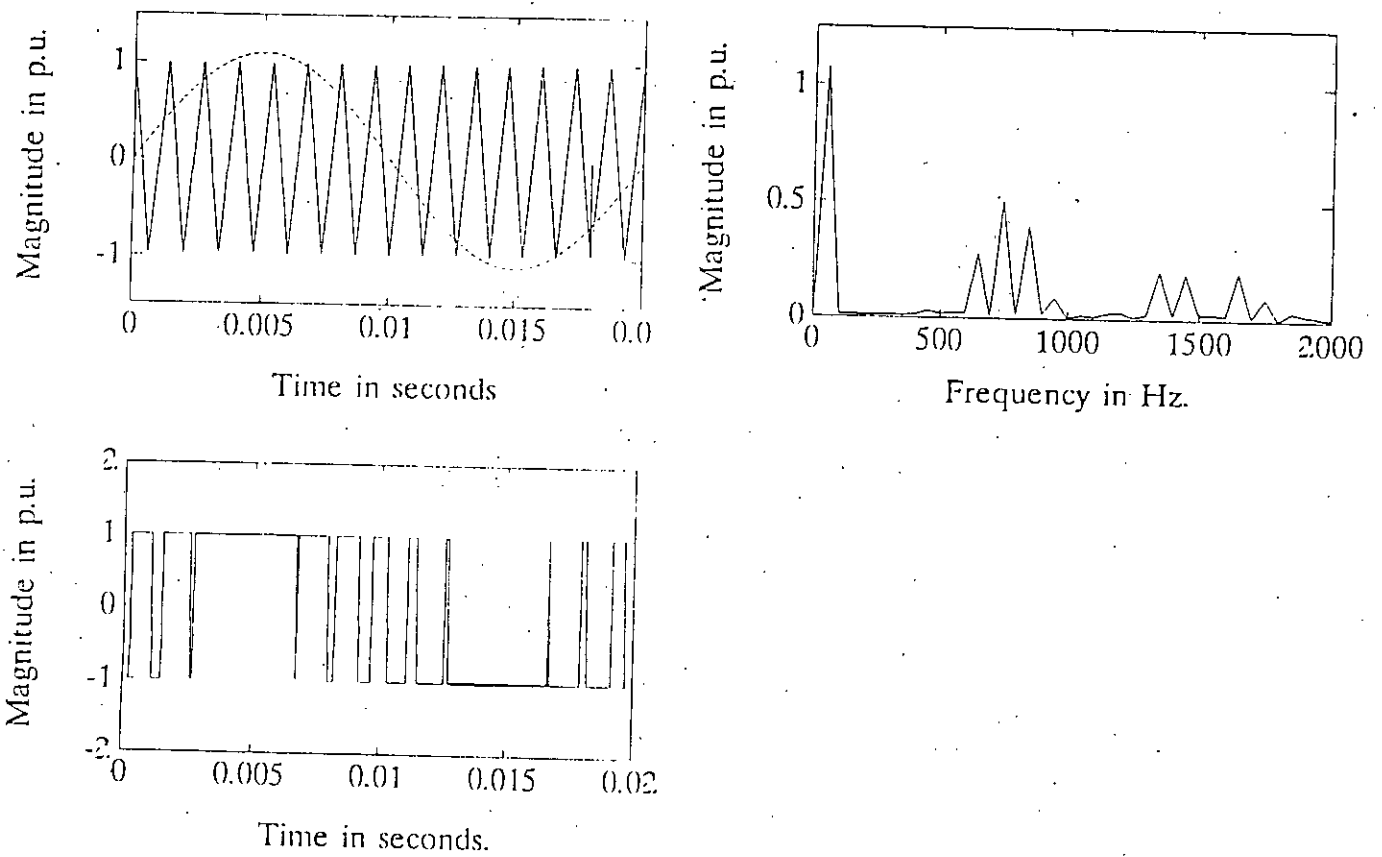


Fig. A.1.15 Waveform of SPWM at Modulation Index $m = 1.1$ and Carrier Frequency $f_c = 750$ Hz
 a) Reference and Carrier Wave
 b) Frequency Spectrum
 c) Switching Function

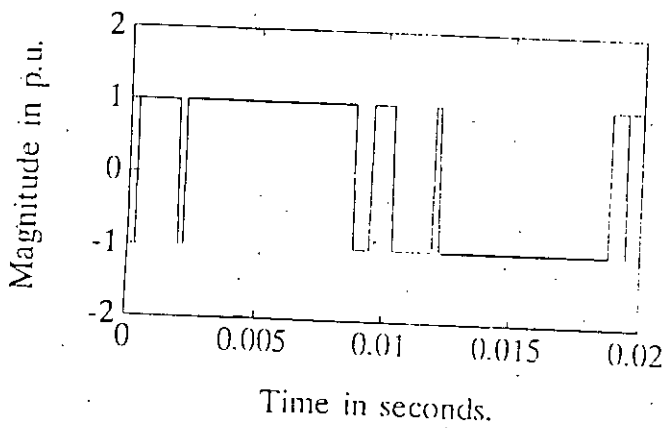
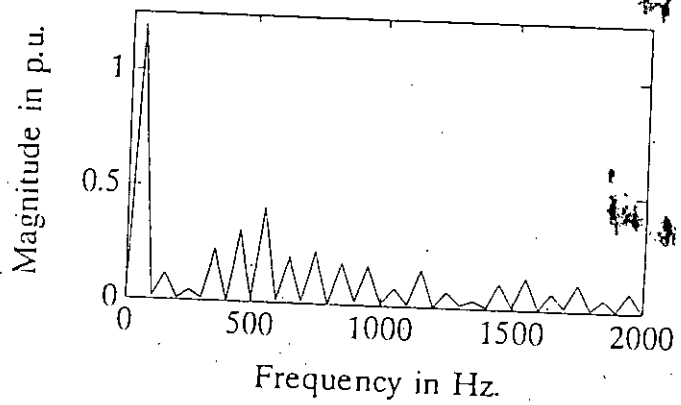
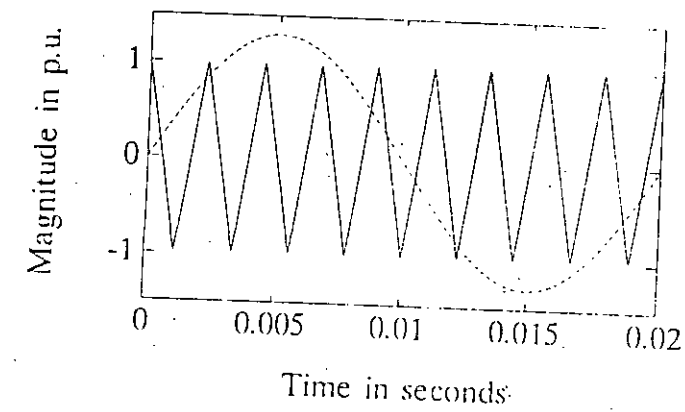


Fig. A.1.16 Waveform of SPWM at Modulation Index $m = 1.3$ and Carrier Frequency $f_c = 450$ Hz
 a) Reference and Carrier Wave
 b) Frequency Spectrum
 c) Switching Function

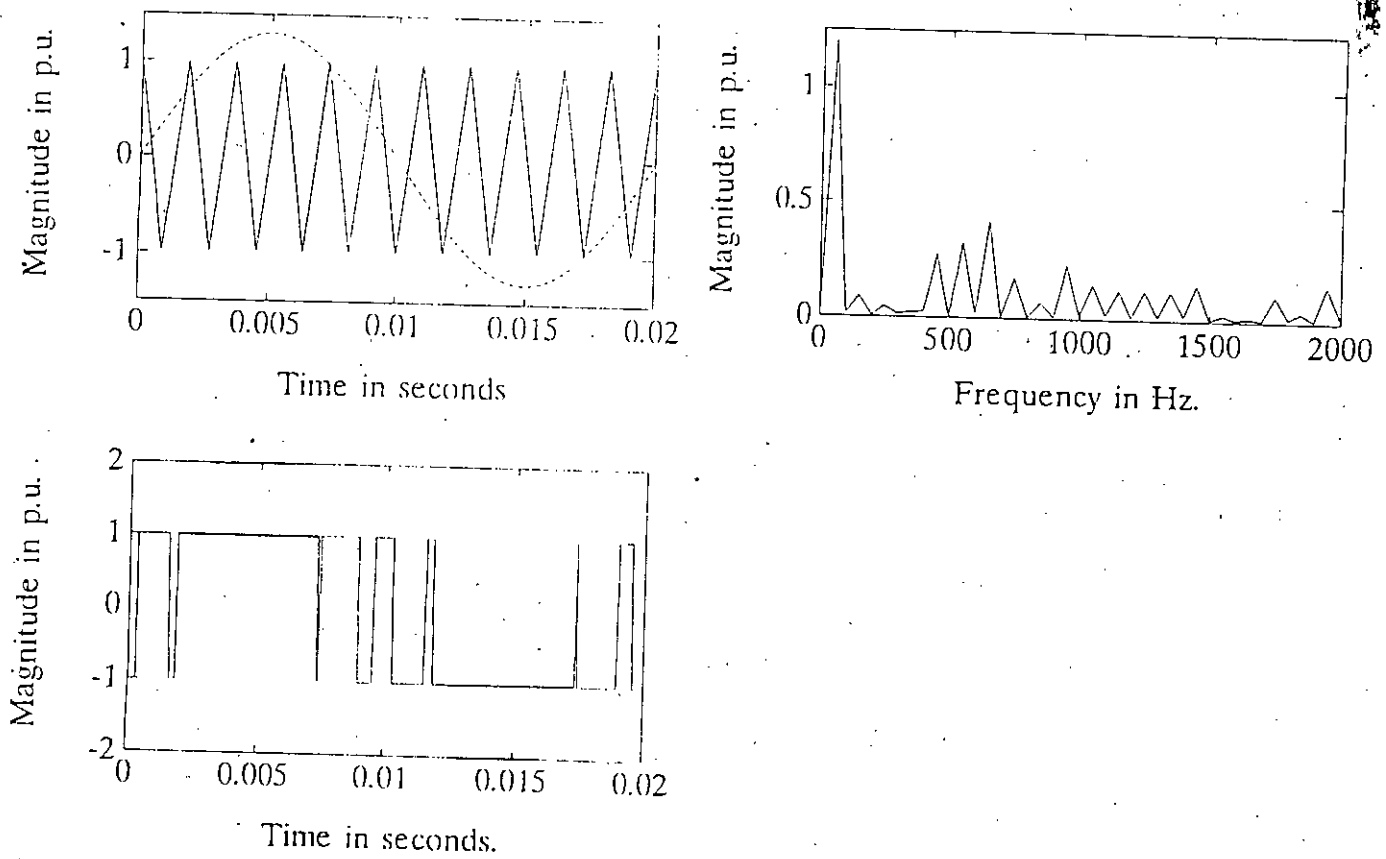


Fig. A.1.17 Waveform of SPWM at Modulation Index $m = 1.3$ and Carrier Frequency $f_c = 550$ Hz
 a) Reference and Carrier Wave
 b) Frequency Spectrum
 c) Switching Function

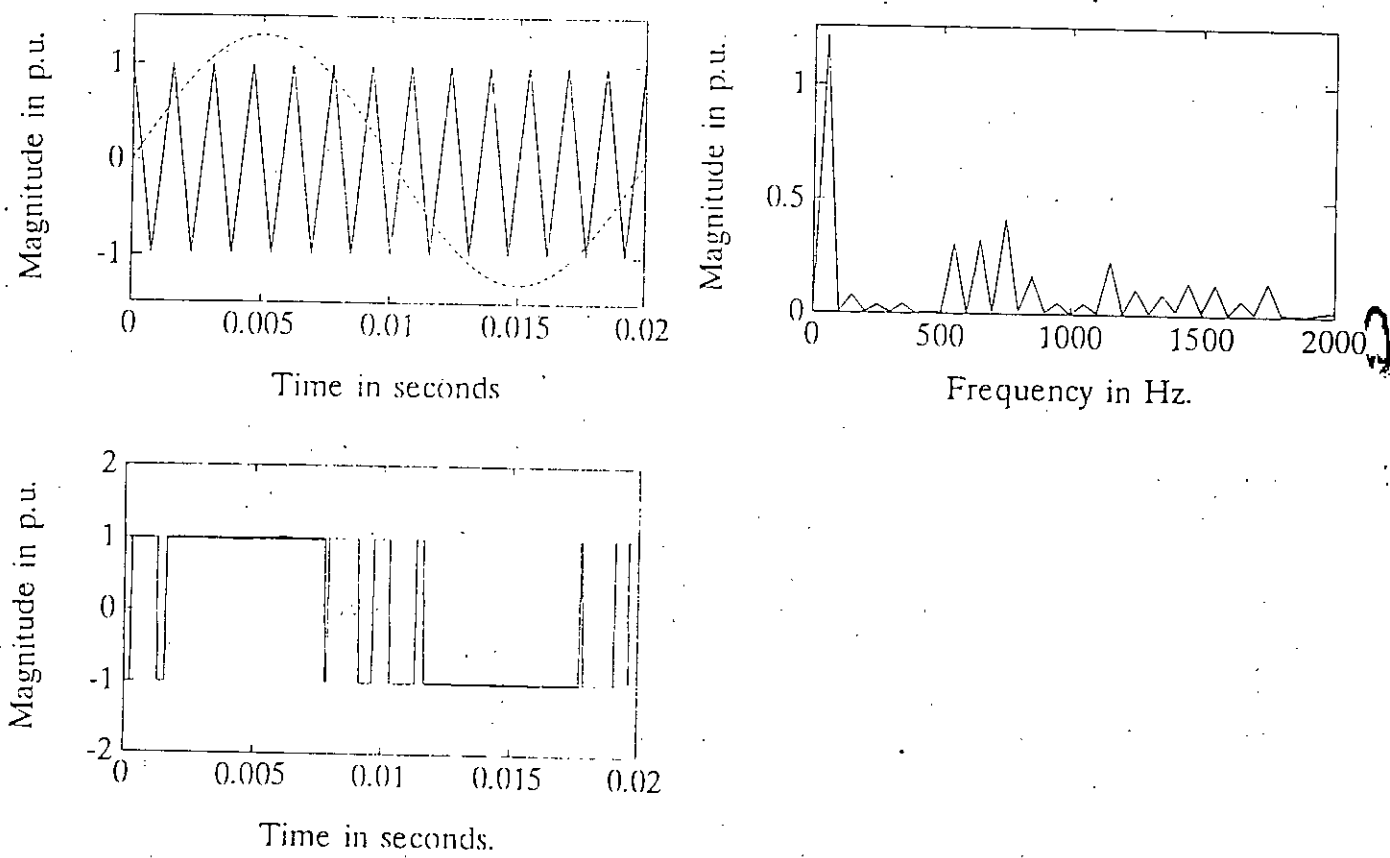


Fig. A.1.18 Waveform of SPWM at Modulation Index $m = 1.3$ and Carrier Frequency $f_c = 650$ Hz
 a) Reference and Carrier Wave
 b) Frequency Spectrum
 c) Switching Function

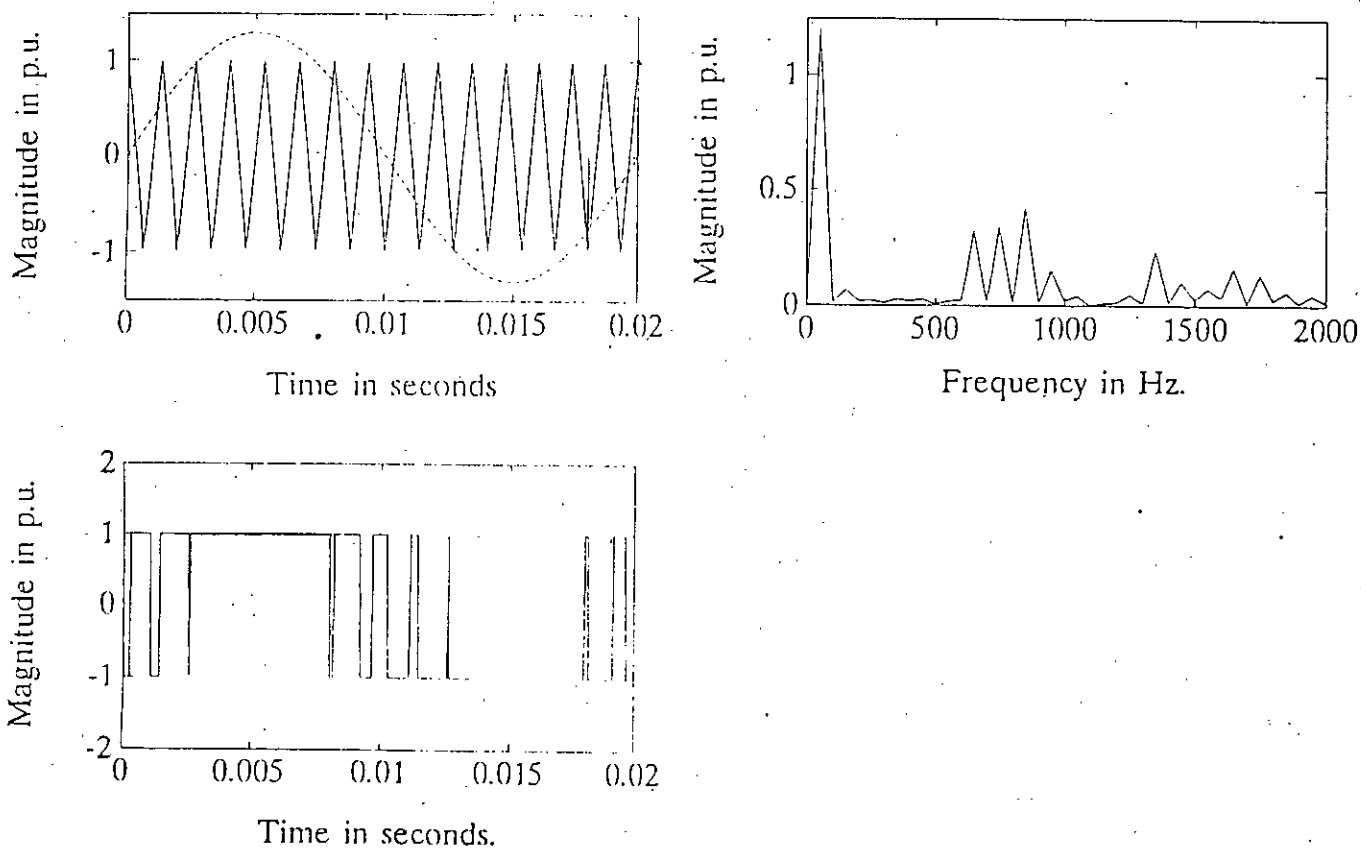


Fig. A.1.19 Waveform of SPWM at Modulation Index $m = 1.3$ and Carrier Frequency $f_c = 750$ Hz
 a) Reference and Carrier Wave
 b) Frequency Spectrum
 c) Switching Function

APPENDIX II

WAVEFORMS AND SPECTRUM OF PWM PHASE SHIFT

CIRCUIT

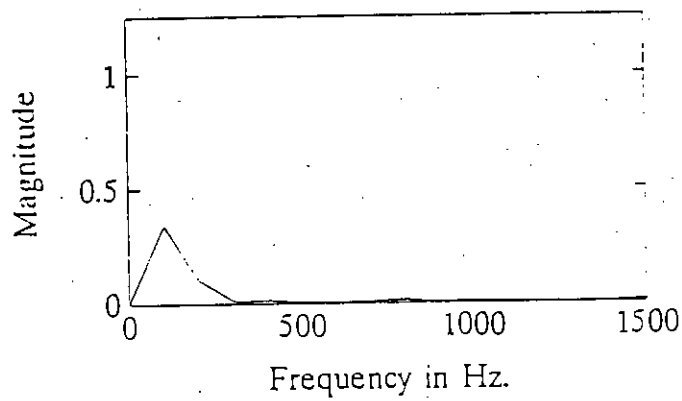
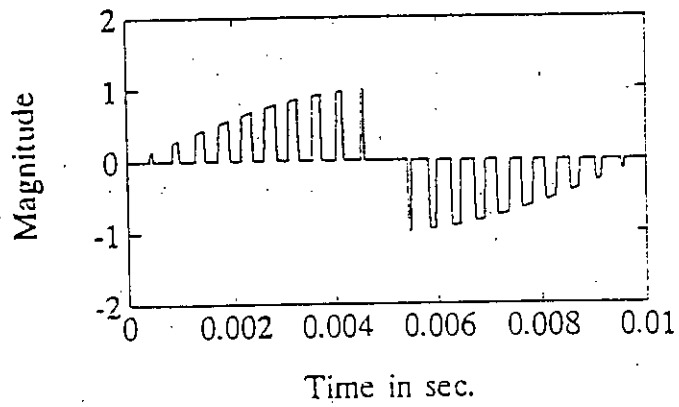


Fig: A.2.1 Modulated Waveform of Phase Shift Circuit at Modulation Index $m = .5$ and Number of Pulse/Quarter Cycle $N = 11$
 a) Modulated Output
 b) Frequency Spectrum

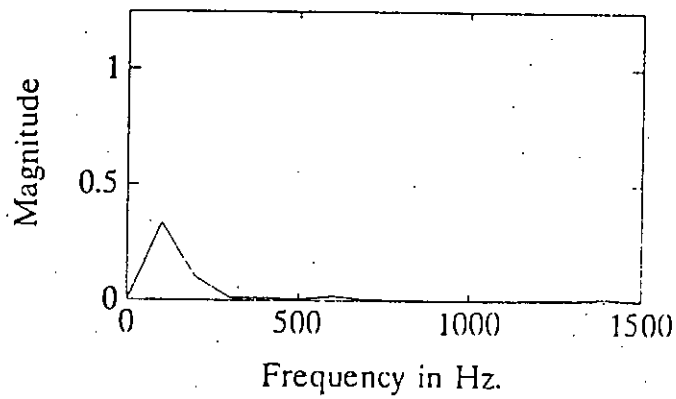
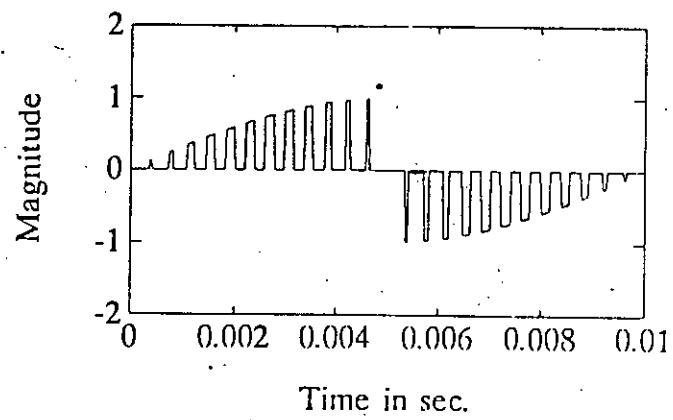


Fig. A.2.2 Modulated Waveform of Phase Shift Circuit at Modulation Index $m = .5$ and Number of Pulse/Quarter Cycle $N = 13$
 a) Modulated Output
 b) Frequency Spectrum

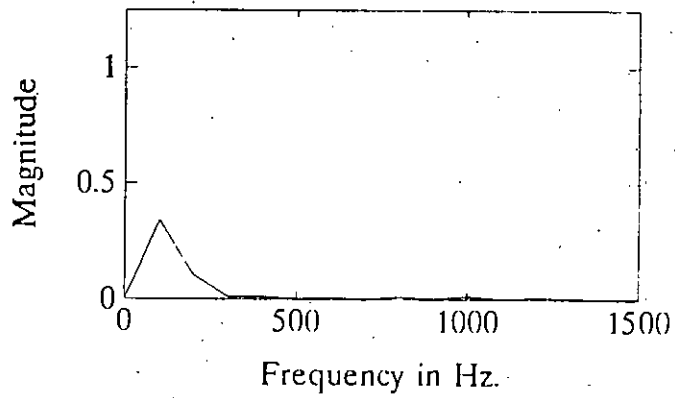
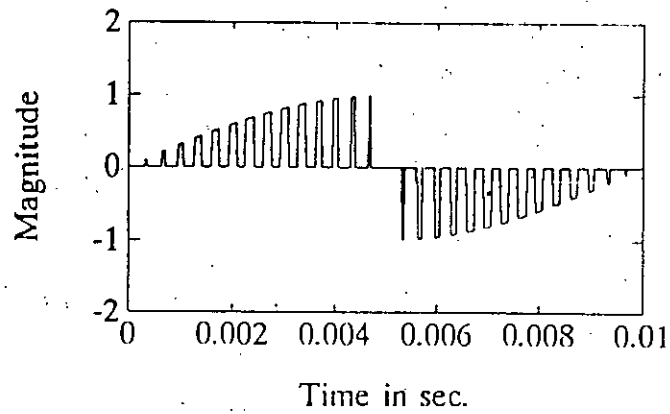


Fig. A.2.3 Modulated Waveform of Phase Shift Circuit at Modulation Index $m = .5$ and Number of Pulse/Quarter Cycle $N = 15$
 a) Modulated Output
 b) Frequency Spectrum

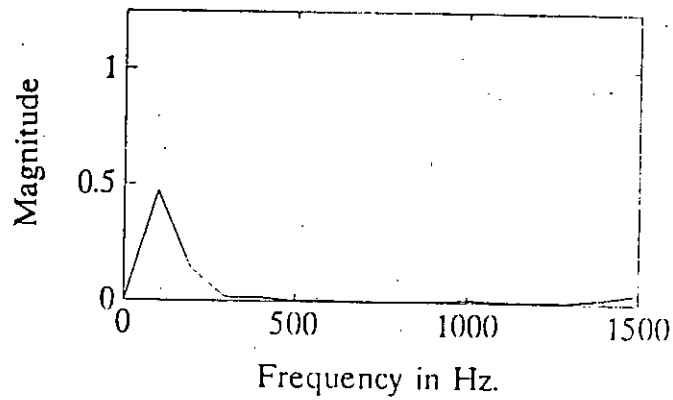
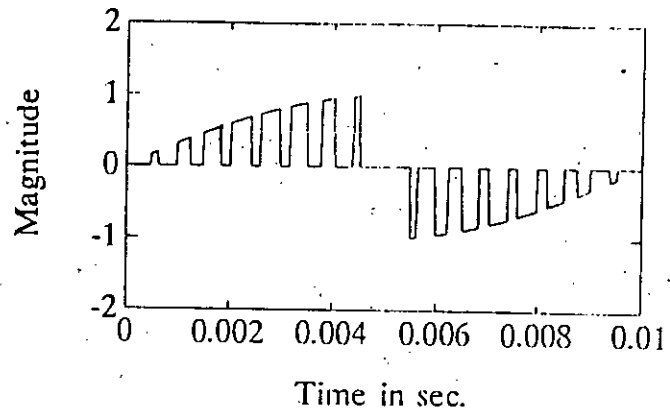


Fig. A.2.4 Modulated Waveform of Phase Shift Circuit at Modulation Index $m = .7$ and Number of Pulse/Quarter Cycle $N = 9$
 a) Modulated Output
 b) Frequency Spectrum

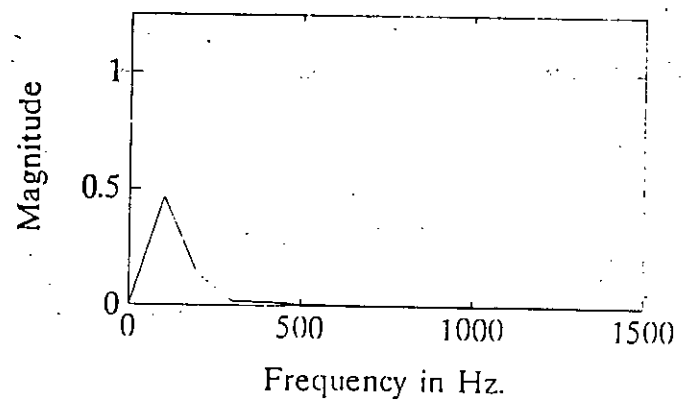
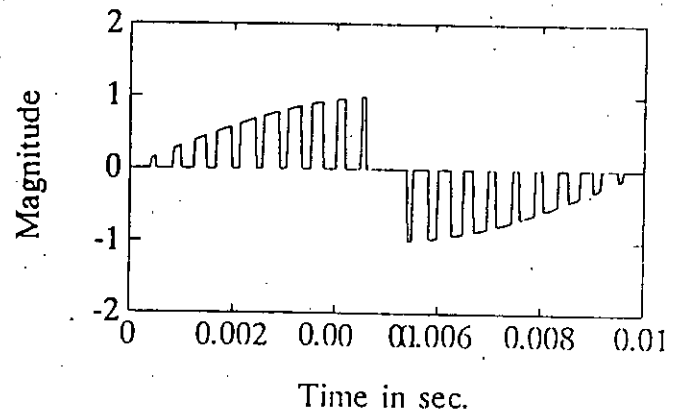


Fig. A.2.5 Modulated Waveform of Phase Shift Circuit at Modulation Index $m = .7$ and Number of Pulse/Quarter Cycle $N = 11$
 a) Modulated Output
 b) Frequency Spectrum

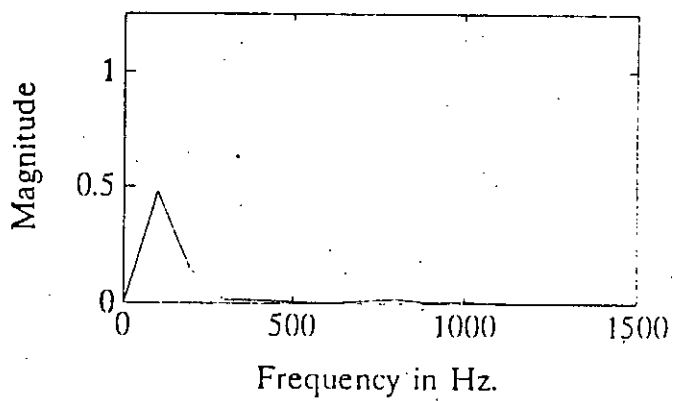
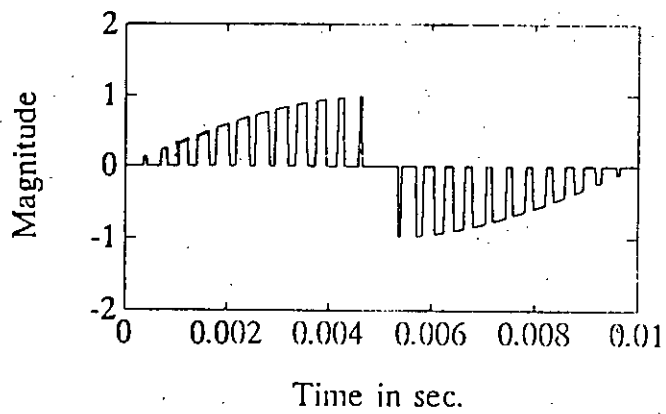


Fig. A.2.6 | Modulated Waveform of Phase Shift Circuit at Modulation Index $m = .7$ and Number of Pulse/Quarter Cycle $N = 13$
 a) Modulated Output
 b) Frequency Spectrum

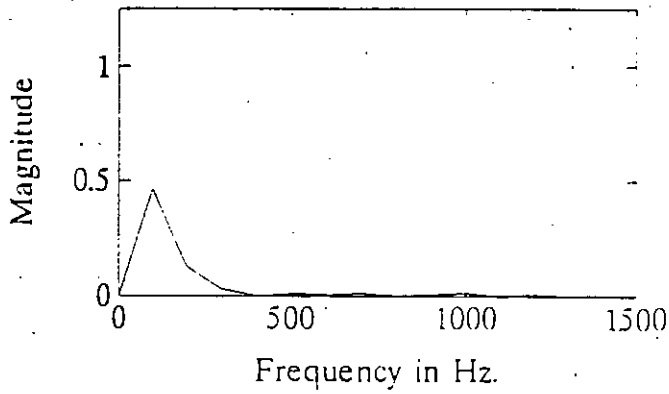
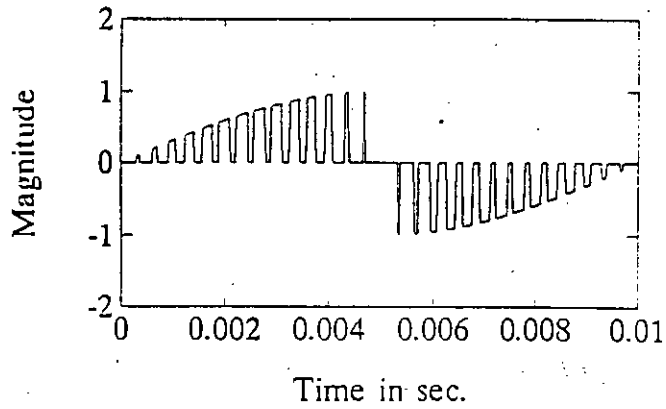


Fig. A.2.7 Modulated Waveform of Phase Shift Circuit at Modulation Index $m = .7$ and Number of Pulse/Quarter Cycle $N = 15$
 a) Modulated Output
 b) Frequency Spectrum

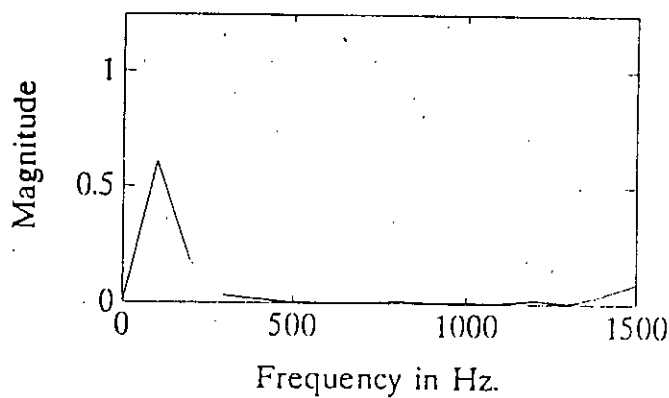
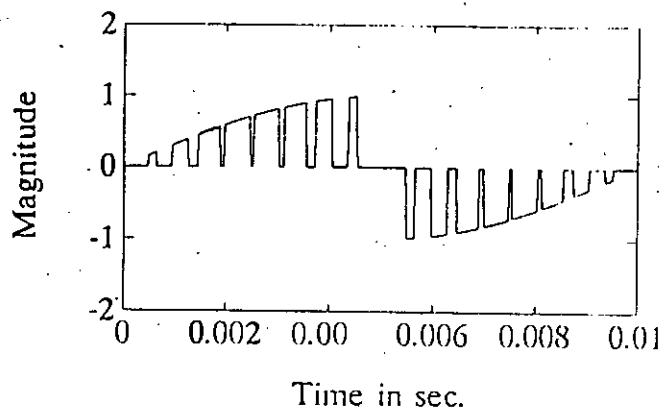


Fig. A.2.8 Modulated Waveform of Phase Shift Circuit at Modulation Index $m = .9$ and Number of Pulse/Quarter Cycle $N = 9$
 a) Modulated Output
 b) Frequency Spectrum

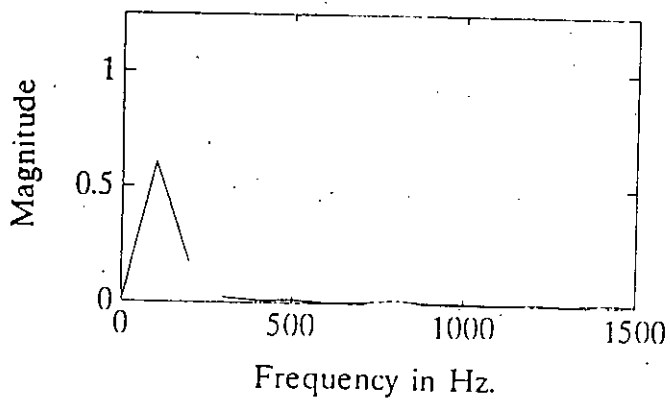
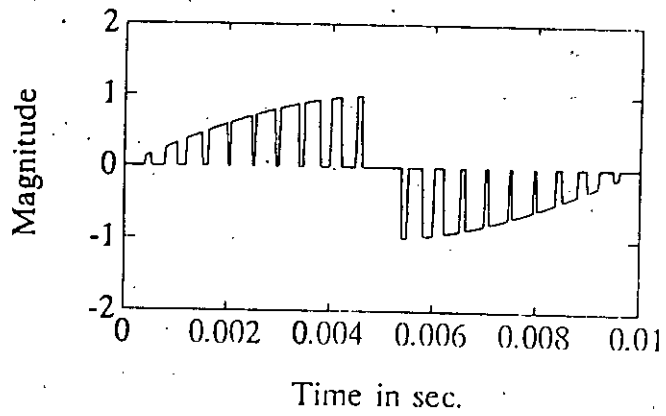


Fig. A.2.9 Modulated Waveform of Phase Shift Circuit at Modulation Index $m = .9$ and Number of Pulse/Quarter Cycle $N = 11$
 a) Modulated Output
 b) Frequency Spectrum

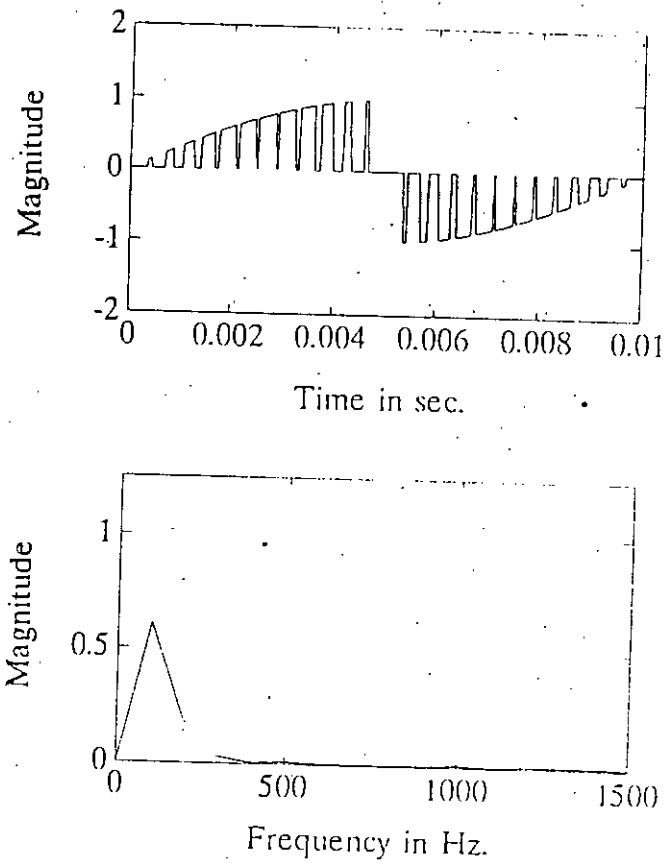


Fig. A.2.10 Modulated Waveform of Phase Shift Circuit at Modulation Index $m = .9$ and Number of Pulse/Quarter Cycle $N = 13$
 a) Modulated Output
 b) Frequency Spectrum

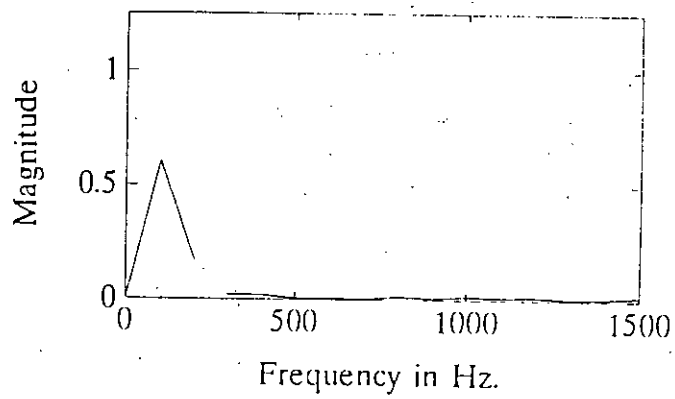
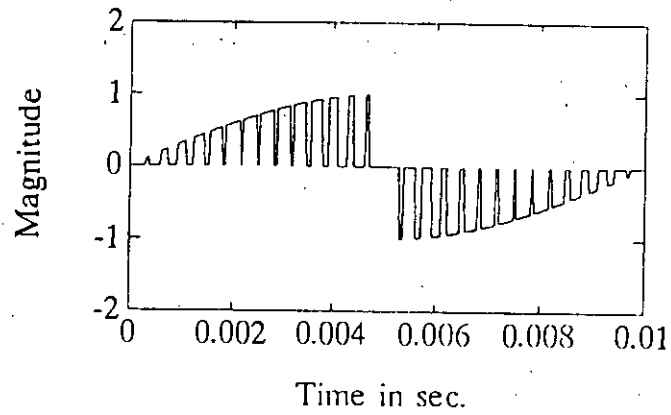


Fig. A.2.11 Modulated Waveform of Phase Shift Circuit at Modulation Index $m = .9$ and Number of Pulse/Quarter Cycle $N = 15$
 a) Modulated Output
 b) Frequency Spectrum

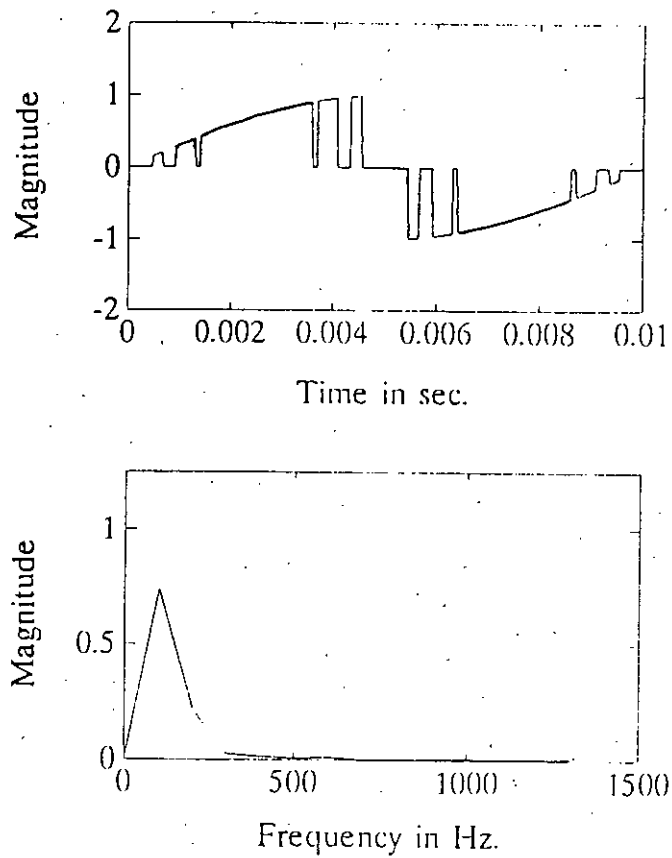


Fig. A.2.12 Modulated Waveform of Phase Shift Circuit at Modulation Index $m = 1.1$ and Number of Pulse/Quarter Cycle $N = 9$
 a) Modulated Output
 b) Frequency Spectrum

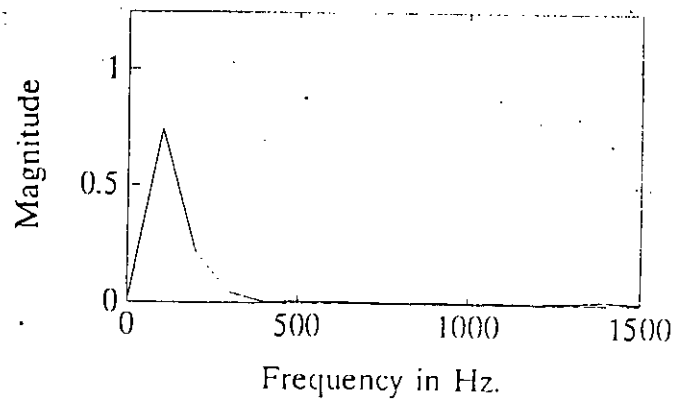
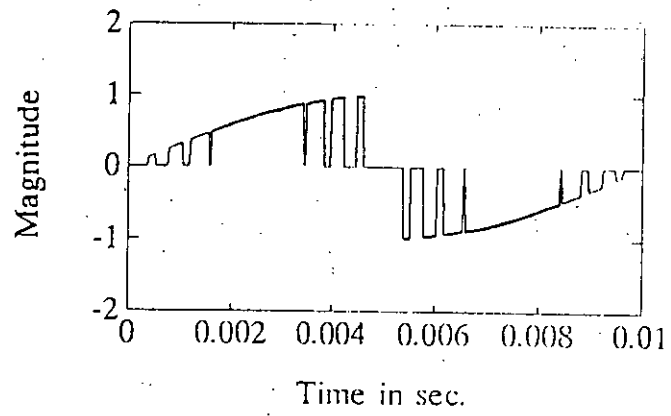


Fig. A.2.13 Modulated Waveform of Phase Shift Circuit at Modulation Index $m = 1.1$ and Number of Pulse/Quarter Cycle $N = 11$
 a) Modulated Output
 b) Frequency Spectrum

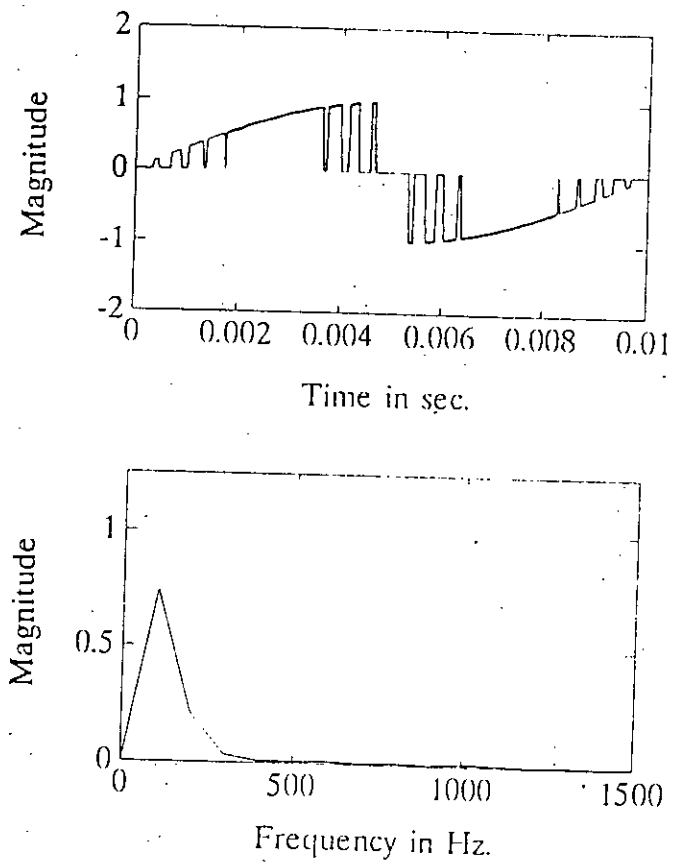


Fig. A.2.14 Modulated Waveform of Phase Shift Circuit at Modulation Index $m = 1.1$ and Number of Pulse/Quarter Cycle $N = 13$
 a) Modulated Output
 b) Frequency Spectrum

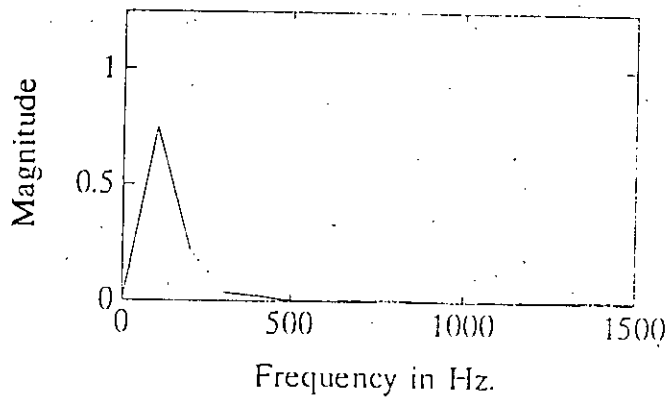
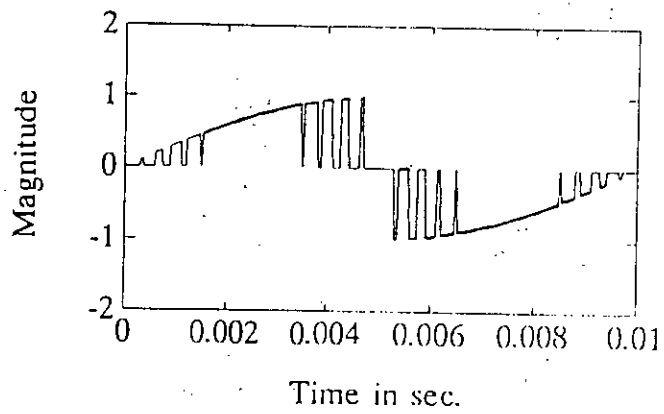


Fig. A.2.15 Modulated Waveform of Phase Shift Circuit at Modulation Index $m = 1.1$ and Number of Pulse/Quarter Cycle $N = 15$
 a) Modulated Output
 b) Frequency Spectrum

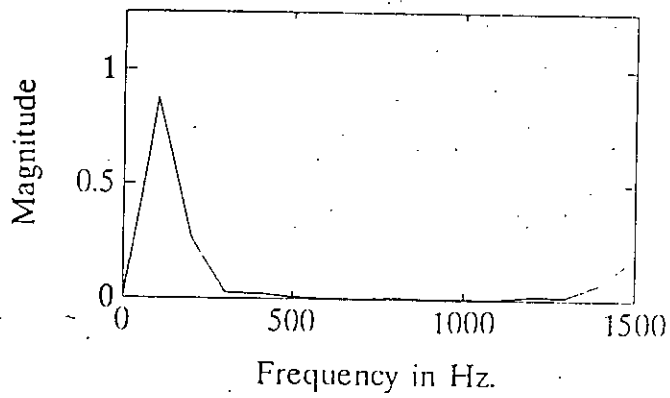
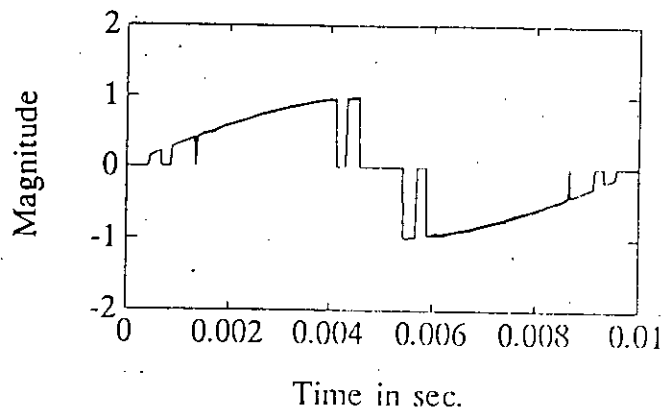


Fig. A.2.16 Modulated Waveform of Phase Shift Circuit at Modulation Index $m = 1.3$ and Number of Pulse/Quarter Cycle $N = 9$
 a) Modulated Output
 b) Frequency Spectrum

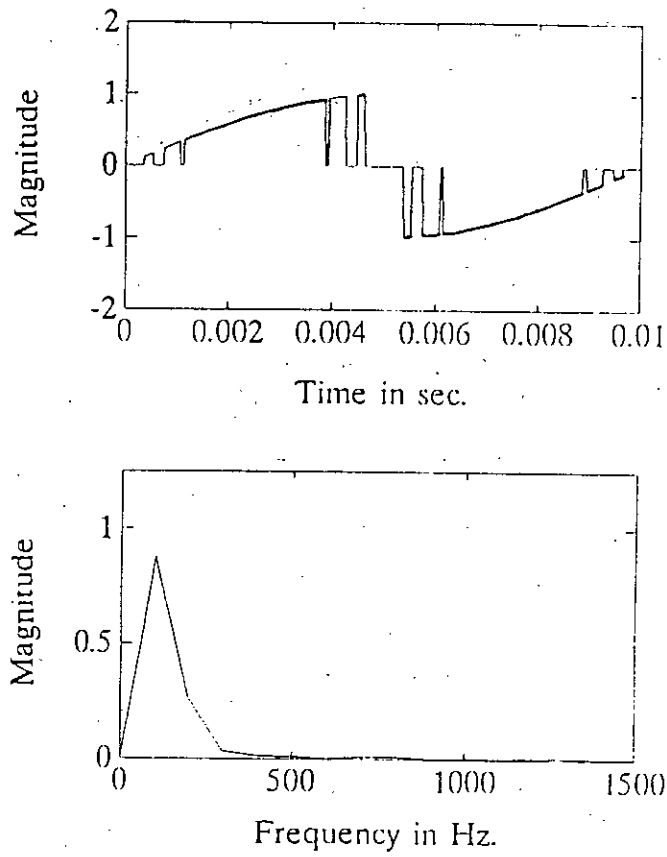


Fig. A.2.17 Modulated Waveform of Phase Shift Circuit at Modulation Index $m = 1.3$ and Number of Pulse/Quarter Cycle $N = 11$
 a) Modulated Output
 b) Frequency Spectrum

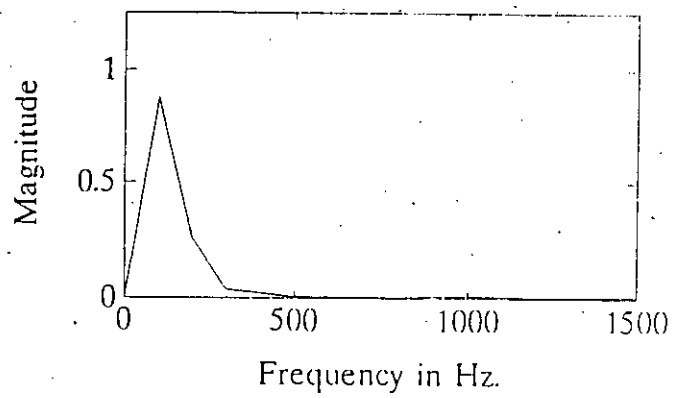
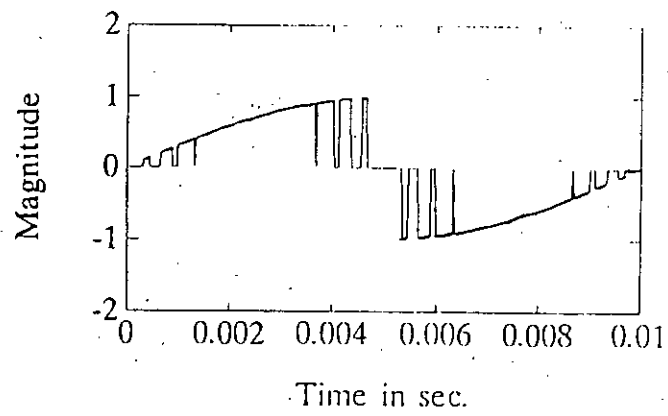


Fig. A.2.18 Modulated Waveform of Phase Shift Circuit at Modulation Index $m = 1.3$ and Number of Pulse/Quarter Cycle $N = 13$
 a) Modulated Output
 b) Frequency Spectrum

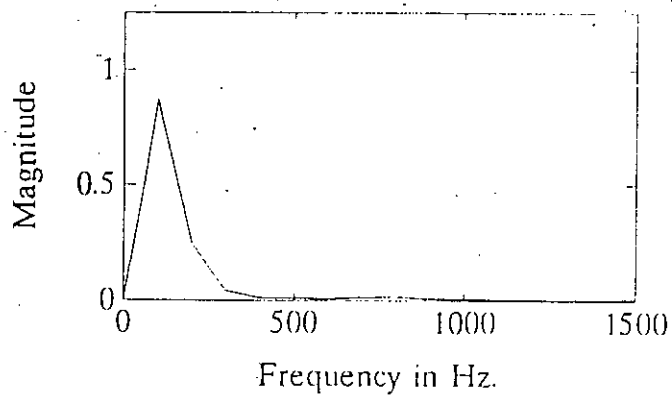
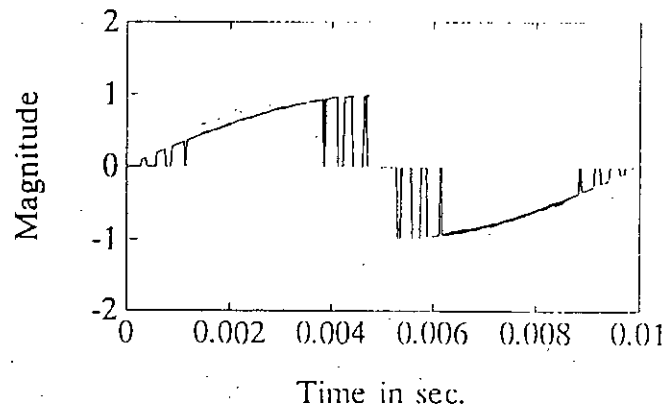


Fig. A.2.19 Modulated Waveform of Phase Shift Circuit at Modulation Index $m = 1.3$ and Number of Pulse/Quarter Cycle $N = 15$
 a) Modulated Output
 b) Frequency Spectrum

APPENDIX III
PROGRAM IN MATLAB

PROGRAM FOR SPWM WAVEFORM ANALYSIS

```
T=1./fm;
Ec=1.0;
t=0:T/2000:T;
bb=0*t;
am=Em/Ec;
N=fc/fm;
tc=1./fc;
tm=1./fm;
s=(4*Ec)/tc;
tw1=0.0;
for i=1:2*N;
    aip=((i-1)/2.)*tc;
    ii=i+1;
    q1=(-1)^i * s * (t-aip)+(-1)^ii *Ec;
    bi=i/2.;
    q2=ga(t,aip+.000000001,bi.*tc);
    w=q1.*q2;
    tw1=tw1+w;
end
tw2=Em*sin(2*pi*fm*t);
axis([0 tm -1.5 1.5])
subplot(221), plot(t,bb,t,tw1,t,tw2)
xlabel('Time in seconds'),ylabel('Magnitude in p.u.')
clear q1;
clear q2;
clear w;
clear tw2;
clear Ec;
clear Em;
clear t;
clear bb;
clear aip;
T=1./fm;
NP=512;
for i=1:N;
    theta(i)=(((2.*i-1.)*pi)/N);
    t(i)=((pi/N)*(1+am*sin(theta(i))))*(1./(2.*pi*fm));
    the(i)=theta(i)*(1./(2.*pi*fm));
    a(i)=the(i)-t(i)/2.;
    b(i)=the(i)+t(i)/2.;
end
t=0:T/511:T;
bb=0*t;
```

```

wsum=0.0;
NN=N/2;
for i=1:NN;
    w1=ga(t,a(i),b(i));
    w2=-ga(t,a(i)+T/2,b(i)+T/2);
    w=w1+w2;
    wsum=wsum+w;
end
clear w1;
clear w2;
axis([0 T -2 2]);
subplot(223),plot(t,bb,t,wsum);
xlabel('Time in seconds. '),ylabel('Magnitude in p.u. ');
fs=(NP-1)/T;
f=(fs/NP)*(0:(NP/2)-1);
y=fft(wsum,NP);
pyy=(y.*conj(y))/(NP/2);
spec=sqrt(pyy/(NP/2));
clear y;
clear pyy;
clear fs;
axis([0 2000 0 1.25]);
subplot(222),plot(f,spec(1:NP/2));
xlabel('Frequency in Hz. '), ylabel('Magnitude in p.u. ')

```

PROGRAM FOR PWM PASE SHIFT CIRCUIT WAVEFORM ANALYSIS

```
Nc=1./2.;
fm=50;
Tm=1/fm;
Tc=Tm*Nc;
fc=1./Tc;
t=0:Tc/511:Tc;
wm=2.*pi*fm;
vm=sin(wm*t);
wsum=0.0;
for i=1:2*Nc;
w=((-1)^(i+1))*ga(t,(Tm/2)*(i-1),(Tm/2)*i);
wsum=wsum+w;
end
vr=wsum.*vm;
gac=ga(t,0,Tc/2)-ga(t,Tc/2,Tc);
vc=vr.*gac;
NP=512;
for i=1:N;
ti=(pi/N)*am*sin((pi*i)/N)*(1./(2.*pi*fc));
thetai=((pi*i)/N)*(1./(2.*pi*fc));
a(i)=thetai-ti/2.;
b(i)=thetai+ti/2.;
end
wsum1=0.0;
for i=1:N;
w1=ga(t,a(i),b(i));
w2=ga(t,a(i)+Tc/2,b(i)+Tc/2);
ww=w1+w2;
wsum1=wsum1+ww;
end
vcpwm=vc.*wsum1;
axis([0 Tc -2 2])
subplot(221),plot(t,vcpwm)
xlabel('Time in sec.')
ylabel('Magnitude')
fs=(NP-1)/Tc;
f=(fs/NP)*(0:(NP/2)-1);
y=fft(vcpwm,NP);
pyy=(y.*conj(y))/(NP/2);
spec=sqrt(pyy/(NP/2));
axis([0 1500 0 1.25]);
subplot(223),plot(f,spec(1:NP/2));
xlabel('Frequency in Hz. '), ylabel('Magnitude')
```

